

|   |  |   |   |   |           |
|---|--|---|---|---|-----------|
| 1. Report No.<br>FHWA/TX-10/0-4822-3  |  | 2. Government Accession No.                         |   | 3. Recipient's Catalog No.  |           |
| 4. Title and Subtitle<br>THE TEXAS PERPETUAL PAVEMENTS: EXPERIENCE OVERVIEW AND THE WAY FORWARD   |  |   |   | 5. Report Date<br>October 2009<br>Resubmitted: April 2010<br>Published: July 2010           |           |
|   |  |   |   | 6. Performing Organization Code   |           |
| 7. Author(s)<br>Lubinda F. Walubita, Wenting Liu, and Tom Scullion  |  |   |   | 8. Performing Organization Report No.<br>Report 0-4822-3                                    |           |
| 9. Performing Organization Name and Address<br>Texas Transportation Institute<br>The Texas A&M University System<br>College Station, Texas 77843-3135   |  |   |   | 10. Work Unit No. (TRAIS)   |           |
|   |  |   |   | 11. Contract or Grant No.<br>Project 0-4822   |           |
| 12. Sponsoring Agency Name and Address<br>Texas Department of Transportation<br>Research and Technology Implementation Office<br>P. O. Box 5080<br>Austin, Texas 78763-5080   |  |   |   | 13. Type of Report and Period Covered<br>Technical Report:<br>September 2005-September 2009 |           |
|   |  |   |   | 14. Sponsoring Agency Code  |           |
| 15. Supplementary Notes<br>Project performed in cooperation with the Texas Department of Transportation and the Federal Highway Administration.<br>Project Title: Monitor Field Performance of Full-Depth Asphalt Pavements to Validate Design Procedures<br>URL: <a href="http://tti.tamu.edu/documents/0-4822-3.pdf">http://tti.tamu.edu/documents/0-4822-3.pdf</a>   |  |   |   |   |           |
| 16. Abstract<br><br><p>Since 2001, the State of Texas has been designing and constructing perpetual pavements on some of its heavily trafficked highways where the expected 20-year truck-traffic estimate of 18 kip ESALs is in excess of 30 million. To date, there are 10 in-service perpetual pavement (PP) sections, typically consisting of about 22 inches total thickness of HMA layers and supported on an 8-inch thick treated (lime or cement) base, resting on a well compacted subgrade soil. This report provides an overview of the Texas construction and evaluation experience of PPs including structural design, materials and mix-designs, construction and quality issues, and performance history. The research methodology and scope of work included data collection, extensive laboratory and field testing, computational modeling, and performance evaluations. Based on the research findings, recommendations for the future Texas PP design, construction, and performance monitoring are provided in this report.</p> <p>Overall, performance to date is satisfactory with no major structural distresses. However, construction-related joint and cracking problems were observed on a few projects. Laboratory and field experience has also indicated workability, compactability, and constructability related problems with the Stone Filled (SF) HMA mixes, which serve as the main structural load-carrying layers. Recommendations have accordingly been made to improve or replace the SF mix-designs. Recommendations are also provided for the structural design of future Texas PPs; the current PP designs were found to be conservative with potential for further optimization. The results generated support the transition to higher design moduli values, yielding a 6 or more inch structural thickness reduction in the total HMA thickness.</p> |  |   |   |   |           |
| 17. Key Words<br>Perpetual Pavement, Stone-Filled HMA, Hamburg, Rutting, Permanent Deformation, Overlay, Cracking, Modulus, Infra-Red, X-ray CT, IRI, GPR, FWD, WIM, MDD, FPS, PerRoad, VESYS, MEPDG  |  |   | 18. Distribution Statement<br>No restrictions. This document is available to the public through NTIS:<br>National Technical Information Service<br>Springfield, Virginia 22161<br><a href="http://www.ntis.gov">http://www.ntis.gov</a> |   |           |
| 19. Security Classif.(of this report)<br>Unclassified   |  | 20. Security Classif.(of this page)<br>Unclassified |   | 21. No. of Pages<br>164   | 22. Price |



**THE TEXAS PERPETUAL PAVEMENTS:  
EXPERIENCE OVERVIEW AND THE WAY FORWARD**

by

Lubinda F. Walubita  
Transportation Researcher  
Texas Transportation Institute

Wenting Liu  
Research Scientist  
Texas Transportation Institute

and

Tom Scullion  
Senior Research Engineer  
Texas Transportation Institute

Report 0-4822-3

Project 0-4822

Project Title: Monitor Field Performance of Full-Depth Asphalt Pavements to  
Validate Design Procedures

Performed in cooperation with the  
Texas Department of Transportation  
and the  
Federal Highway Administration

October 2009

Resubmitted: April 2010

Published: July 2010

TEXAS TRANSPORTATION INSTITUTE  
The Texas A&M University System  
College Station, Texas 77843-3135



## **DISCLAIMER**

The contents of this report reflect the views of the authors, who are responsible for the facts and the accuracy of the data presented herein. The contents do not necessarily reflect the official view or policies of the Federal Highway Administration (FHWA) or the Texas Department of Transportation (TxDOT). This report does not constitute a standard, specification, or regulation, nor is it intended for construction, bidding, or permit purposes. The United States Government and the State of Texas do not endorse products or manufacturers. Trade or manufacturers' names appear herein solely because they are considered essential to the object of this report. The engineer in charge was Tom Scullion, P.E. (Texas No. 62683).

## **ACKNOWLEDGMENTS**

This project was conducted for TxDOT, and the authors thank TxDOT and FHWA for their support in funding this research project. In particular, the guidance and technical assistance provided by the project director Joe Leidy, P.E., of TxDOT and the program coordinator Miles Garrison, P.E., proved invaluable. Special thanks are also extended to Lee Gustavus, Stephen Sebesta, Rick Canatella, Gerry Harrison, Tony Barbosa, and Vivekram Umashankar from the Texas Transportation Institute (TTI) for their help with laboratory and field testing. The assistance provided by the various TxDOT districts (Fort Worth, Laredo, San Antonio, and Waco) is also gratefully acknowledged.

The following project advisors also provided valuable input throughout the course of the project: Billy Pigg, P.E., Waco District; Andrew Wimsatt, P.E., formally Fort Worth District; Rosa Trevino, Laredo District; and Patrick Downey, P.E., San Antonio District.

# TABLE OF CONTENTS

|   |      |
|---|------|
| List of Figures .....                                     | x    |
| List of Tables .....                                      | xiii |
| List of Notations and Symbols.....                        | xv   |
| Chapter 1. Introduction .....                             | 1-1  |
| Objectives and Scope of Work .....                        | 1-1  |
| Description of Contents .....                             | 1-3  |
| Summary .....   | 1-3  |
| Chapter 2. The Texas In-Service PP Projects .....         | 2-1  |
| The Texas PP Design Concept.....                          | 2-1  |
| The Existing in-Service PP Structures.....                | 2-3  |
| PP Materials and Mix-Designs .....                        | 2-8  |
| Summary .....   | 2-12 |
| Chapter 3. PP Construction and Lessons Learned .....      | 3-1  |
| Subgrade and Base Stabilization.....                      | 3-1  |
| HMA Placement and Quality Control Issues.....             | 3-3  |
| Construction Joint Problems.....                          | 3-11 |
| Coring and AV Distribution.....                           | 3-13 |
| Summary .....   | 3-17 |
| Chapter 4. Laboratory Testing and Material Property ..... |      |
| Characterization .....                                    | 4-1  |
| Laboratory Test Protocols.....                            | 4-1  |
| HMA Test Specimens, AV, and Replicates.....               | 4-2  |
| Asphalt Binder Content and Aggregate Extractions.....     | 4-2  |
| Asphalt Binder DSR Test Results .....                     | 4-4  |
| HMA Lab Test Results .....                                | 4-5  |
| X-Ray CT Scanning and AV Characterization.....            | 4-14 |
| Summary .....   | 4-17 |
| Chapter 5. Field Testing and Performance Evaluation ..... | 5-1  |
| Visual Surveys .....                                      | 5-1  |

## TABLE OF CONTENTS (Continued)

|   |      |
|---|------|
| Cracking.....   | 5-2  |
| Surface Rut Measurements .....                                  | 5-5  |
| Surface Profiles and IRI Measurements .....                     | 5-6  |
| FWD Measurements .....  | 5-9  |
| GPR Measurements and Forensic Evaluations .....                 | 5-17 |
| Summary .....   | 5-18 |
| Chapter 6. Traffic WIM and MDD Response Measurements .....      | 6-1  |
| WIM Traffic Measurements .....                                  | 6-1  |
| MDD Response Measurements.....                                  | 6-7  |
| Summary .....   | 6-18 |
| Chapter 7. Computational Modeling and Software Evaluation ..... | 7-1  |
| Validation of the Texas PP Design Concept.....                  | 7-1  |
| Comparative Software Evaluation .....                           | 7-2  |
| The FPS 21W Software .....                                      | 7-3  |
| The MEPDG 1.00 Software.....                                    | 7-7  |
| Summary .....   | 7-9  |
| Chapter 8. Texas PP Performance Comparisons .....               | 8-1  |
| SH 114 (Fort Worth) - SFHMA versus Type B/C Mixes.....          | 8-1  |
| General Texas PP Performance Comparison.....                    | 8-6  |
| Texas PP Comparison with NCAT Test Track PP Sections.....       | 8-7  |
| Summary .....   | 8-13 |
| Chapter 9. Future Texas PP Design and Recommendations.....      | 9-1  |
| Future PP Structural and Mix Design Proposals.....              | 9-1  |
| Future PP Construction.....                                     | 9-6  |
| Future PP Testing and Performance Evaluation .....              | 9-7  |
| Summary .....   | 9-8  |
| Chapter 10. Summary and Conclusions.....                        | 10-1 |
| References.....   | R-1  |



## TABLE OF CONTENTS (Continued)

|   |     |
|---|-----|
| Appendix A: Existing Texas Perpetual Pavement Sections .....            | A-1 |
| Appendix B: Example of Material Properties for SH 114.....              | B-1 |
| Appendix C: Field Performance Testing of Selected PP Sections .....     | C-1 |
| Appendix D: MDD Deflections and Strain Analyses for IH 35 (Laredo)..... | D-1 |

## LIST OF FIGURES

| Figure   | Page |
|--|------|
| 2-1 A Typical Texas PP Structural Section .....                                  | 2-2  |
| 2-2 Map of Texas and PP Project Locations (Projects #1-10).....                  | 2-6  |
| 2-3 The 1-inch SF Coarse Aggregate Gradations and Coarse Surface Texture .....   | 2-11 |
| 3-1 Lime Treatment Process on SH 114 .....                                       | 3-1  |
| 3-2 Field-Extracted Base Core from SH 114.....                                   | 3-2  |
| 3-3 Comparison of MTDs and HMA Mat Temperature Profiles on SH 114 .....          | 3-4  |
| 3-4 Effects of the Compacted Lift Thickness for the 1-in SFHMA Layer .....       | 3-5  |
| 3-5 Steel Wheel versus Pneumatic Breakdown Roller (IH 35–Laredo).....            | 3-6  |
| 3-6 SH 114 Conventional- 17 Total Compaction Rolling Passes.....                 | 3-7  |
| 3-7 GPR Density Variations and Forensic Defects in Core (IH 35 San Antonio)..... | 3-8  |
| 3-8 Substandard Cores from SH 114 and IH 35 .....                                | 3-8  |
| 3-9 Localized Voided Areas and Segregation on IH 35 Price (NB, Laredo) .....     | 3-9  |
| 3-10 Evidence of Subsurface Defects/Moisture Presence on IH 35 (McLennan).....   | 3-9  |
| 3-11 Examples of Ideal GPR Readings with No Subsurface Defects .....             | 3-10 |
| 3-12a Open Joint and Moisture Presence on IH 35 Price (Laredo, 2008).....        | 3-12 |
| 3-12b Non-Ideal GPR Readings Indicating Moisture Presence on IH 35 (Price) ..... | 3-12 |
| 3-13 Clean GPR Readings after Strip Sealing on IH 35 Price (Laredo, 2009).....   | 3-13 |
| 3-14 Core AV Distribution–IH 35 (NB, Price, Laredo) .....                        | 3-14 |
| 3-15 Core AV Distribution–IH 35 (SB, Price, Laredo).....                         | 3-15 |
| 3-16 Coring and AV Distributional .....  | 3-15 |
| 3-17 Core AV Distribution as a Function of Depth (IH 35, San Antonio).....       | 3-16 |
| 4-1 Binder $G^*/\sin \delta$ (delta) versus Temperature .....                    | 4-4  |
| 4-2 Phase Angle versus Temperature .....   | 4-4  |
| 4-3 $ E^* $ Master-Curves (Reference Temperature = 70 °F).....                   | 4-12 |
| 4-4 Permanent Deformation Results.....   | 4-15 |
| 4-5 X-Ray CT Results for IH 35 Laredo Cores (Price).....                         | 4-16 |

## LIST OF FIGURES (Continued)

|      |   |      |
|------|---|------|
| 5-1  | Examples of Open Longitudinal and Transverse Construction Joints .....          | 5-2  |
| 5-2  | Longitudinal Cracking on IH 35 (Gilbert Job) .....                              | 5-3  |
| 5-3  | Coring along the Longitudinal Crack on IH 35 (Gilbert Job) .....                | 5-3  |
| 5-4  | GPR Measurements and Coring from the Wheel Path (IH 35 Gilbert Job) .....       | 5-4  |
| 5-5  | Example of Summer 2009 Surface Rut Measurements on IH 35 (Price Job) .....      | 5-5  |
| 5-6  | Average Summer 2009 Surface Rut Measurements–All PP Projects .....              | 5-6  |
| 5-7  | Average IRI Plots for SH 114 (Superpave)–Outside EB Lane. ....                  | 5-7  |
| 5-8  | Average IRI Plots for IH 35 (Hillsboro)–Outside NB Lane.....                    | 5-7  |
| 5-9  | Extrapolative Plot of the Overall Average IRI. ....                             | 5-8  |
| 5-10 | Plot of FWD Deflections on IH 35 Gilbert (Laredo).....                          | 5-10 |
| 5-11 | Average FWD Surface Deflections (Winter and Summer).....                        | 5-10 |
| 5-12 | Summary Curvature Index Results for IH 35 Zumwalt 01 Project (Laredo) .....     | 5-12 |
| 5-13 | Average Curvature Indices for All the PP Projects .....                         | 5-13 |
| 5-14 | Extrapolative Plot of the Curvature Indices .....                               | 5-13 |
| 5-15 | Example of FWD Moduli Plots (HMA Layers) for IH 35 Gilbert (Laredo).....        | 5-15 |
| 5-16 | FWD Moduli Plots (Base and Subgrade) for IH 35 Gilbert (Laredo).....            | 5-15 |
| 5-17 | Plot of Base and Subgrade FWD Moduli for IH 35 Zumwalt 02 (Laredo).....         | 5-17 |
| 5-18 | Summer 2009 GPR Measurements on IH 35 (San Antonio).....                        | 5-17 |
| 5-19 | Clean GPR Readings (Summer 2009) with No Indication of Subsurface Defects ..... | 5-18 |
| 6-1  | WIM Station 531–IH 35 Zumwalt02 (Laredo).....                                   | 6-1  |
| 6-2  | WIM Station 527–SH 114 Superpave (Fort Worth).....                              | 6-1  |
| 6-3  | Truck Gross-Vehicle Weight Distributions.....                                   | 6-3  |
| 6-4  | Hourly 18 kip Distributions over 24 Hours .....                                 | 6-4  |
| 6-5  | Example of Monthly 18 kips Distributions for August 2008 .....                  | 6-4  |
| 6-6  | Axle Load Distributions .....   | 6-5  |
| 6-7  | Truck GVW Distribution by Lane.....   | 6-6  |
| 6-8a | MDD Instrumentation Set-Up .....  | 6-7  |
| 6-8b | MDD Installation.....   | 6-8  |
| 6-9  | MDD Depth Locations within the Zumwalt02 PP Structure.....                      | 6-9  |
| 6-10 | Typical 18 Wheeler-Truck MDD Deflection Response with Time Passage.....         | 6-10 |

## LIST OF FIGURES (Continued)

|       |   |      |
|-------|---|------|
| 6-11  | Example MDD Deflection Measurements as a Function Pavement Depth.....   | 6-11 |
| 6-12a | Vertical Strain Plot for the HMA Layers.....  | 6-13 |
| 6-12b | Vertical Strain Plot for the Base.....  | 6-13 |
| 6-12c | Vertical Strain Plot in the Subgrade Top 8-inches .....   | 6-14 |
| 6-13  | Surface Deflection versus Subgrade Microstrains in the Top 8-inches.....  | 6-14 |
| 7-1   | FPS 21W Main Screen .....   | 7-5  |
| 7-2   | FPS 21W Built-In Layer Options .....  | 7-5  |
| 7-3   | Example FPS 21W Design Output Data.....   | 7-6  |
| 7-4   | Example FPS 21W Mechanistic Analysis .....  | 7-6  |
| 8-1   | Pictorial Location of the SH 114 PP Sections .....  | 8-2  |
| 8-2   | SH 114 PP Structural Sections .....   | 8-2  |
| 8-3   | Non-Ideal GPR Readings, Defective Core, and High Non-Uniform Core<br>AV Distribution from SH 114 Superpave..... | 8-5  |
| 8-4   | Ideal GPR Readings, Non-Defective Intact Core, and Uniform AV Core From<br>SH 114 Conventional.....             | 8-5  |
| 8-5   | Overview of the NCAT Test Track.....  | 8-8  |
| 8-6   | Aggregate Gradation Comparisons .....   | 8-11 |
| 8-7   | Texas SH 114 vs. NCAT PP Sections (GPR, Cores, and AV Distribution) .....                                       | 8-12 |

## LIST OF TABLES

| <b>Table</b>  | <b>Page</b> |
|---|-------------|
| 2-1 In-Service Texas PP Structural Sections.....                                | 2-4         |
| 2-2 Project TRM and GPS Location Details.....                                   | 2-5         |
| 2-3 Traffic Design Data.....  | 2-7         |
| 2-4 In-Service Typical Mix-Designs and Material Characteristics.....            | 2-8         |
| 2-5 Laboratory Comparison of Aggregate Properties.....                          | 2-9         |
| 4-1 Laboratory Test Protocols.....  | 4-1         |
| 4-2 Asphalt Binder Content Results Based on the Troxler Ignition Oven Test..... | 4-2         |
| 4-3 Aggregate Extraction Results for 1-Inch SFHMA Layer (SH 114 Superpave)..... | 4-3         |
| 4-4 Average HMA Mix Results.....  | 4-5         |
| 4-5 HMA Moduli Values at 77 °F, 10 Hz.....                                      | 4-7         |
| 4-6 District Average Moduli at 77 °F, 10 Hz.....                                | 4-8         |
| 4-7 District Average Hamburg Results.....                                       | 4-8         |
| 4-8 District Average Overlay Results.....                                       | 4-8         |
| 4-9 Moduli Comparison–Field Cores.....  | 4-9         |
| 4-10 Hamburg Rutting Performance Comparison–Field Cores.....                    | 4-10        |
| 4-11 Overlay Cracking Performance Comparison–Field Cores.....                   | 4-10        |
| 4-12 Lab-Molded Samples and Plant-Mixes.....                                    | 4-11        |
| 4-13 Field- Extracted Cores.....  | 4-11        |
| 5-1 Average IRI Measurements (All PP Projects).....                             | 5-8         |
| 5-2 District Average In Situ FWD Moduli Values at 77°F.....                     | 5-16        |
| 6-1 WIM Traffic Counts.....   | 6-6         |
| 6-2 Peak Vertical Deflections and Strain Computations.....                      | 6-11        |
| 6-3 FPS Strain Computations in the Subgrade.....                                | 6-15        |
| 6-4 PP Re-Designs with FPS 12W and Actual Measured Input Data.....              | 6-17        |
| 6-5 Example Comparison of Moduli Values for SH 114.....                         | 6-17        |
| 7-1 Summary Results of Computational Modeling.....                              | 7-1         |
| 7-2 Software Comparisons.....   | 7-3         |
| 7-3 Example of Sensitivity Analysis for Rutting.....                            | 7-8         |

## LIST OF TABLES (Continued)

|     |  |      |
|-----|--|------|
| 7-4 | MEPDG Distress Analysis (SH 114) at 95 Percent Reliability Level ..... | 7-8  |
| 8-1 | Comparative Evaluation of the SH 114 PP Sections.....                  | 8-3  |
| 8-2 | Comparative Evaluation of Selected PP Sections .....                   | 8-6  |
| 8-3 | SH 114 Comparison with NCAT N8 and N9 Sections .....                   | 8-10 |
| 8-4 | Comparison of OT Results–Field Cores (SH 114 vs. Alabama).....         | 8-13 |
| 9-1 | Future Texas PP Design Proposals.....                                  | 9-2  |
| 9-2 | Proposed Future Design Moduli Values at 77 °F .....                    | 9-4  |
| 9-3 | Comparison Validation of the Proposed PP Structural Designs .....      | 9-5  |
| 9-4 | Comparison of Some Performance Thresholds.....                         | 9-7  |

## LIST OF NOTATIONS AND SYMBOLS

|        |  |
|--------|--|
| AASHTO | American Association of State Highway and Transportation Officials |
| ADT    | Average daily traffic  |
| BCI    | Base curvature index   |
| DSR    | Dynamic shear rheometer  |
| DM     | Dynamic modulus  |
| ESAL   | Equivalent single axle load  |
| FDAP   | Full-depth asphalt pavement  |
| FPS    | Flexible pavement system   |
| FWD    | Falling weight deflectometer                                       |
| GPR    | Ground penetrating radar   |
| HDSMA  | Heavy-duty stone mastic asphalt                                    |
| HMA    | Hot-mix asphalt  |
| HMAC   | Hot-mix asphalt concrete   |
| HWTT   | Hamburg wheel tracking test  |
| IR     | Infra-red  |
| IRI    | International roughness index                                      |
| MDD    | Multi-depth deflectometer  |
| MEPDG  | Mechanistic empirical design guide                                 |
| MTD    | Material transfer device   |
| NCAT   | National Center for Asphalt Technology                             |
| NDT    | Non-destructive test (ing)   |
| NMAS   | Nominal maximum aggregate size                                     |
| OT     | Overlay tester   |
| PFC    | Porous friction course   |
| PG     | Performance grade  |
| PI     | Plasticity Index   |
| PP     | Perpetual pavement   |
| PSI    | Present Serviceability Index                                       |
| QA     | Quality assurance  |

## LIST OF NOTATIONS AND SYMBOLS (CONTINUED)

|                        |  |
|------------------------|--|
| QC                     | Quality control  |
| RBL                    | Rich-bottom layer  |
| RLPD                   | Repeated load permanent deformation test                             |
| RR                     | Research report  |
| RRL                    | Rut-resistant layer  |
| SCI                    | Surface curvature index  |
| SF                     | Stone-fill or Stone filled   |
| SFHMA(C)               | Stone-fill hot-mix asphalt (concrete)                                |
| Subgrade <sub>w7</sub> | Subgrade curvature index   |
| SMA                    | Stone mastic asphalt   |
| SP                     | Superpave  |
| SS                     | Special specification  |
| TIOT                   | Troxler ignition oven test   |
| WIM                    | Weigh-in-motion  |
| $W_i$                  | FWD surface deflection from $i^{\text{th}}$ sensor                   |
| $\varepsilon_t$        | Horizontal tensile strain measured in microns ( $\mu\varepsilon$ )   |
| $\varepsilon_v$        | Vertical compressive strain measured in microns ( $\mu\varepsilon$ ) |
| "                      | Inch as dimensional unit (e.g., 1" = 1 inch [ $\cong$ 25 mm])        |
| $\phi$                 | Symbol phi used to mean diameter                                     |



# CHAPTER 1

## INTRODUCTION

Since 2001, the State of Texas has been designing and constructing full-depth asphalt pavements (also commonly known as perpetual pavements) on some of their heavily trafficked highways where the expected 20-year truck-traffic estimate of 18 kip ESALs is in excess of 30 million. To date, there are 10 perpetual pavement (PP) sections in-service. Typical sections consist of about 22 inches total thickness of HMA layers and supported on an 8 or more inch thick treated (lime or cement) base material that is resting on a well compacted in-situ subgrade soil material.

This report provides an overview of the evaluation of the Texas perpetual pavements and related experiences including structural design, materials and mix-designs, construction and quality issues, and performance history. Where necessary, this report should be read in conjunction with technical reports 0-4822-1 and 0-4822-2 ([Scullion, 2005](#); [Walubita and Scullion, 2007](#)) that constitute Volumes 1 and 2 of the same work. Reference can also be made to the companion database entitled “The Texas Perpetual Pavement (PP) Database ([Walubita et al., 2009](#)).

### OBJECTIVES AND SCOPE OF WORK

The research work contained in this report was initiated to monitor the construction and performance history of the Texas perpetual pavements, including evaluating and validating the Texas PP design concept. Accordingly, this report provides an overall evaluation and documentation of the Texas PP experience including highlighting the lessons learned and the remedial measures taken thereof as well as providing recommendations on the future designs, construction, and performance monitoring/evaluation of the Texas PP structures. Overall, the project research goals were:

- 1) validation of the Texas PP design concept by relating field and laboratory results to actual pavement performance monitored after construction;
- 2) material testing and database development, with a focus on design moduli;

- 3) performance monitoring and data collection to verify and enhance TxDOT's PP design, materials, and construction specifications;
- 4) formulation of recommendations for future Texas PP design, construction, and performance evaluation;
- 5) evaluation and recommendation of appropriate software for design, modeling, and performance prediction of Texas PP structures; and
- 6) development of test plans and specifications for future Texas PP construction, testing, and performance monitoring/evaluation.

To achieve these objectives, the research methodology and scope of work included the following:

- 1) Laboratory testing and material property characterization. The laboratory tests included the asphalt-binder extractions, asphalt-binder properties, rutting and moisture damage susceptibility with the Hamburg, cracking resistance, dynamic modulus, permanent deformation, permeability, etc.
- 2) Construction monitoring and evaluations included workability and compactability aspects. Construction quality (QC) monitoring tests included IR thermal imaging of the HMA mat temperatures.
- 3) Field testing and performance monitoring/evaluation. Non-destructive and performance evaluation tests included visual surveys (surface defects, surface rutting, and cracking), surface profiles (IRI and ride quality), FWD, and the GPR.
- 4) Coring and forensic evaluations including X-ray CT scanning of field-extracted cores for air void characterization.
- 5) Traffic WIM and MDD response measurements. These measurements included actual traffic counts and in situ deflections/strain evaluations on selected PP projects.
- 6) Computational modeling and comparative software evaluation including the FPS, PerRoad, VESYS, and the MEPDG.
- 7) Texas PP performance comparison including evaluation of the PP structures at the NCAT test track in Alabama.
- 8) Comparative synthesis of the research findings and making pertinent recommendations.

## DESCRIPTION OF CONTENTS

This report consists of 10 chapters, including this chapter ([Chapter 1](#)) that provides the introduction, research objectives, research methodology, and scope of work. [Chapter 2](#) provides a description of the existing in-service PP structures including the project location details, pavement structures, materials, and mix-designs. [Chapter 3](#) gives a presentation of the PP construction experiences and lessons learned, followed by a discussion of laboratory and field testing results in [Chapters 4](#) and [5](#), respectively.

Traffic measurements and computational modeling are subsequently presented in [Chapters 6](#) and [7](#), respectively. [Chapter 8](#) shows a comparative analysis of the Texas PP performance history including comparative evaluation of the PP structures in Alabama at the NCAT test track. [Chapter 9](#) provides a synthesis of the results and research findings including recommendations and specifications for future Texas PP designs, construction, testing, and performance evaluation. The report concludes in [Chapter 10](#) with a summary of findings and the future prospects of perpetual pavements in Texas. The research product deliverables are also discussed in this chapter ([Chapter 10](#)). Appendices of detailed test data and analysis results are also included at the end of the report.

## SUMMARY

In this introductory chapter, the background and the research objectives were discussed. The research methodology and scope of work were described followed by a description of the report contents.

Throughout this report, all the Superpave and Stone Filled HMA mixes including the SMA are specified by their nominal maximum aggregate size (NMAS), e.g., 1-inch SFHMAC, ¾-inch SFHMAC, and ½-inch HDSMA; NMAS is defined as one sieve size larger than the first sieve to retain more than 10 percent of the aggregate material. Additionally, as some of the laboratory tests such as the Hamburg, Dynamic Shear Rheometer, and Permeability use standard metric (SI) units, some of the test results have consequently been reported in metric units, e.g., use of “mm” for the Hamburg test results. Note also that the abbreviation SFHMAC has been used interchangeably with the term SFHMA.



## CHAPTER 2

### THE TEXAS IN-SERVICE PP PROJECTS

This chapter discusses the existing PP sections that are in service. The discussion includes the project location details, structural layer thicknesses, materials and mix-designs, traffic design data, and the environment. The Texas PP design concept is also discussed in this chapter. A summary is then provided to wrap up the chapter.

#### THE TEXAS PP DESIGN CONCEPT

The general PP design philosophy is to mitigate rutting and bottom-up fatigue cracking in the pavement structure, with a design structural life of up to 50 years. However, they are subject to periodic surface maintenance and/or renewal in response to surface distresses in the upper layers of the pavement during their service lives. Deep seated structural distresses such as fatigue cracking (bottom-up) and/or rutting should not occur or if present are very minimal. The current PP mechanistic-empirical (M-E) design principle is, therefore, based on the following two response limiting criteria, for bottom-up fatigue cracking and rutting, respectively:

- Horizontal tensile strain at the bottom of the lowest HMA layer ( $\epsilon_t$ ):  $\leq 70 \mu\epsilon$   
(bottom-up fatigue cracking)
- Vertical compressive strain on the top of subgrade ( $\epsilon_v$ ):  $\leq 200 \mu\epsilon$   
(rutting)

A PP structure meeting these strain response criteria is considered to be structurally adequate both in terms of fatigue cracking (bottom-up) and full-depth rutting. Otherwise, the layer thicknesses and/or material properties would need to be modified for compliance.

The Texas PP structural section that was devised based on the PP concept developed by the Asphalt Institute is shown in [Figure 2-1](#), including the material-layer type and the proposed minimum layer thicknesses ([TxDOT, 2001](#); [APA, 2002](#); [Walubita and Scullion, 2007](#)). The definitions and functional characteristics of each layer are discussed in the subsequent text.

| Layer Designation, Materials, and Functions |                                      |                        |  |  | Thickness<br>(inches) |
|---|--------------------------------------|------------------------|--|--|-----------------------|
| Layer 1                                     | PFC<br>(SS3231)                      | Porous Friction Course |  | Sacrificial layer                        | 1.0 – 1.5             |
| Layer 2                                     | HDSMA<br>(SS3248)                    | Heavy-Duty<br>SMA      | 1/2" Aggregate + PG 76-XX  | Impermeable<br>load carrying<br>layer    | 2.0 – 3.0             |
| Layer 3                                     | SFHMAC<br>(SS3249)                   | Stone-Filled<br>HMAC   | 3/4" Aggregate + PG 76-XX  | Transitional layer                       | 2.0 – 3.0             |
| Layer 4                                     | SFHMAC<br>(SS3248)                   | Stone-Filled<br>HMAC   | 1.0-1.5" Aggregate + PG 76-XX  | Stiff load carrying<br>layer             | 8.0 - Variable        |
| Layer 5                                     | Superpave<br>(SS3248)                | Superpave<br>(RBL)     | 1/2" Aggregate + PG 64-XX<br>(Target lab density=98%)                      | Stress relieving<br>impermeable<br>layer | 2.0 – 4.0             |
| Layer 6                                     | Stiff base or stabilized<br>subgrade |                        | Construction working table or compaction platform<br>for succeeding layers |  | 6.0-8.0               |
| Subgrade                                    |                                      |                        |  |  | ∞                     |

**Figure 2-1. A Typical Texas PP Structural Section.**

In [Figure 2-1](#), SMA stands for stone matrix (or mastic) asphalt, HMAC for hot-mix asphalt concrete, RBL for rich bottom layer, and PG for performance grade. SF, HD, SS, and PFC stand for stone-filled, heavy-duty, special specification, and porous friction course, respectively. The preceding number in front of the term aggregate such as ½ inch, ¾ inch, 1 inch, and 1.5 inch refers to the NMAS in inches. For the PG asphalt-binder, the double X (i.e., XX) refers to the lower PG temperature grade (°C) of the asphalt-binder, e.g., -22, -28, etc., ([AI, 1996](#)).

In [Figure 2-1](#), layers 1 (PFC) and 2 (SMA) are intended to improve the resistance to oxidation/weathering, thermal cracking, rutting, and permeation. A PFC surface further improves drainage and safety by reducing splash/spray and hydroplaning potential. In particular, SMAs (about 2- to 3-inches thick) provide very good stone-on-stone contact with generally high stiffness values (i.e., modulus greater than 500 ksi at 77 °F). The PFC, typically 1.0- to 1.5-inches thick, is optional in the current Texas PP design criteria but is generally provided to reduce traffic noise and improve the pavement surface drainage characteristics.

Layer 4 represents the main structural load-carrying and stiff rut-resistant layer with a minimum thickness of 8 inches to ensure adequate structural capacity in terms of the load spreading capability. A 1-inch NMAAS HMA mix is typically used for this layer. Layer 5 represents the flexible and typically high asphalt-binder content fatigue-resistant layer, i.e., 2.0 to 4.0 inches in thickness. Because of its characteristically high asphalt-binder content, Layer 5 is generally referred to as the Rich-Bottom Layer denoted as RBL. Layer 3 is a transitional load-carrying layer, also composed of a SFHMAC mix with a NMAAS of around  $\frac{3}{4}$  inch.

Layer 6 (typically about 6 to 8 inches thick) and the subgrade provide the working platform and pavement foundation, respectively. Layer 6, in fact, constitutes the base, often 8 inches thick and composed of treated subgrade material, typically about 3.0 to 6.0 percent lime treatment (added in liquid slurry form). However, cement treatment (about 2.0 percent) has also been utilized on one of the Texas PP projects.

According to [Figure 2-1](#), the total minimum HMA layer thickness is 14 inches, with the main structural loading carrying layer (the RRL) comprising 57 percent of the total HMA layer thickness. These total HMA layer thicknesses and mixture types are considered structurally necessary to mitigate the two major structural distresses of rutting and bottom-up fatigue cracking based on the general PP design concept ([APA, 2002](#)).

## THE EXISTING IN-SERVICE PP STRUCTURES

To date, there are 10 PP sections in-service constructed since 2001 in four Texas districts, namely:

- |                |                          |
|----------------|--------------------------|
| 1) Fort Worth  | 2 sections on SH 114,    |
| 2) Laredo      | 4 sections on IH 35,     |
| 3) San Antonio | 2 sections on IH 35, and |
| 4) Waco        | 2 sections on IH 35.     |

[Table 2-1](#) provides a summary of the PP structural sections in terms of the design materials and layer thicknesses. Full layer thickness details for each PP section are included in [Appendix A](#).

**Table 2-1. In-Service Texas PP Structural Sections.**

| Layer#                                | Material              | Average PP Layer Thickness (Inches) |                     |                |                     |              | Overall Average |
|---------------------------------------|-----------------------|-------------------------------------|---------------------|----------------|---------------------|--------------|-----------------|
|                                       |                       | Design Spec                         | Fort Worth (SH 114) | Laredo (IH 35) | San Antonio (IH 35) | Waco (IH 35) |                 |
| 1                                     | PFC (Optional)        | 1.0-1.5                             | -                   | -              | 1.5                 | 1.5          | 1.5             |
| 2                                     | SMA                   | 2.0-3.0                             | 2.0                 | 3.0            | 2.0                 | 3.0          | 3.0             |
| 3                                     | ¾-inch SF (or Type C) | 2.0-3.0                             | 3.0                 | 3.0            | 3.0                 | 3.0          | 3.0             |
| 4                                     | 1-inch SF (or Type B) | ≥ 8.0                               | 13.0                | 9.0            | 12.0                | 11.0         | 10.5            |
| 5                                     | RBL                   | 2.0-3.0                             | 4.0                 | 3.0            | 4.0                 | 4.0          | 4.0             |
| 6                                     | Base                  | 6.0-8.0                             | 8.0                 | 8.0            | 7.0                 | 11.0         | 8.0             |
| Subgrade                              |                       | Natural in situ soil material       |                     |                |                     |              |                 |
| Total HMA thickness (Inches)          |                       | ≥ 14.0                              | 22.0                | 20.0           | 21.5                | 22.5         | 22.0            |
| Total PP structure thickness (Inches) |                       | ≥ 20.0                              | 30.0                | 28.0           | 29.5                | 30.5         | 30.0            |

Clearly, [Table 2-1](#) shows that the majority of these PP structures are conservatively thicker than the minimum proposed in [Figure 2-1](#), with a total HMA layer and base thicknesses averaging 22 and 8 inches, respectively. Thus, a typical in-service Texas PP structure is about 30 inches total thickness, comparatively more conservative than the design proposal in [Figure 2-1](#), particularly for the 1-inch SFHMA layer.

### Project Location Details

[Table 2-2](#) provides a summary of the project location details in terms of the road mile-marker posts (TRM) and GPS coordinates. A map layout of the projects is shown in [Figure 2-2](#). Full details of the project locations including geographical limits and elevations are included in [Appendix A](#).



**Table 2-2. Project TRM and GPS Location Details.**

| #                     | Hwy       | CSJ#        | District<br>(County)   | TRM Location |  | GPS Location                   |                                | Length<br>(mile) |
|-----------------------|-----------|-------------|------------------------|--------------|--|--------------------------------|--------------------------------|------------------|
|                       |           |             |                        | Begin        | End                                      | Start                          | End                            |                  |
| 1                     | IH 35     | 0018-05-062 | Laredo<br>(Webb)       | 08+0.403     | 13+0.828                                 | N 27° 37.131'<br>W 99° 29.492' | N 27° 41.421'<br>W 99° 27.581' | 6.000            |
| 2                     | IH 35     | 0018-02-049 | Laredo<br>(La Salle)   | 49+0.431     | 53+0.427                                 | N 28° 11.242'<br>W 99° 18.785' | N 28° 14.629'<br>W 99° 17.722' | 4.000            |
| 3                     | IH 35     | 0018-01-063 | Laredo<br>(La Salle)   | 58+0.000     | 65+0.362                                 | N 28° 18.366'<br>W 99° 16.392' | N 28° 24.578'<br>W 99° 15.265' | 7.362            |
| 4                     | IH 35     | 0017-08-067 | Laredo<br>(La Salle)   | 69+0.439     | 74+0.003                                 | N 28° 27.708'<br>W 99° 13.939' | N 28° 31.544'<br>W 99° 12.786' | 5.442            |
| 5                     | IH 35     | 0016-04-091 | San Antonio<br>(Comal) | 188+0.774    | 190+0.368                                | N 29° 41.850'<br>W 98° 05.841' | N 29° 44.163'<br>W 98° 04.207' | 1.740            |
| 6                     | IH 35     | 0016-04-094 | San Antonio<br>(Comal) | 190+0.368    | 191+1.015                                | N 29° 43.084'<br>W 98° 05.296' | N 29° 44.163'<br>W 98° 04.207' | 1.300            |
| 7                     | IH 35     | 0015-01-164 | Waco<br>(McLennan)     | 340+0.052    | 342+0.622                                | N 31° 37.096'<br>W 97° 05.974' | N 33° 39.017'<br>W 97° 06.034' | 2.200            |
| 8                     | IH 35     | 0048-09-023 | Waco<br>(Hill)         | 368+0.724    | IH35E:<br>371+0.916<br>IH35W:<br>1+0.238 | N 32° 01.152'<br>W 97° 05.728' | N 32° 03.868'<br>W 97° 05.869' | 3.250            |
| 9                     | SH<br>114 | 0353-01-026 | Fort Worth<br>(Wise)   | 580+0.804    | 583+0.500                                | N 33° 02.203'<br>W 97° 25.730' | N 33° 02.192'<br>W 97° 23.996' | 2.200            |
| 10                    | SH<br>114 | 0353-01-026 | Fort Worth<br>(Wise)   | 583+0.500    | 586+0.200                                | N 33° 02.192'<br>W 97° 23.996' | N 33° 02.169'<br>W 97° 23.542' | 1.740            |
| Average length (mile) |           |             |                        |              |  |                                |                                | 3.5              |

**Project legend:** #1 = Price, #2 = Zumwalt02 (ZMW02), #3 = Gilbert, #4 = Zumwalt01 (ZMW01), #5 = San Antonio, #6 = New Braunfels, #7 = McLennan, #8 = Hillsboro, #9 = Fort Worth 01, & #10 = Fort Worth 02.

Figure 2-2 shows that all but two (numbers 9 and 10 on State Highway SH 114) of the Texas PP sections have been constructed on IH 35, the primary north-south highway in Texas. However, sections on both IH 35 and SH 114 had a 20-year traffic design estimate of over 30 million ESALs (18 kips).

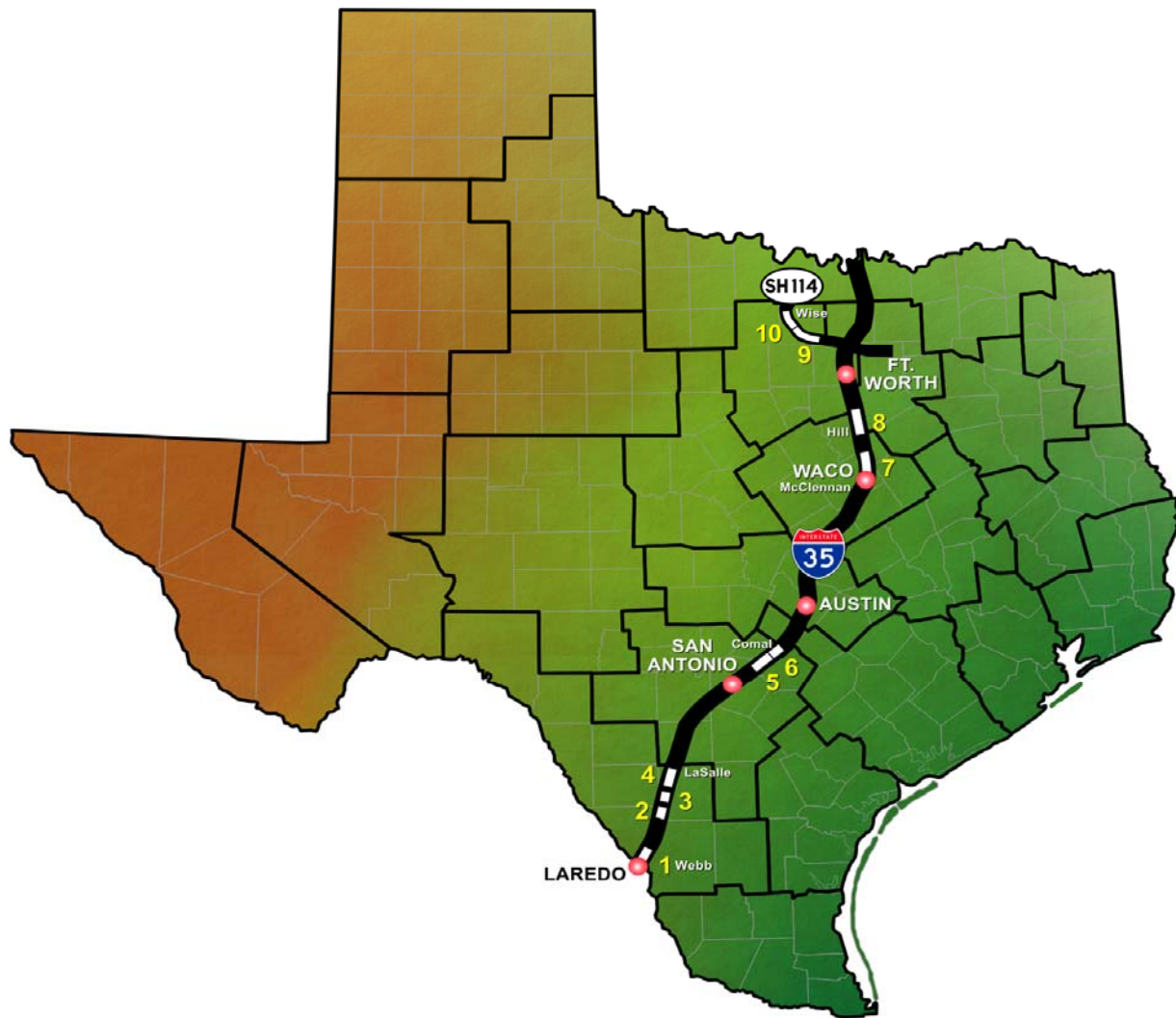


**Figure 2-2. Map of Texas and PP Project Locations (Projects #1-10).**

### **Traffic Design Data and Environment**

The average traffic design data that were used for the current existing PP sections are summarized in [Table 2-3](#). Full traffic design data for each PP section are included in [Appendix A](#). As mentioned previously, the Texas PP concept was formulated for highways where the 20-year 18 kips estimate is over 30 million ESALs, which is consistent with the average numbers shown in [Table 2-3](#). Note, however, that some of these PP sections, in particular those on IH 35, had as much as 75 million design 18-kip ESALs with the truck percentage as high as 46 percent and up to a total of 8 lanes; see [Appendix A](#).

**Table 2-3. Traffic Design Data.**

| <b>Item</b>  | <b>Average</b>           |
|--|--------------------------|
| Average begin ADT                                  | 29, 155                  |
| Average end ADT (after 20 years)                   | 40, 390                  |
| Average traffic growth rate (percent)              | 3.0                      |
| Average 20-year design 18 kips ESALs (million)     | 30                       |
| Average percentage of trucks (percent)             | 28                       |
| Average PP sectional length (mile)                 | 3.5                      |
| Minimum number of lanes (both directions)          | ≥ 4                      |
| Average lane width (ft)                            | 12                       |
| Average shoulder width (ft)                        | 10                       |
| Average speed limit (mph)                          | 70                       |
| Highways where PP structures have been constructed | IH 35 (8) and SH 114 (2) |

The typical design life of perpetual pavements is 50 years (APA, 2002). For conventional flexible HMA pavements, the typical design life is 20 years. Although designed for 50 years, the engineering expectation is that at least one minor surface renewal (such as an overlay) for restoration of functional characteristics (among others) will be required within or at the end of a PP's first 20 years of service. An 18-kip axle load is typically used as the design load when evaluating the 70 and 200  $\mu\epsilon$  endurance limits at the bottom of the lowest HMA layer and on top of the subgrade, respectively. However, some countries such as Israel, due to extraordinary heavier truck loads, use 29 kips as the design ESAL (Sidess and Uzan, 2008).

Based on Figure 2-2, several (projects 1 thru 4) of the Texas PP sections are located in the dry-warm regions where subgrade or base moisture problems are not expected. However, Waco (projects 7 and 8) and Fort Worth (projects 9 and 10) fall within the moderate to wet-cold environmental zones. Therefore, the potential for moisture related problems exists for the PP projects located in these areas. Projects 5 thru 8 are on highly plastic soils, so swelling soil damage is a possibility.

## PP MATERIALS AND MIX-DESIGNS

Table 2-4 summarizes the typical mix-designs and material characteristics that have been used on the 10 Texas PP structures (in-service).

**Table 2-4. In-Service Typical Mix-Designs and Material Characteristics.**

| Layer#                | Mix/Material                 | Average In-Service Typical Material Characteristics   |
|-----------------------|------------------------------|---|
| Layer 1<br>(Optional) | PFC                          | 6.0-6.1%PG 76-22S + 0.0-1.0% lime + 0.3-0.4% cellulose fibers + igneous/limestone aggregates (19 mm NMAS open-graded) (Avg OAC = 6.0%)  |
| Layer 2               | SMA                          | 5.9-6.8% PG 76-22S + 5.0-11.0% mineral filler + 0.0-1.5% lime + 0.0-0.4% cellulose fibers + 0.0-4.5% fly ash + igneous/limestone aggregates (12.5 mm NMAS gap-grade) (Avg OAC = 6.0%) |
| Layer 3               | ¾-inch SF<br>(HMAC)          | 4.2-5.2% PG 76-22 + 0.0-1.5% lime + 0.0-1.0% anti-strip + limestone aggregates (19 mm NMAS dense to coarse graded) (Avg OAC = 4.4%)   |
| Layer 4               | 1-inch SF<br>(HMAC)<br>(RRL) | 4.0-4.5% PG 70-22 + 0.0-1.5% lime + 0.0-0.5% anti-strip + limestone (25 mm NMAS coarse-graded with low fines) (Avg OAC = 4.2%)  |
| Layer 5               | RBL                          | 4.2-6.1% PG 64-22 + 0.0-1.5% lime + 0.0-0.5% anti-strip + limestone aggregates (12.5 mm NMAS dense-graded) (Avg OAC = 5.4%)   |
| Layer 6               | Base                         | Cement ( 2.0%) or lime (3.0 to 6.0%) treated subgrade soil materials (lime is typically added in liquid slurry form)  |
| Subgrade              |                              | Compacted natural in-situ soil material   |

Legend: Avg = average; OAC = optimum asphalt content

### Asphalt-Binders

In contrast to the recommendations in Figure 2-1, Table 2-4 shows that most of the existing 1-inch SFHMAC mixes (layers) used an average of 4.2 percent PG 70-22 asphalt-binder instead of a PG 76-grade. This was partly on account of workability and cost related issues as PG 70-22 is relatively cheaper and more workable than PG 76-22. PG 76-22 is a comparatively stiffer asphalt-binder, often modified with about 5 percent styrene-butadiene-styrene (SBS).

Anti-stripping agents (in the order of 0.5 to 1.0 percent) and hydrated lime (in the range of 0.5 to 1.5 percent) are typically added to improve the HMA mixes' moisture damage-resistance characteristics. These additives are typically incorporated by percent weight of the total aggregate blend proportions, mostly to the aggregates and/or HMA mixes that are considered to be potentially susceptible to stripping and moisture damage.

## Aggregates

As can be seen in [Table 2-4](#), limestone was the most commonly used aggregate, and was used exclusively in all sections at the transitional layer and below. However, other aggregate types such as crushed gravel, granite, sandstone, and trap rock were also used on some in-service Texas PP sections, particularly those in the Laredo District. Although competitively cheaper and readily available in Texas compared to the other aggregate types, limestone was found to be problematic on some of the Texas PP projects in service. It is highly absorptive and thus, detrimentally reduces the net effective asphalt-binder content that is available for lubrication (during compaction), coating, and bonding with the aggregates. [Table 2-5](#) compares some of the limestone properties to that of crushed gravel.

**Table 2-5. Laboratory Comparison of Aggregate Properties.**

| Test Parameter                            | Limestone | Crushed Gravel | Threshold |
|---|-----------|----------------|-----------|
| Soundness (average)                       | 18        | 4              | ≤ 30      |
| LA abrasion (average)                     | 29        | 18             | ≤ 40      |
| Polish value (average)                    | 21        | 27             | -         |
| Aggregate bulk specific gravity (average) | 2.65      | 2.62           | -         |
| Water absorption capacity (WAC) (average) | 2.25%     | 1.17%          | ≤ 2.0%    |

In terms of soundness, LA abrasion, and WAC, it is clear from [Table 2-5](#) that the crushed gravel aggregate has superior properties but is usually more costly compared to limestone. Evidently, the limestone is more absorbent with a laboratory measured WAC value greater than 2.0 percent. Thus, the probability of the limestone absorbing some of the asphalt-binder is considerably higher. On one project (SH 114 in the Fort Worth District), the estimated asphalt-binder content (using the Troxler Ignition oven method) from a field core of the 1-inch SFHMAC layer using limestone aggregates was only 3.3 percent versus the 4.0 percent design, suggesting about 17 percent absorption (or loss) ([Walubita and Scullion, 2007](#)). This ultimately may have a negative impact on the performance of the 1-inch SFHMAC layer and the whole PP structure.

Researchers (Zhou et al., 2006) proposed WAC thresholds as follows: (1) high absorption:  $WAC > 2.0$  percent; (2) intermediate absorption:  $1.0 \text{ percent} \leq WAC \leq 2.0$  percent; and (3) low absorption:  $WAC < 1.0$  percent. The results in Table 2-5 indicate that the limestone aggregate falls within the high absorption category, with a WAC value greater than 2.0 percent.

### **The PFC, SMA, ¾-inch SFHMAC, and RBL Mix-Designs**

As indicated in Table 2-4, the PFC is optional in the current Texas PP design, and is not considered a structural component. It may be included as a functional component to enhance the skid resistance or reduce splash/spray effects during wet weather. As of summer 2009, only four out of the 10 in service Texas PP sections had actually utilized a surfacing PFC mix. Like the PFC, the SMA and RBL mix designs were found to be reasonably satisfactory. However, the mix design for the coarse-graded ¾ inch SFHMAC showed potential for further optimization to improve both the workability and other material characteristic properties such as durability and cracking resistance by increasing the asphalt-binder content and the fine aggregate content.

### **The 1-inch SFHMAC Mix-Design**

As will be discussed in the subsequent chapters of this report, the 1-inch SFHMAC mix-design was found to be very problematic, associated with workability and constructability related-problems among others. Workability and compactability problems were also experienced in the laboratory with these mixes during sample fabrication. This was primarily attributed to the moderately low asphalt-binder content (about 4.2 percent) and coarser aggregate gradation with low fines content. Recommendations for mix-design improvements were made and are discussed subsequently in this report. Note that the 1 inch SFMAC was primarily designed as the main load bearing layer with an expected high resistance to rutting, and thus, the coarse aggregate gradation.

Figure 2-3 shows some examples of the 1 inch SFHMAC coarse gradations and the resulting coarse surface texture. The current in-service mixes have a percent passing the No. 8 sieve ranging from 19.0 to 26.8 percent with an average of 23.3 percent thus meeting the No. 8 gradation requirement (Walubita and Scullion, 2007).

The aggregate blend proportions typically consist of a higher percentage of the coarser rock, an average of about 40 percent ( $\geq 3/4$ -inch NMAS rock), and a relatively lower percentage of the fine, an average of around 23 percent ( $\leq$  No. 4 NMAS mostly screenings or sand). On average, the combined aggregate gradation consists of about 13.3 percent retained on the number  $3/4$  inch sieve, with a design range of 10.0 percent to 20.0 percent.

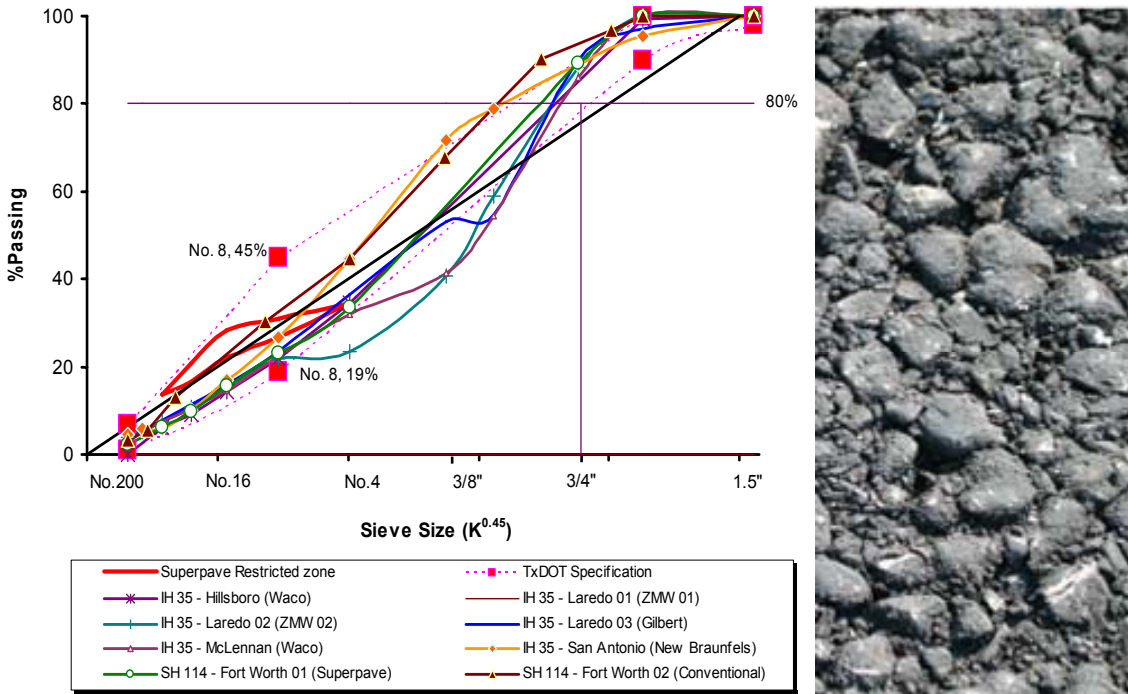


**Figure 2-3. The 1-inch SF Coarse Aggregate Gradations and Coarse Surface Texture.**

The greater proportion of the coarser rock or bigger stones, combined with lower percentages of mid-sized fractions, is one of the reasons these mixes are often referred to as the Stone-Fill (or stone filled) HMA mixes.

### The Base and Subgrade Materials

For most of the existing Texas PP sections, the base consists of 3 to 6 percent lime stabilization of the subgrade soil material, added as slurry, with an average treatment depth of 8 inches. On one project (IH 35, Zumwalt02 in Laredo), 2 percent cement treatment was used to treat the existing material, which constituted the base. Results from both lime and cement treatments are satisfactory, yielding stiff non-moisture susceptible bases.

However, localized heaving and swelling problems were experienced with the sulfate-rich clay soils on the Hillsboro project in the Waco District. Upon hydration in the presence of water, the lime (or Calcium Oxide [CaO]) chemically reacts with sulfates in the clay soil to produce a swelling and highly expansive mineral compound called ettringite and/or thaumasite, typically causing bumps or swells in the pavement structure. The speed of swelling activity is related to the fineness of the sulfate compounds and the availability of water. A short section approximately 300-ft long was replaced on the Hillsboro project during construction because of sulfate heave problems. No subsequent problems have been found.

## **SUMMARY**

The main points from this chapter are summarized as follows:

- The general PP design philosophy is to mitigate rutting and bottom-up fatigue cracking in pavement structures by minimizing the horizontal tensile strains ( $\leq 70 \mu\epsilon$ ) and compressive strains ( $\leq 200 \mu\epsilon$ ) in the lowest HMA layer and top of the subgrade, respectively. Structural design life of up to 50 years is postulated.
- The Texas PP design theory was conceptualized based on the Asphalt Institute PP design philosophy for highways with a minimum 20-year 18-kip ESAL projection of 30 million and a total structural design thickness of about 20 inches (at least 14-inch thickness of HMA and minimum 6-inch thick base).
- The average structural thickness for the 10 existing PP structures is 30 inches (22-inch thick HMA and 8-inches thick base), which is conservatively thicker than the proposed design concept.
- With respect to materials and mix-designs, limestone was the most preferred aggregate, primarily for economical reasons and local availability. The main load-bearing layer (the 1-inch SFHMAC) was intentionally designed with a coarse aggregate gradation and moderately low asphalt-binder content to contribute to its rutting resistance properties; however, these mix-design characteristics tended to compromise the mix's workability and constructability properties.



- The Texas PP base material is typically 3 to 6 percent lime treated subgrade soil. Cement (2 percent) treatment was also used on one project; all projects show satisfactory base stabilization results. Localized heaving and swelling problems were, however, encountered in the Waco District, where the clay soils contain some sulfates that are prone to swelling/expansion in the presence of hydrating calcium-based stabilizers.



## **CHAPTER 3**

### **PP CONSTRUCTION AND LESSONS LEARNED**

This chapter discusses construction and quality issues related to the Texas PP structures. In particular, focus was on the evaluation of the workability and compactability aspects of the stone-fill mixes that serve as the main structural load-carrying layers. A summary is then presented at the end of the chapter to highlight the lessons learned and the remedial measures taken thereof including providing recommendations on the future construction of perpetual pavements in Texas.

#### **SUBGRADE AND BASE STABILIZATION**

Subgrade soil compositions vary widely throughout Texas, ranging from highly plastic clays to low plasticity index (PI) silts and sands. With the exception of West Texas, most districts prefer to treat the subgrade with calcium-based stabilizers to either provide a stable working platform to allow compaction of subsequent layers, or to permanently stabilize the upper subgrade to provide a moisture-resistant structural layer. A permanently stabilized soil layer constitutes the base layer for most Texas PP sections to date. Lime (3 to 6 percent) or cement (2 percent) was applied directly to the subgrade (in some cases to recycled base material), taking PI, sulfate content, and organic content into consideration ([Scullion and Hilbrich, 2004](#)).

To date, satisfactory results have been obtained with both lime and cement stabilization yielding stiff non-moisture susceptible base layers. [Figure 3-1](#) shows an example of lime stabilization with a treatment depth of up to 8 inches on SH 114 ([Walubita and Scullion, 2007](#)). The lime dosage was 6 percent by dry weight, added in a liquid form as slurry, so as to optimize the stabilization process.



**Figure 3-1. Lime Treatment Process on SH 114.**

As shown in [Figure 3-2](#) (from subsequent field coring), the 6 percent lime treatment provided a highly bound stable foundation, i.e., stiff non-moisture susceptible layer. The stabilized subgrade material was cored in an intact state with no deterioration, which is unusual for a lime-treated layer ([Walubita and Scullion, 2007](#)).



**Figure 3-2. Field-Extracted Base Core from SH 114.**

However, there were some localized problems of heaving and swelling on one of the Texas PP projects on IH 35 in the Waco District where the lime stabilization reacted with the minerals in the subgrade soil. The subgrade soil (clay) material in this area contains sulfates. The hydration of the lime (or Calcium Oxide [CaO]) chemically reacts with sulfates in the clay soil to produce a swelling and highly expansive mineral compound called ettringite and/or thaumasite.

## **HMA PLACEMENT AND QUALITY CONTROL ISSUES**

With the exception of the PFC at 80 percent and the RBL at 97 percent, the targeted density for all the HMA mixes was 96 percent. The high in-situ AV (20 percent) for the PFC is necessary for desired surface drainability. The low in-situ AV (3 percent) of the RBL contributes to this layer's fatigue-cracking resistance, durability, and impermeability properties. At 96 percent in-place density, the recommended compacted lift thickness for the thicker RRL ( $\geq 8$  inches thick) with the 1-inch SFHMAC mix was 3 to 5 inches. The mat placement temperature generally varied between 260 and 300 °F depending on the asphalt-binder type, typically 260 °F for mixes with PG 64-22, 275 °F for mixes with PG 70-22, and 300 °F for HMA mixes with PG 76-22 (TxDOT, 2004).

While no major problems were experienced with the other HMA mixes, constructability problems and quality issues were experienced with the SFHMA mixes, i.e., workability and compactability issues. Due to their coarseness (with low fines) and moderately low asphalt-binder content (compounded by absorptive limestone aggregates in some instances), the SFHMAC mixes were found difficult to work with and difficult to attain the target in-place density. The following sections summarize some of the field observations and experiences together with some remedial measures undertaken and recommendations made to mitigate these undesirable characteristics.

### **Material Transfer Device (MTD) and IR Thermal Imaging**

Use of the belly-dump trucks and windrow elevator (i.e., windrow pick-up system) as the MTD was observed to be less effective than the Roadtec® in eliminating thermal segregation in the HMA mat during either the cold (winter) or hot (summer) weather placement. The Roadtec, with its internal remixing capability, was observed to yield a more consistent mix with greater temperature uniformity. Thus, the Roadtec or equivalent MTD would be preferred for future jobs. [Figure 3-3](#) shows a comparative example of the Infra-Red thermal profiles on SH 114, for a target HMA mat placement temperature of 300 °F.

[Figure 3-3](#) shows the surface temperature profiles for the full lane width (12 ft) of new HMA mats. With respect to the thermal color coding scheme, red represents HMA mat temperatures near 300 °F, the target mat temperature; green represents mat temperatures between 235 and 270 °F, and blue represents mat temperatures less than 235 °F.



**Figure 3-3. Comparison of MTDs and HMA Mat Temperature Profiles on SH 114 (Red  $\cong$  300 °F [Good], 235 °F  $\leq$  Green  $\leq$  270 °F, Blue  $\cong$  220 °F [Thermal Segregation]).**

Blue is generally the undesired color as it often represents thermally segregated cold spots with poor compaction properties. Solid red throughout is the ideal and desired color, representing high temperature uniformity at the appropriate compaction temperature. As shown in Figure 3-3, the target mat placement temperature was hardly attained nor was it uniform using the windrow pick-up MTD system. There are intermittent sections of green coloring and blue spots representing thermal segregation with mat temperatures below 270 °F. Clearly, the Roadtec MTD system exhibits a greater potential to place a more uniform mat minimizing mechanical and thermal segregation.

It was also noted that the intermittent blue cold spots observed in the IR thermal profiles in Figure 3-3 coincided with end of HMA delivery truck loads and paver stoppages. Thus, it is important to ensure pavers are supplied with sufficient mix at uniform temperature to allow continuous, uninterrupted operations. On the same basis, it would be highly desirable to have a smooth placement/compaction operation with minimal paver stoppages. These thermal variations could negatively impact the compaction operation, which could ultimately lead to non-uniformity in the target compaction thickness, variations in the in-place density, and appearance of other defects such as bumps in the completed mat.

### Compacted Lift Thickness

Compacting at the lower end of the allowable lift thickness range ( ~3 inches) was observed to yield a more constructible mix as gauged by attaining the target in-place density and layer interface bonding than using thicker lifts. Additionally, this also required less compactive effort in terms of the rolling pattern and number of passes. Compacting at a greater lift thickness tended to cause the mixes to segregate vertically, creating highly voided areas capable of detrimentally trapping moisture. [Figure 3-4](#) shows a comparative illustration of the compacted lift thickness for the 1-inch SFHMA layer.



**Figure 3-4. Effects of the Compacted Lift Thickness for the 1-inch SFHMA Layer.**

Clearly, [Figure 3-4](#) shows better construction quality for the 3- and 4-inch layer lift-thickness (#1, #8, and #3) with no visual evidence of vertical segregation, honey combining, or debonding. Also, the measured AV at 7.3 percent was fairly reasonable as opposed to about 12.6 percent for the 5-inch layer lift-thickness. Based on these observations, a 4-inch compacted lift thickness would thus be considered reasonable for these mixes (i.e., SFHMA compacted lift thickness  $\leq 4.0$  inches). Conjecture in the case of these SFHMA mixes is that the large angular aggregate particles do not receive sufficient compactive energy at the bottom of thicker lifts to promote adequate reorientation. This problem is exacerbated by the low asphalt-binder content that limits the effective lubrication to allow reorientation.

## Compaction and Rolling Pattern

On most of the projects, the rolling pattern was as follows: (1) breakdown roller – two vibratory passes (steel wheel); (2) intermediate roller – three passes pneumatic rollers; and (3) one vibratory pass plus one static (steel wheel) pass. However, one project (Zamwalt01) also used the pneumatic as the breakdown roller with satisfactory results. From Figure 3-5, it is apparent that the pneumatic roller appears to have helped the 1-inch SFHMA compaction; the GPR readings after the first mile are clean with no indication of serious subsurface anomalies or density variations in the HMA layers.

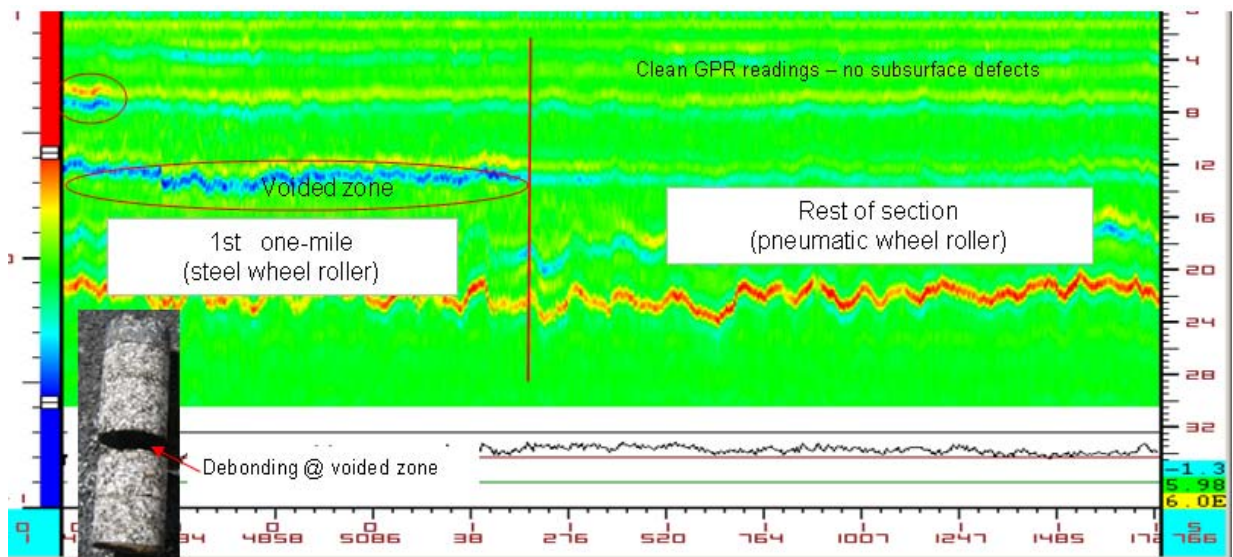


**Figure 3-5. Steel Wheel versus Pneumatic Breakdown Roller (IH 35 – Laredo).**

In terms of the GPR color coding scheme and data interpretation, green represents ideal GPR readings with no indication of potential subsurface defects, i.e., about zero voltage returned. A strong blue color signature within the GPR COLORMAP is indicative of high voided areas or low density spots within the pavement structure. A strong red-blue color stacking signature is indicative of moisture presence, i.e., the location where water is trapped is signified by a pattern of strong red color signature immediately underlain by a strong blue color signature in the GPR COLORMAP. So, blue spots and red-blue color stacking are undesired as they indicate subsurface anomalies.



As would be expected, applying more rolling passes tended to improve the SFHMA compaction and uniform density attainment. Figure 3-6 shows an example of a core and AV distribution where the compaction pattern was as follows: five vibratory and two static passes for the breakdown roller, eight pneumatic passes for the intermediate roller, and one vibratory pass plus one static pass for the finishing roller. Overall, a total of 17 rolling passes were applied on this section. As can be seen in Figure 3-6, the core from this section is intact with no visible defects; the AV distribution based on X-ray CT scanning is also fairly uniform, averaging 7 percent and for the most part is below 10 percent. Also, the GPR readings are clean with no indication of subsurface anomalies.

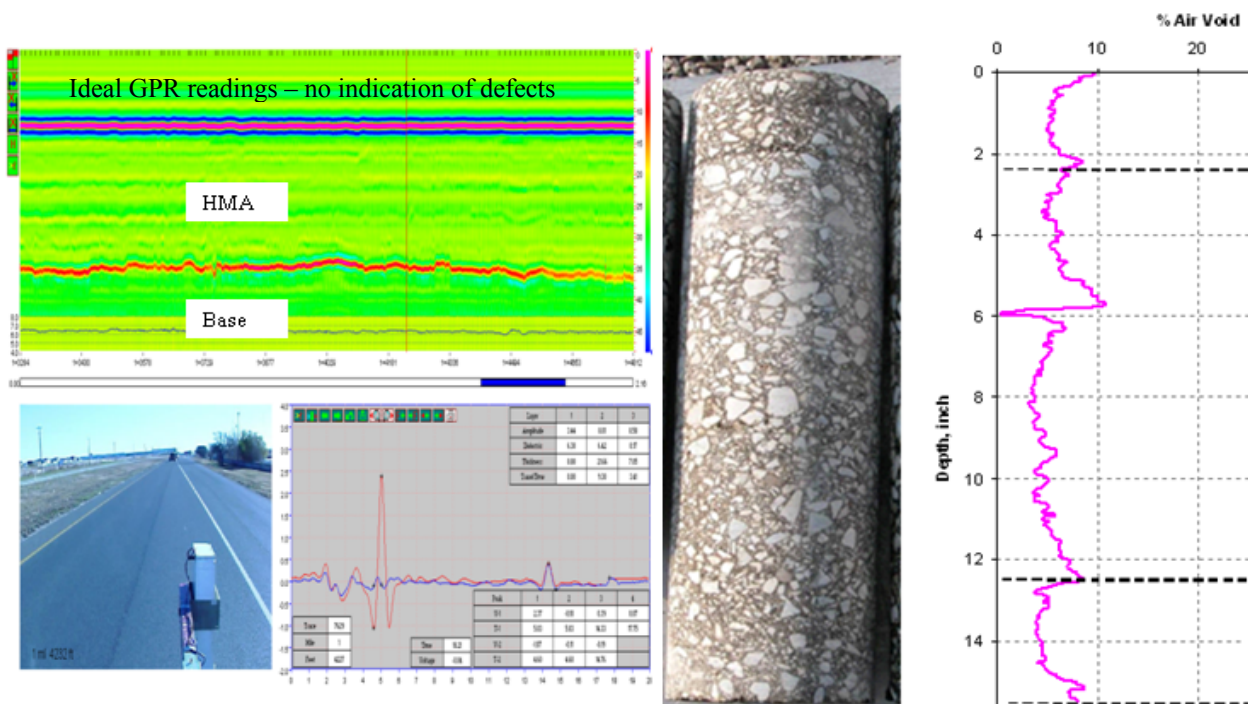


Figure 3-6. SH 114 Conventional – 17 Total Compaction Rolling Passes.

### In-Place Density Variations and Forensic Defects

Due to the poor constructability of the SFHMA mixes, the target in-place density was in most cases not attained, with an average of about 11.8 percent core AV versus the  $4\pm 1$  percent target. GPR testing indicated considerable variations in the HMA mat densities and presence of entrapped moisture on some projects. Forensic evaluations through coring indicated various subsurface defects such as high localized voided areas, vertical segregation, and debonding, particularly within the SFHMA layers.

Figures 3-7 through 3-10 show some examples of non-ideal GPR measurements and substandard cores. These forensic defects are undesirable as they pose a potential problem for both the PP structural integrity and moisture damage.

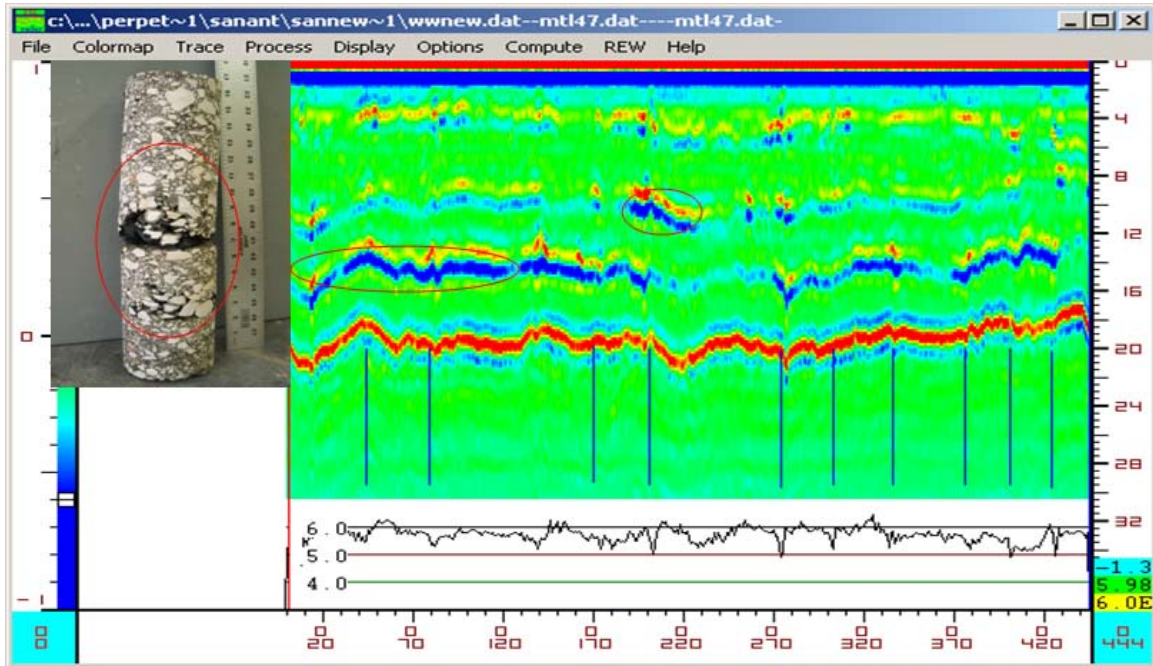


Figure 3-7. GPR Density Variations and Forensic Defects in Core (IH 35 San Antonio).



Figure 3-8. Substandard Cores from SH 114 and IH 35.

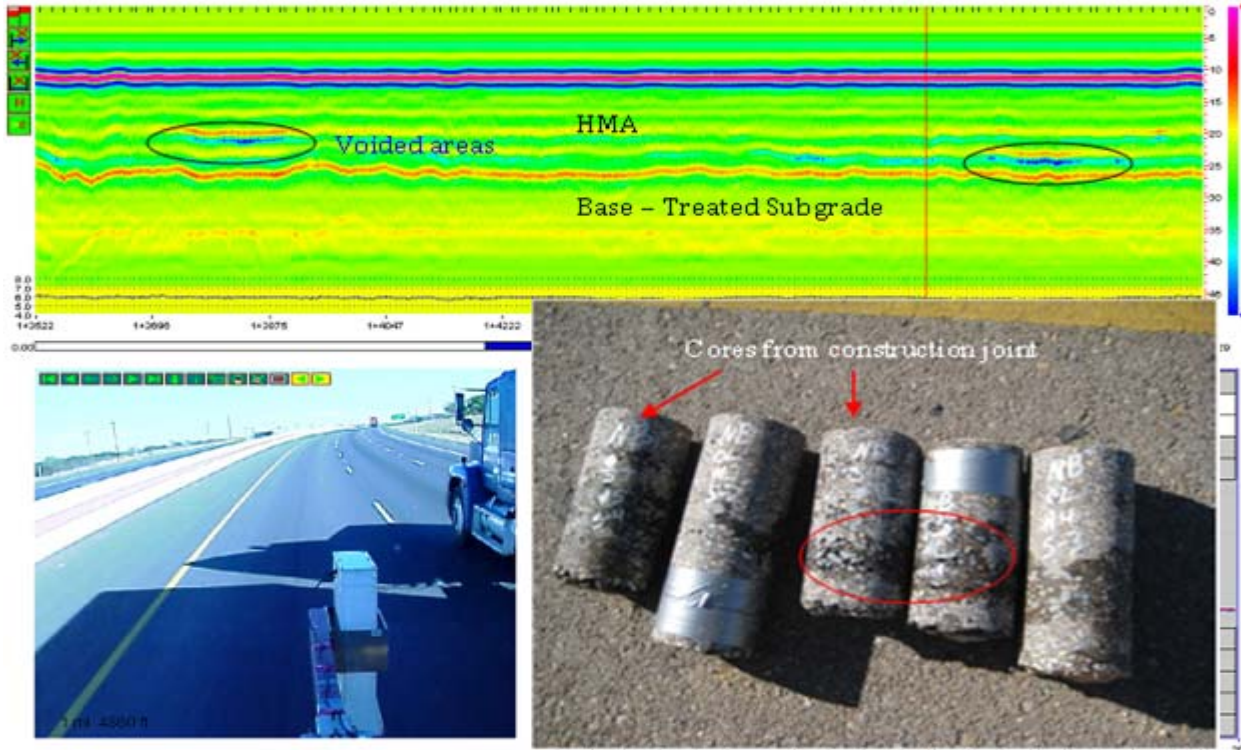


Figure 3-9. Localized Voided Areas and Segregation on IH 35 Price (NB, Laredo).

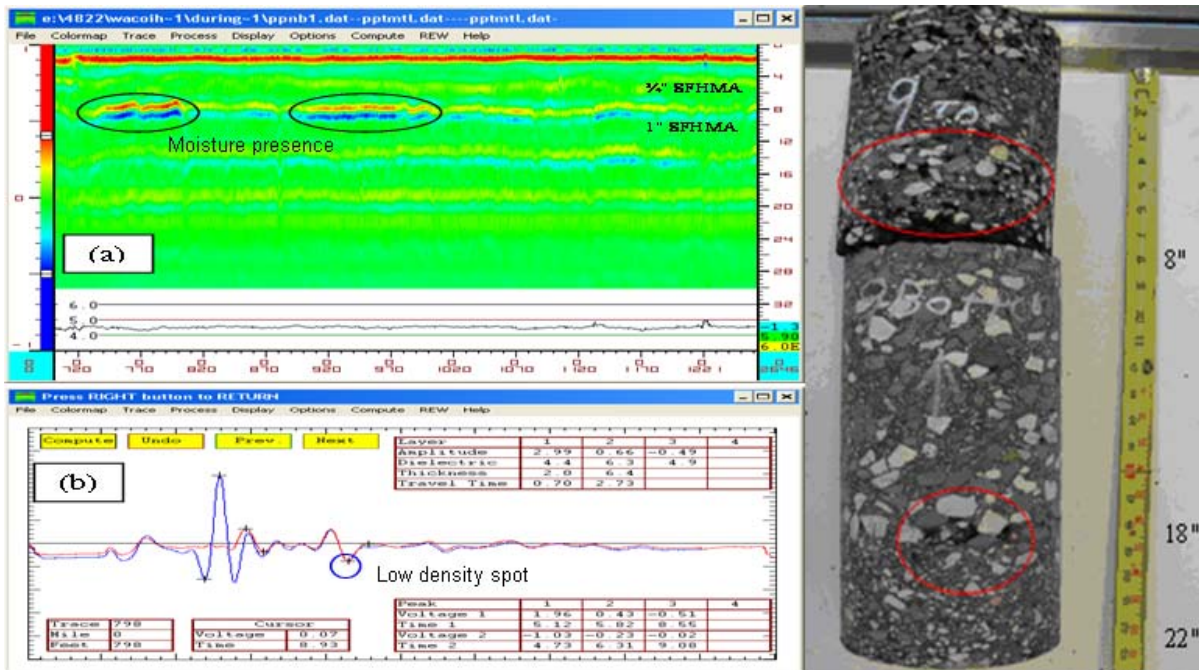
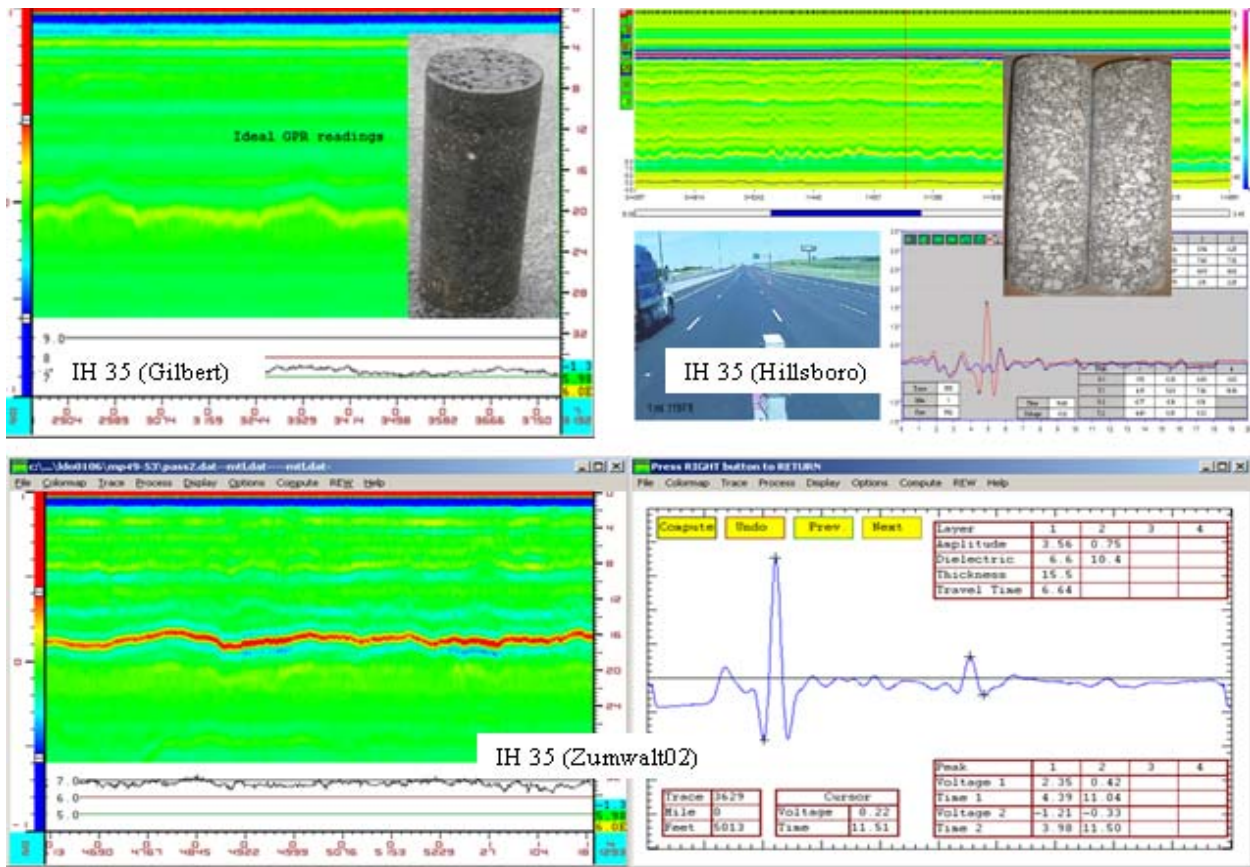


Figure 3-10. Evidence of Subsurface Defects/Moisture Presence on IH 35 (McLennan).

### Ideal GPR Readings with No Subsurface Defects

Despite the workability and compactability problems of the SFHMA mixes, construction quality was fairly satisfactory on some projects (or sections of the project), particularly those constructed at a later stage, such as the SH 114 (Conventional), IH 35 (Hillsboro), IH 35 (Zumwalt 01 and 02), IH 35 (Gilbert), and IH 35 (Price). Some examples of ideal GPR readings with no indication of subsurface defects are shown in [Figure 3-11](#).



**Figure 3-11. Examples of Ideal GPR Readings with No Subsurface Defects.**

In general, these projects exhibit some of the most uniformly well placed HMA of all the PP sections in Texas. Some notable construction changes on these projects aimed at improving the PP constructability included compacting the 1-inch SFHMA layer in 3 (Hillsboro) and 4 (Gilbert and Zumwalt02)-inch lift thicknesses as opposed to the construction specification of 5 inches. From [Figure 3-11](#), it is apparent that these construction changes appear to have yielded satisfactory compaction results.

On a comparative basis, greater constructability problems with the SFHMA mixes were experienced with the San Antonio projects on IH 35 and most of the earlier constructed PP sections. GPR readings and cores from these projects exhibited the severest subsurface anomalies in terms of forensic defects such as in-place density variations, voided areas, vertical segregation, and debonding. The best construction quality was observed with the SH 114 (Conventional) project in Fort Worth, where conventional dense-graded Type C and B mixes were used instead of the coarse-graded SFHMA mixes. IH 35 (Hillsboro) in Waco and the Laredo projects also exhibited fairly acceptable construction quality, especially considering that it was the first time the contractors were building perpetual pavements and placing the coarse-graded SFHMA mixes in Texas.

No major constructability or forensics defects were experienced with the other HMA layers/mixes. Overall, the RBL exhibited the best workability and compactability characteristics attributed to its dense aggregate gradation and high asphalt-binder content. No forensic defects were detected in this layer; the in-situ AV was fairly uniform, and the layer was impermeable.

## **CONSTRUCTION JOINT PROBLEMS**

Construction joint problems were experienced on some projects due to poor joint staggering, effects of trench construction, low density, and poor joint compaction on part of the contractor. Trench construction is the process of removing, then rebuilding the existing structure one lane width at a time, allowing little latitude for joint staggering or proper density control along the mat free edge. Furthermore, particles from the wall of the adjacent structure, worked loose by construction equipment, are free to fall in the trench contaminating the new mat. These problems resulted in open permeable construction joints that detrimentally allow moisture to infiltrate into the PP structure. GPR measurements along and within the vicinity of the construction joints detected the presence of both low density spots and moisture entrapment. [Figure 3-12](#) shows these results for IH 35 Price (Laredo). Based on these GPR measurements, recommendations were subsequently made to strip seal all the open joints to limit moisture infiltration; see [Figure 3-13](#).

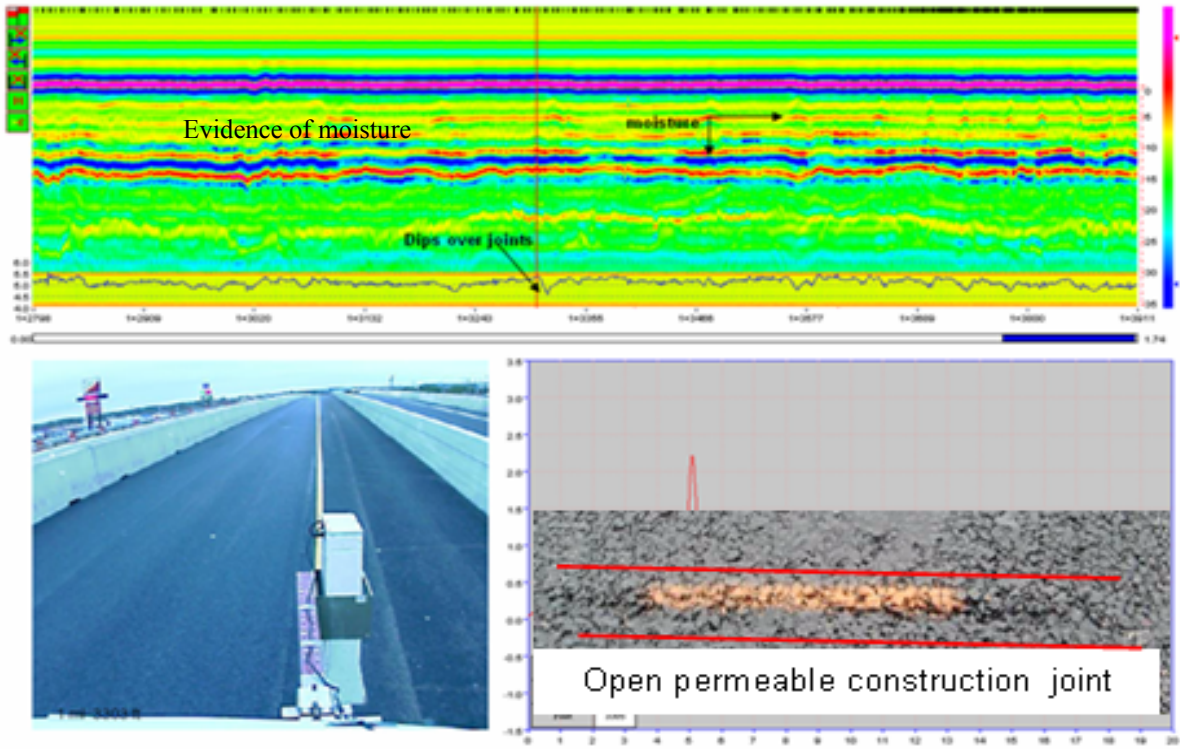


Figure 3-12a. Open Joint and Moisture Presence on IH 35 Price (Laredo, 2008).

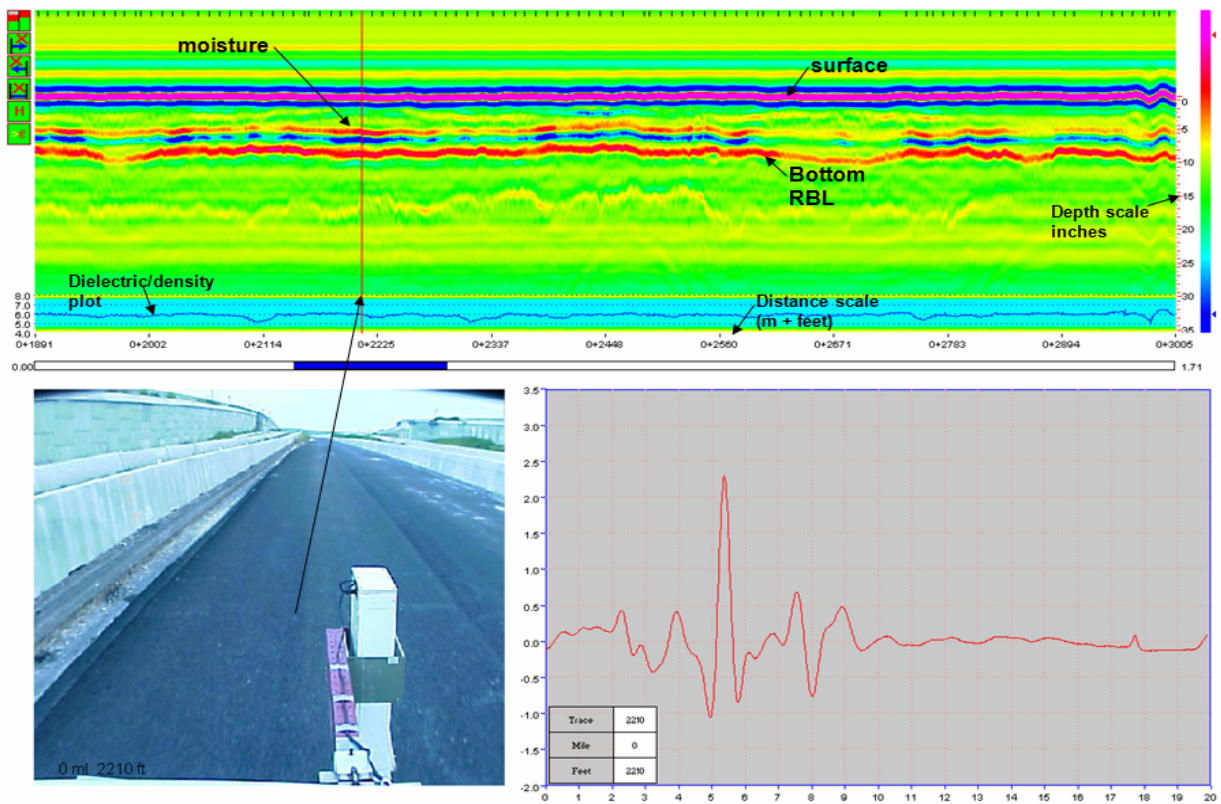
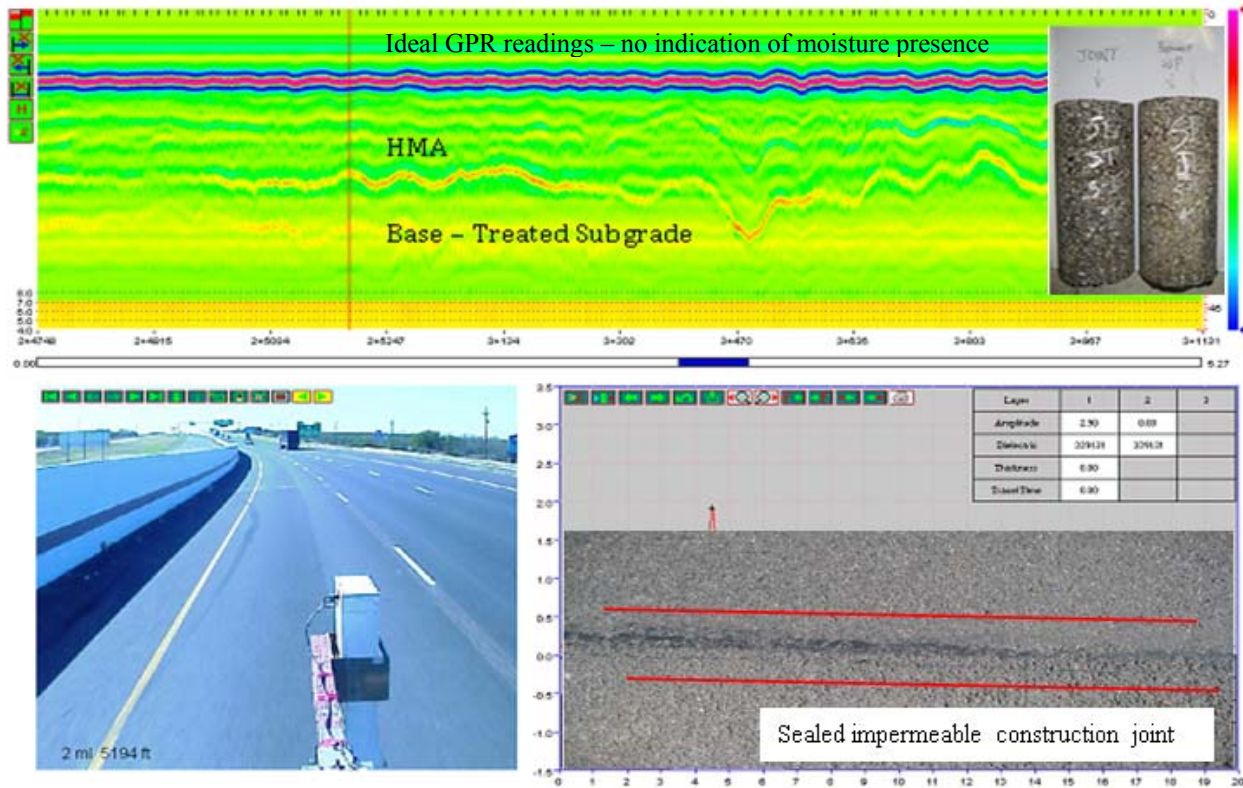


Figure 3-12b. Non-Ideal GPR Readings Indicating Moisture Presence on IH 35 (Price).



**Figure 3-13. Clean GPR Readings after Strip Sealing on IH 35 Price (Laredo, 2009).**

As can be seen in Figure 3-13, GPR measurements taken later in 2009 after the strip sealing operation did not detect any moisture presence in the vicinity of the construction joint, indicating that the sealing operation was satisfactory and that the joints were adequately sealed. Based on these observations, mitigation measures on future jobs should include better construction joint staggering, tighter enforcement of the joint compaction specification, and elimination of trench construction where possible.

### **CORING AND AV DISTRIBUTION**

X-ray CT scanning of the field-extracted cores was also conducted to characterize the core AV distribution as a function of depth. Scanning results indicated non-uniform distribution of the AV, particularly in the SFHMA layers. The AV content was found to be especially high and non-uniform in the 1-inch SFHMA layers indicating that these layers are highly permeable with potential for moisture entrapment, particularly considering that the bottom RBL is impermeable.

The AV content was generally found to be extremely high at the layer interfaces, thus explaining the rampant occurrence of interface layer debonding. Also, there was evidence of high non-uniform AV distribution for cores extracted from the construction joints. Figures 3-14 through 3-17 show some examples of the AV characterization for selected projects.

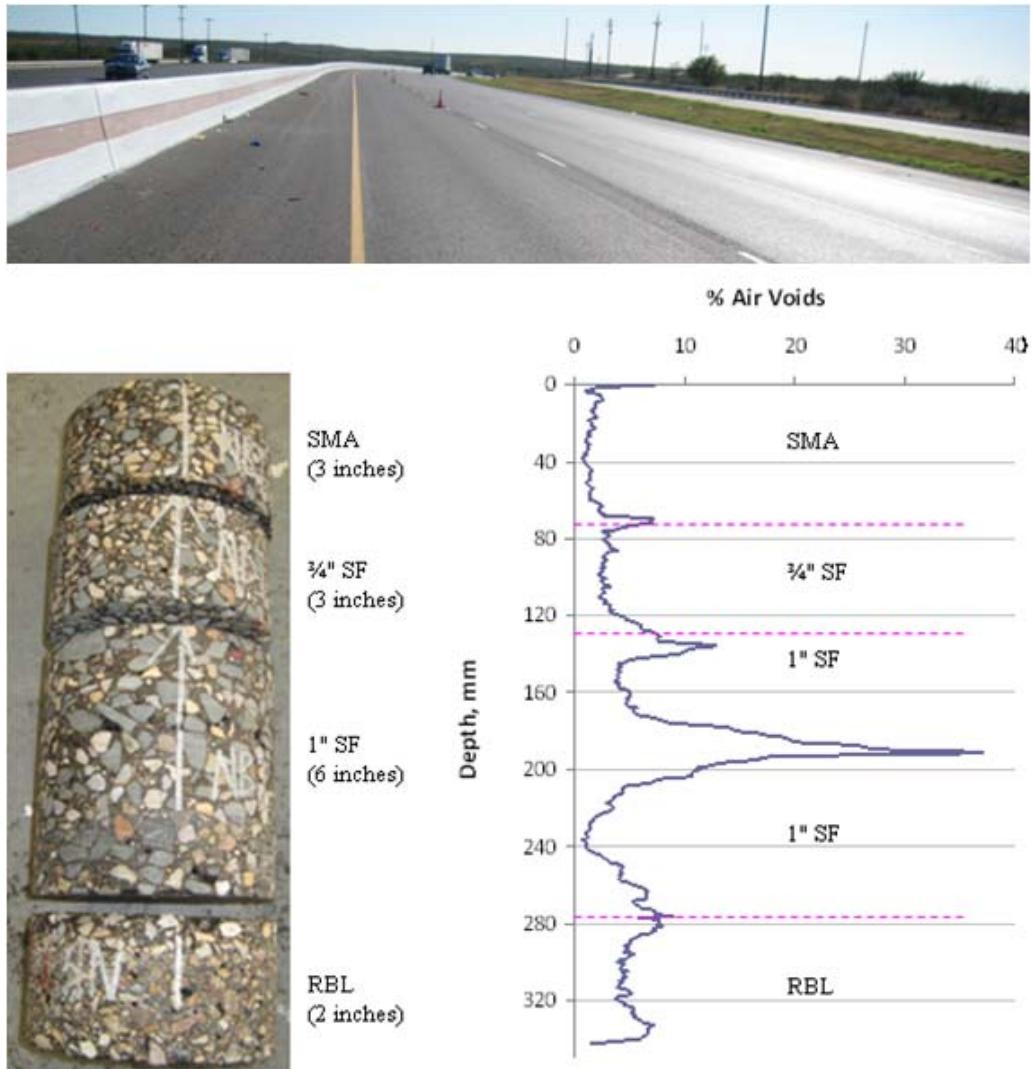


Figure 3-14. Core AV Distribution – IH 35 (NB, Price, Laredo).



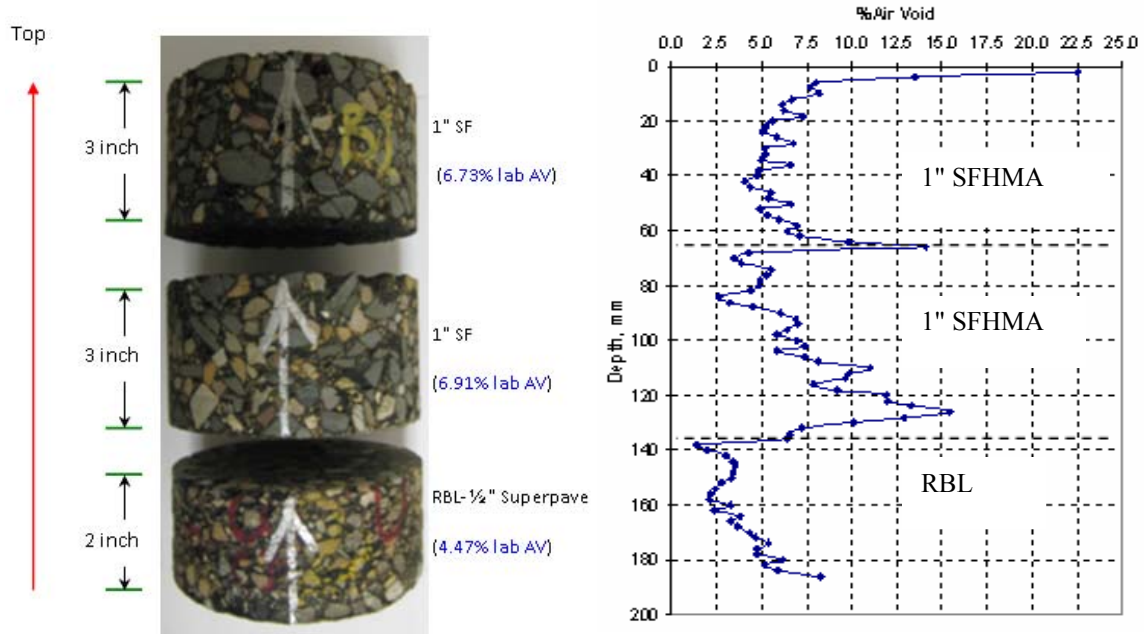


Figure 3-15. Core AV Distribution – IH 35 (SB, Price, Laredo).

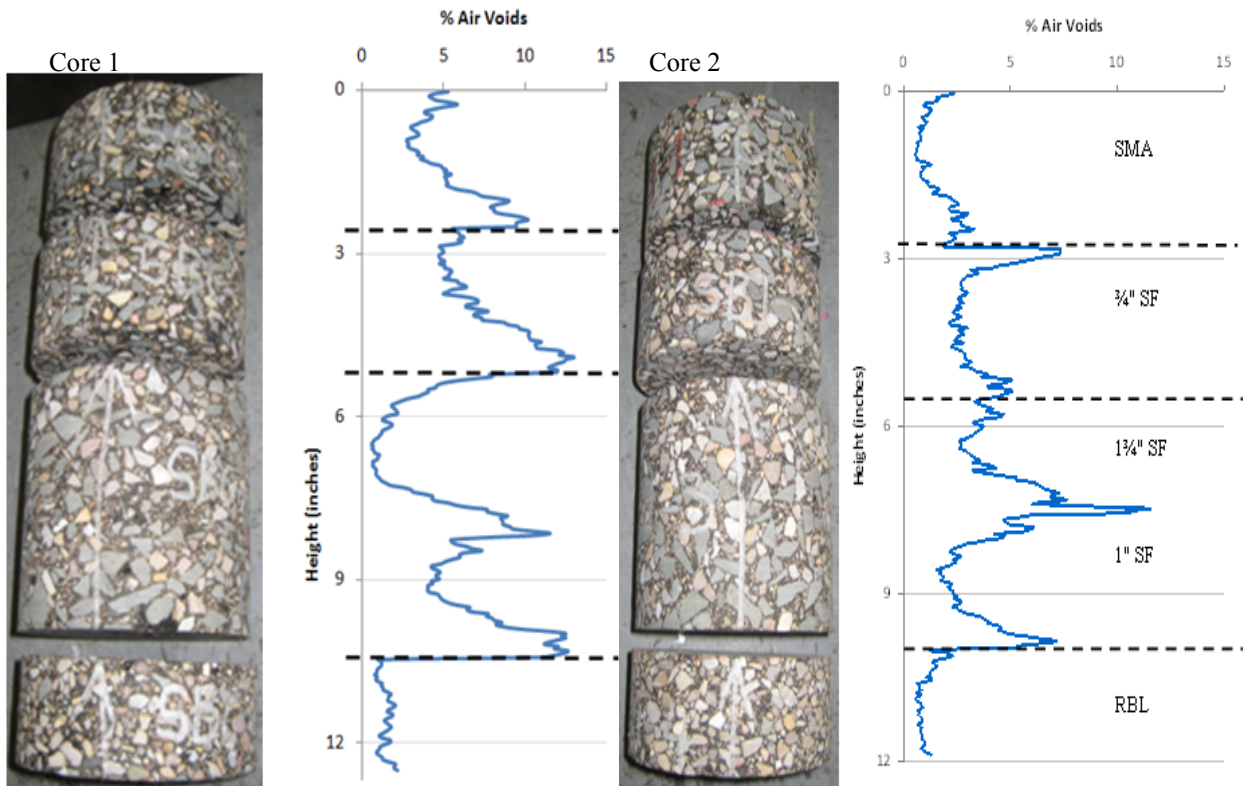


Figure 3-16. Coring and AV Distribution (Core 1 – along the construction joint; Core 2 – from inside lane) – IH 35 (SB Lane, Price, Laredo).

Figure 3-16 compares the AV distribution between cores from a construction joint and in between the wheel path. On average, the AV distribution for the core from the construction joint is higher in magnitude than the core from in between the wheel path. Nonetheless, these results are within theoretical expectations but emphasize the need to enforce the joint compaction specification and tighten up the QC/QA test protocols.

Figure 3-17 below is the core AV distribution from IH 35 in San Antonio and shows high AV content in the top PFC layer as expected. As designed, the AV content is the lowest in magnitude and also appears to be more uniformly distributed in the RBL.

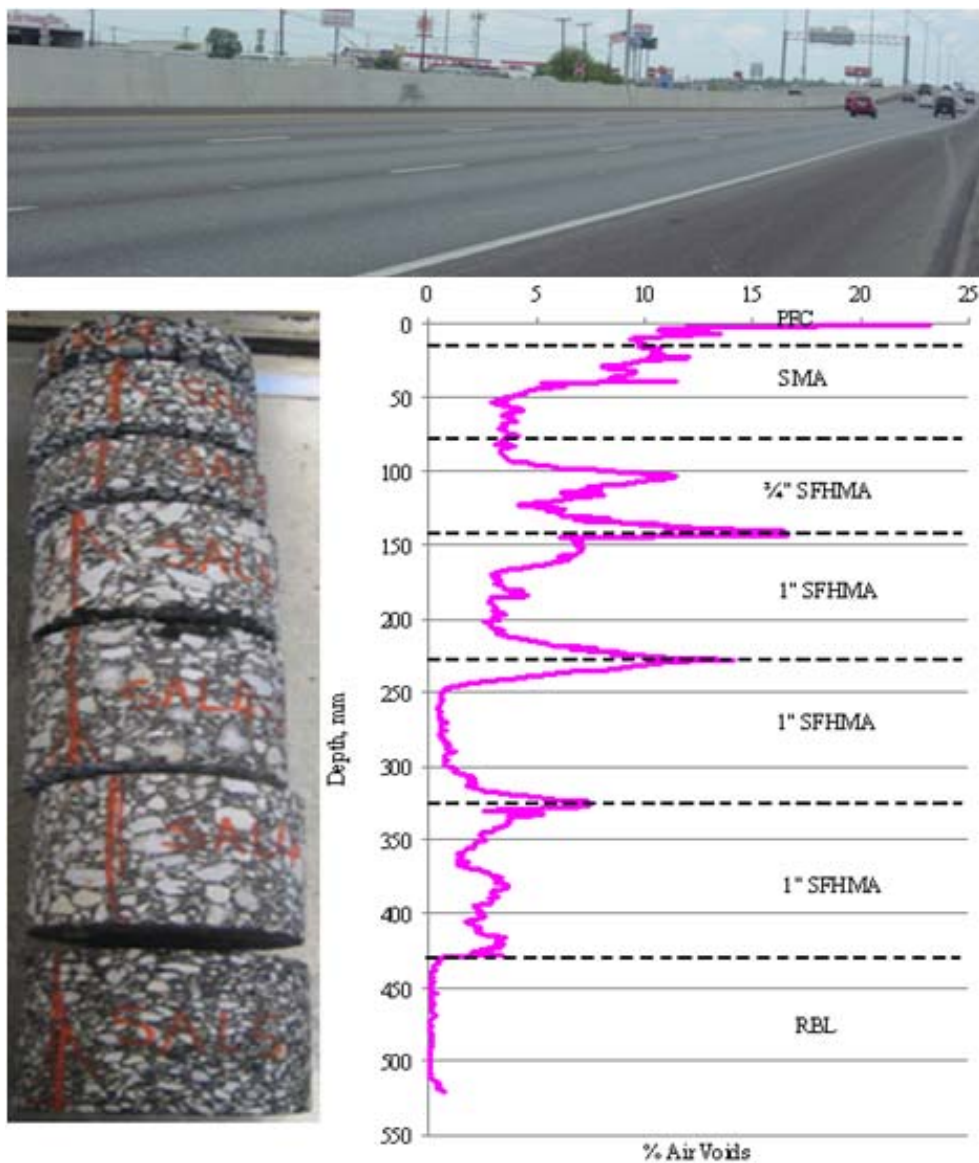


Figure 3-17. Core AV Distribution as a Function of Depth (IH 35, San Antonio).

Figures 3-14 through 3-17 indicate fairly uniform AV distribution within the RBL compared to the SFHMA layers. Looking at Figures 3-16 and 3-17, the AV distribution for the RBL is way less than 5 percent, which is consistent with the 97 percent target density (Chapter 2) and indicates that the RBL is non-porous (impermeable) as designed. In terms of mix-design, the RBL is composed of a dense aggregate gradation and relatively high asphalt binder content (on order of about 5.4 percent), characteristics that tend to improve the mix's workability and compactability properties.

For the SFHMA layers, AV peaks are clearly evident at the layer interface within the lifts. These high AV peaks suggest potential for debonding problems, which is undesirable. Note that debonding problems were experienced with the SFHMA cores; see Figures 3-5, 3-8, and 3-10. As expected, the porous PFC layer exhibited the highest AV distribution in terms of magnitude; see Figure 3-17.

## SUMMARY

This chapter presented the constructability aspects of the Texas perpetual pavements, with a focus on the SFHMA mixes. The list below summarizes the lessons learned and the recommendations made:

- The SFHMA mixes are associated with constructability (workability and compactability) problems arising from their lean mix-design (coarse aggregate gradation and low asphalt-binder content).
- Due to their poor constructability properties, the SFHMA mixes were found to be highly susceptible to forensic defects such as low density/in-place density variations (non-uniform AV distribution, highly localized honeycombing), vertical segregation, debonding, and permeability problems. These defects pose a great risk for moisture damage as well as compromising the structural integrity of the whole pavement.
- Constructability properties must be improved to minimize the occurrence of forensic defects evident in the placed SFHMA mixes, e.g., by increasing the OAC, adjusting the gradation, etc. Alternatively, using mixes such as the dense-graded Type B or standard Superpave that are relatively more workable is recommended.

- Three- to four-inch compacted lift thickness yielded better results than 5 inches. Future jobs using SFHMA should consider limiting the compacted lift thickness to 4 inches.
- The Roadtec MTD exhibited less thermal segregation in the HMA mat compared to the non-remixing windrow elevator set-up. The Roadtec offers on-board mix storage (surge bin) and HMA remixing, allowing for uninterrupted delivery of a more uniformly graded and thermally uniform product to the paving machine. The Roadtec or equivalent MTD should be given preference in future Texas PP jobs.
- Open, permeable construction joints were observed in some instances, and are primarily associated with poor construction practices. Mitigation measures on future jobs should include the following: (1) better enforcement of specification requirements to stagger construction joints, (2) exceed minimum evaluation requirements of the joint compaction specification, (3) exceed minimum intervals in the QC/QA test protocols, and (4) eliminate trench construction where possible.
- The GPR and IR thermal imaging (supplemented with coring and AV characterization) were found to be ideal and effective NDT tools for construction QC monitoring and evaluation. These NDT tools should be incorporated in future PP construction jobs.

# CHAPTER 4

## LABORATORY TESTING AND MATERIAL PROPERTY CHARACTERIZATION

An extensive laboratory test program was completed to characterize the material properties of the asphalt binders and the HMA mixes/layers. The test results are presented and analyzed in this chapter. A brief description of the test protocols is presented first, followed by the test results. A summary of the major findings is then presented at the end of the chapter.

### LABORATORY TEST PROTOCOLS

Table 4-1 lists the numerous tests that were conducted, including the test name, pictorial/schematic overview (where applicable), test loading parameters, and the output data.

**Table 4-1. Laboratory Test Protocols.**

| # Test | Name                          | Picture/Schematic | Test Parameters  | Output Data  |
|--------|-------------------------------|-------------------|--|--|
| 1      | Troxler ignition oven (TIOT)  |                   | $\geq 250$ °F  | Asphalt binder (aged) content and aggregate extraction |
| 2      | Dynamic shear rheometer (DSR) |                   | 10 rad/s, temperature range: 122 – 180 °F in water bath                                    | Asphalt binder (virgin) rheological properties         |
| 3      | Hamburg (HWTT)                |                   | 158 lb load, 122 °F water bath, 52 passes/min  | HMA rutting and stripping (moisture damage) potential  |
| 4      | Overlay (OT)                  |                   | 0.025-inch displacement @ 10 s/cycle (5s loading and 5s unloading), 77 °F                  | HMA cracking potential                                 |
| 5      | Permanent deformation (RLPD)  |                   | 20 and 30 psi loads, 1 Hz, 5 000 cycles, 77 and 104 °F, 0.1 s loading and 0.9s rest period | HMA permanent deformation and visco-elastic properties |
| 6      | Dynamic modulus (DM)          |                   | Frequency: 0.1 – 25 Hz, Temperature: 14– 130 °F  | HMA modulus  |
| 7      | X-ray CT scanning             |                   | At room temperature ( $\approx 77$ °F)   | AV distribution characterization                       |
| 8      | Permeability                  |                   | At room temperature ( $\approx 77$ °F)   | Permeability properties                                |

## HMA TEST SPECIMENS, AV, AND REPLICATES

HMA specimens consisted of plant-mixes, lab-molded samples (from raw materials), and field-extracted cores. With the exception of the PFC (designed at 20±1 percent) and RBL (designed at 3±0.5 percent), the target AV was 7±0.5 percent for all the plant-mixes and lab-molded samples. Considering all mixes used, the field core AV varied between 4.3 (RBL) to 21.8 (PFC) percent. When looking exclusively at the SFHMA cores, the AV ranged from 7.3 to 13 percent with an average of 11.8 percent and a COV of 31 percent. The AV range for the RBL cores was 4.3 to 7.1 percent with an average of 6.7 percent and a COV of 12 percent. Test method Tex-207-F was used to evaluate density and calculate the AV content. Test method Tex-236-F was used to determine AC content.

For each test shown in [Table 4-1](#), a minimum of three replicate specimens were used per mix type (for plant-mix, lab-molded samples, or field-extracted cores). Twenty-five percent coefficient of variation was arbitrarily utilized as the acceptable variability.

## ASPHALT BINDER CONTENT AND AGGREGATE EXTRACTIONS

Based on the Troxler ignition oven testing of field extracted-cores, there were some instances of deviation in the asphalt binder content from the ±0.3 percent specification tolerance, particularly for the SFHMA layers. [Table 4-2](#) shows some examples of the ignition oven-derived asphalt binder contents.

**Table 4-2. Asphalt Binder Content Results Based on the Troxler Ignition Oven Test.**

| Layer        | Highway               | Design OAC | Burned Off AC Content | Deviation by Weight of Total Mix | Meets ±0.3% Specification Tolerance |
|--------------|-----------------------|------------|-----------------------|----------------------------------|-------------------------------------|
| SMA          | SH 114                | 6.8%       | 6.7%                  | -0.09%                           | Yes                                 |
| Type C       | SH 114                | 4.4%       | 4.5%                  | +0.09%                           | Yes                                 |
| ¾-inch SFHMA | IH 35 (San Antonio)   | 5.3%       | 4.9%                  | -0.36%                           | No                                  |
| 1-inch SFHMA | SH 114 (Superpave)    | 4.0%       | 3.4%                  | -0.56%                           | No                                  |
| 1-inch SFHMA | IH 35 (Gilbert)       | 4.3%       | 3.8%                  | -0.46%                           | No                                  |
| 1-inch SFHMA | IH 35 (Hillsboro)     | 4.1%       | 4.1%                  | 0.00%                            | Yes                                 |
| 1-inch SFHMA | IH 35 (McLennan)      | 4.1%       | 3.9%                  | -0.18%                           | Yes                                 |
| 1-inch SFHMA | IH 35 (New Braunfels) | 4.5%       | 4.1%                  | -0.37%                           | No                                  |
| 1-inch SFHMA | IH 35 (Zumwalt02)     | 4.1%       | 3.9%                  | -0.18%                           | Yes                                 |
| Type B       | SH 114                | 4.5%       | 4.5%                  | 0.00%                            | Yes                                 |
| RBL          | SH 114                | 5.3%       | 5.2%                  | -0.09%                           | Yes                                 |
| RBL          | IH 35 (Hillsboro)     | 5.3%       | 5.3%                  | 0.00%                            | Yes                                 |

Clearly, [Table 4-2](#) shows deviations of over 0.3 percent for the SFHMA cores from IH 35 (San Antonio), SH 114 (Superpave), IH 35 (Gilbert), and IH 35 (New Braunfels). This lower than design AC could have a detrimental impact on the long-term PP performance, which is undesirable. While constructability problems of these SFHMA mixes ([Chapter 3](#)) can not be ignored, aggregate absorption may equally have played a role. Most of these SFHMA layers used limestone aggregates, which may be very absorptive. For instance, the SH 114 limestone was tested to have a laboratory WAC value of 2.3 percent, which is considered high and indicative of a potential for asphalt binder absorption. Evidently, these results emphasize the need for tighter QC/QA protocols in future SFHMA construction projects. By contrast, however, the dense-graded layers/mixes such as the RBL, Type C, and Type B were fairly consistent, with the ignition oven-derived AC contents being within the  $\pm 0.3$  percent tolerance limit.

In an effort to improve their rutting resistance, the SFHMA layers are typically designed with a coarse aggregate gradation. This mix-design philosophy apparently compromises the mixture workability and compactability characteristics ([Chapter 2](#)). Furthermore, the aggregate extraction tests indicated a much coarser gradation for some of the SFHMA layers than the job mix formula (JMF) design, compounding their constructability problems even worse. The 1-inch SFHMA layer on SH 114 (Superpave) for instance had about 15.1 percent cumulative retained on the number  $\frac{3}{4}$ -inch sieve instead of the design 10.7 percent; see the results in [Table 4-3](#).

**Table 4-3. Aggregate Extraction Results for 1-Inch SFHMA Layer (SH 114 Superpave).**

| Sieve Size<br>(mm)  | Percent Passing |        |             | Deviation | Operational<br>Tolerance | Meets<br>Tolerance |     |
|---------------------|-----------------|--------|-------------|-----------|--------------------------|--------------------|-----|
|                     | Spec            | Design | Extractions |           |                          |                    |     |
| 1½-inch             | 37.50           | 100    | 100         | 100       | 0.0%                     | ±5%                | Yes |
| 1-inch              | 25.00           | 90-100 | 100         | 100       | 0.0%                     | ±5%                | Yes |
| $\frac{3}{4}$ -inch | 19.00           | -      | 89.3        | 84.9      | -4.9%                    | ±5%                | Yes |
| No. 4               | 4.75            | -      | 33.6        | 28.7      | -14.6%                   | ±5%                | No  |
| No. 8               | 2.36            | 19-45  | 23.2        | 20.0      | -13.8%                   | ±5%                | No  |
| No. 16              | 1.18            | -      | 15.6        | 14.1      | -9.6%                    | ±3%                | No  |
| No. 200             | 0.075           | 1.0-7  | 2.3         | 3.4       | +47.8%                   | ±2%                | No  |

As was discussed in [Chapter 3](#), this coarseness in the gradation appears to cause workability and compactability related problems, resulting in undesirable in-place material characteristics. Inevitably, this also impacts on other performance characteristics such as durability, permeability, and cracking resistance of the PP structures.

## ASPHALT BINDER DSR TEST RESULTS

The majority of the asphalt binders used on the Texas PP projects was sourced from Valero and Wright asphalt in Texas. DSR test results for PG 64-22, PG 70-22, PG 70-28, and PG 76-22 asphalt binders (virgin) are shown in Figures 4-1 and 4-2. A detailed tabulation of these results ( $G^*$ ,  $\delta$ , and  $G^*/\text{Sin } \delta$ ) can be found in the Texas PP database (Walubita et al., 2009).

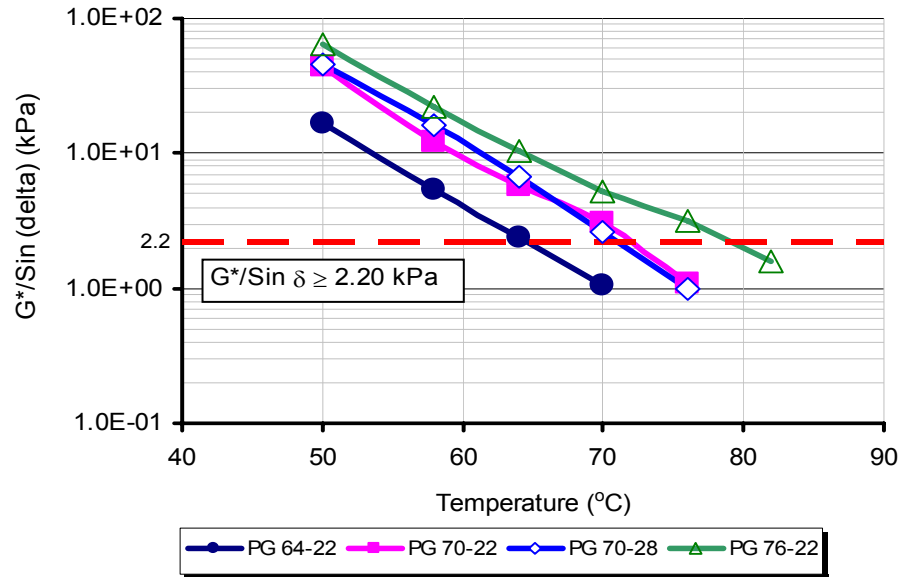


Figure 4-1. Binder  $G^*/\text{Sin } \delta$  (delta) versus Temperature.

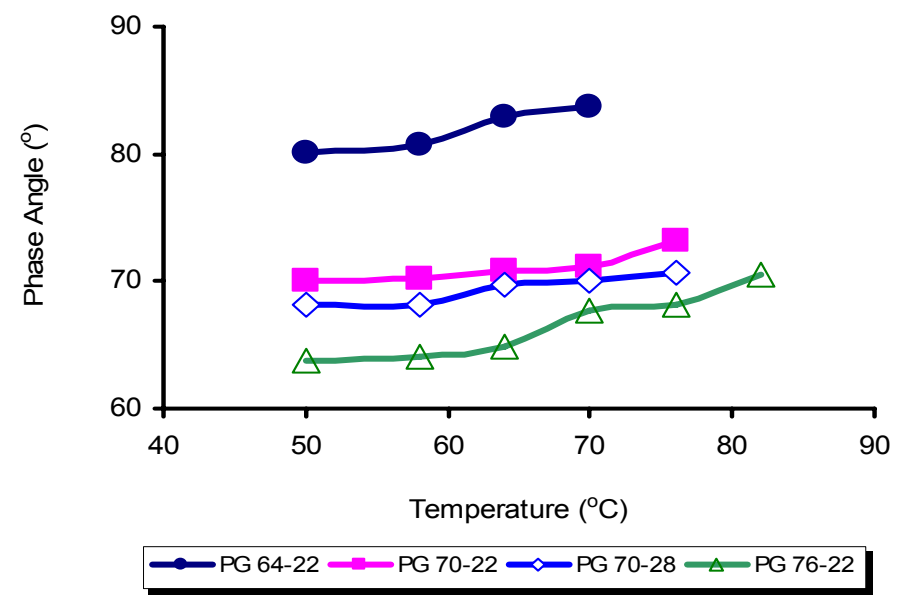


Figure 4-2. Phase Angle versus Temperature.



In general, the rheological results shown in [Figures 4-1](#) and [4-2](#) are consistent with the typical visco-elastic behavior of asphalt-binders. Additionally, all the virgin asphalt binders met the PG specification (for the high temperature properties) consistent with the prescribed  $G^*/\sin \delta \geq 2.20$  kPa threshold for Superpave performance-graded binders ([AI, 1996](#)).

## HMA LAB TEST RESULTS

The HMA lab test results are discussed in this section and include summaries from (1) the Overlay Test for cracking resistance; (2) the Hamburg Wheel-tracking test for rutting resistance; (3) the dynamic modulus test for modulus characterization; and (4) permeability test for transmissive flow rate. Full details of these laboratory test results can be found in the Texas PP database ([Walubita et al., 2009](#)).

### Average Test Results by HMA Mix Type

[Table 4-4](#) provides a comparative summary of the HMA mix test results. These results are an average representation of all the Texas PP projects.

**Table 4-4. Average HMA Mix Results.**

| HMA Mix   | Average Numbers           |                        |   |  |
|---|---------------------------|------------------------|---|--|
|   | Overlay Cycles            | Hamburg Rut (mm)       | Modulus (ksi)                                 | Permeability (cm/sec)                                  |
| PFC (surface porous layer)                      | 147                       | 9.0 (@ 20 k)           | 357   | $1.63 \times 10^{-3}$                                  |
| SMA   | 300                       | 5.9 (@ 20 k)           | 726   | $0.38 \times 10^{-3}$                                  |
| Type C  | 324                       | 14.5 (@ 15 k)          | 680   | $0.21 \times 10^{-3}$                                  |
| ¾-inch SFHMA <sup>a</sup> (rut-resistant layer) | 132                       | 9.0 (@ 20 k)           | 1 060   | $0.98 \times 10^{-3}$                                  |
| Type B  | 175                       | 13.2 (@ 10 k)          | 937   | $0.57 \times 10^{-3}$                                  |
| 1-inch SFHMA <sup>a</sup> (RRL)                 | 77                        | 6.2 (@ 20 k)           | 1 286   | $1.42 \times 10^{-3}$                                  |
| RBL (fatigue-resistant layer)                   | 900                       | 12.6 (@ 10 k)          | 605   | $0.00 \times 10^{-3}$                                  |
| Test threshold utilized <sup>b</sup>            | $\geq 300$ cycles @ 77 °F | $\leq 12.5$ mm @ 50 °C | Typical value is about 500 ksi @ 10 Hz, 77 °F | $\leq 1.2 \times 10^{-3}$ cm/sec @ ambient temperature |

<sup>a</sup>Note: Based on their design and position in the PP structure, the SFHMA mixes are generally not subjected to large tensile stress/strain demands and so, their poor OT performance is not unexpected. They are primarily designed for rutting resistance.

<sup>b</sup>Note: The  $1.2 \times 10^{-3}$  cm/sec permeability threshold is not applicable to PFC mixes.

Legend: k stands for x1000, i.e., 20k = 20 000 HWTT load passes.

Of particular interest in [Table 4-4](#) is the poor OT performance and porous nature of the 1-inch SFHMA layers/mixes but superior Hamburg rutting performance and a high modulus value. This laboratory performance was not unexpected as these mixes were primarily designed for rutting resistance and serves as the main structural load-carrying layer in the current Texas PP structures. The SFHMA mix-design, with its coarse aggregate gradation and low asphalt-binder content, results in considerably stiffer (high modulus value of about 1286 ksi) mixes/layers that are highly resistant to rutting (only 6.2 mm rutting after 20,000 load passes) but poor in cracking resistance. In fact, [Table 4-4](#) shows the lowest number of OT cycles (i.e., 77) for the 1-inch SFHMA, indicating that it is the least resistant to cracking among all the HMA mixes/layers tested. Provided these mixtures are protected from high loading tensile strains by sufficient cover and depth of structure, this shortcoming may not in itself hurt performance.

However, the high permeability nature ( $1.42 \times 10^{-3}$  cm/sec) of the 1-inch SFHMA is a cause for concern, particularly in terms of moisture damage from water infiltrating through the surface layers (after rain). According to [Degussa \(2007\)](#),  $1.2 \times 10^{-3}$  cm/sec is considered an acceptable permeability level for coarse-graded HMA mixes. By contrast, the permeability value of the 1-inch SFHMA is  $1.42 \times 10^{-3}$  cm/sec, 18 percent higher than the threshold and almost the same magnitude as the porous PFC. This could be a potential cause for water entrapment within the PP structure especially considering that the bottom RBL is impermeable (zero cm/sec). Also, high permeability means easy air infiltration into the pavement, leading to asphalt-binder oxidative aging that reduces durability as well as cracking resistance. Again, this permeability problem is directly related to the SFHMA mix design (low percentage of finer fractions [i.e., below the #8 sieve size] and high potential for interconnected AV).

The high permeability nature ( $1.63 \times 10^{-3}$  cm/sec) of the PFC, though on the higher side, is considered acceptable as this mix is purposely designed to be a porous surface layer (see [Chapter 2](#)). As expected, the fatigue-resistant RBL exhibited the best laboratory cracking resistance with the highest number of OT cycles at 817, much greater than the 300 that was utilized as the benchmark. The RBL was also found to be highly impermeable (zero cm/sec), but had the poorest rutting performance in the Hamburg test. However, because of the RBL location in the pavement structure, rutting resistance is not a performance concern.

## HMA Moduli Values at 77 °F, 10 Hz

Dynamic modulus test results are listed in [Table 4-5](#); typical HMA moduli values at a reference temperature of 77 °F (and 10 Hz) were generated.

**Table 4-5. HMA Moduli Values at 77 °F, 10 Hz.**

| HMA Mix Type                                   | Lab Range      | Lab Average | Recommended for Design |
|--|----------------|-------------|------------------------|
| PFC  | 300 – 450 ksi  | 357 ksi     | 350 ksi                |
| SMA  | 500 – 750 ksi  | 726 ksi     | 650 ksi                |
| ¾-inch SFHMA<br>(¾-inch NMAS; performance mix) | 600 – 1200 ksi | 1060 ksi    | 800 ksi                |
| 1-inch SFHMA<br>(1-inch NMAS; performance mix) | 800 – 1500 ksi | 1286 ksi    | 1000 ksi               |
| RBL<br>(e.g., ½-inch Superpave; dense-graded)  | 400 – 650 ksi  | 605 ksi     | 500 ksi                |
| Type A (coarse-graded)                         | 750 – 1200 ksi | 900 ksi     | 800 ksi                |
| Type B (⅞-inch NMAS)                           | 700 – 1000 ksi | 937 ksi     | 800 ksi                |
| Type C and D* (dense-graded)                   | 450 – 700 ksi  | 500 ksi     | 500 ksi                |
| Type F* (fine-graded)                          | 300 – 400 ksi  | 360 ksi     | 350 ksi                |

\*Note: Type D and F mixes were not used in the Texas PP structures; values are provided for comparative purposes only.

The HMA moduli values in column 4 of [Table 4-5](#) “Recommended for Design” are the proposed design values that are based on all of the available DM laboratory test data tempered with the need to be conservative. These are the reference moduli values (at 77 °F) proposed for consideration in future designs of Texas perpetual pavements.

Notice in [Table 4-5](#) the high stiffness nature of the 1-inch SFHMA mix with a minimum modulus of 800 ksi. This is consistent with the mix-design volumetrics given previously in [Chapter 2](#). The 1-inch SFHMA is in fact a performance mix that is typically used as the main structural rut-resistant layer in the Texas PP structural designs. As expected, the fine-graded Type F mix constitutes one of the least stiff mixes with a modulus value of less than 500 ksi at 77 °F. In the current Texas PP design concept, the PFC mixes are optional; they are a functional component addressing wet weather safety by reducing splash/spray effects, rapidly draining to improve wet weather frictional characteristics.

## District Average Results

Tables 4-6 through 4-8 are the district average results for modulus, Hamburg rutting, and Overlay cracking resistance, respectively. These results represent the average of both lab-molded and field-extracted core specimens. Evidently, the results indicate that Laredo District has the stiffest mixes (highest moduli values) with the best laboratory rutting performance (lowest Hamburg rut depths) but the poorest cracking resistance performance based on the OT results (Table 4-8).

**Table 4-6. District Average Moduli at 77 °F, 10 Hz.**

| HMA Mix      | Average Lab Modulus (ksi) |        |             |      | Overall Avg. (ksi) | COV |
|--------------|---------------------------|--------|-------------|------|--------------------|-----|
|              | Fort Worth                | Laredo | San Antonio | Waco |                    |     |
| PFC          | --                        |        | 368         | 345  | 357                | 5%  |
| SMA          | 640                       | 878    | 702         | 683  | 726                | 14% |
| Type C       | 680                       | -      | -           | -    | 680                |     |
| ¾-inch SFHMA | 825                       | 1347   | 1025        | 1043 | 1060               | 20% |
| Type B       | 937                       | -      | -           | -    | 937                |     |
| 1-inch SFHMA | 1275                      | 1462   | 1267        | 1139 | 1286               | 10% |
| RBL          | 565                       | 658    | 623         | 574  | 605                | 7%  |

**Table 4-7. District Average Hamburg Results.**

| HMA Mix              | Average Hamburg Rutting (mm) |        |             |      | Overall Avg. (mm) | COV |
|----------------------|------------------------------|--------|-------------|------|-------------------|-----|
|                      | Fort Worth                   | Laredo | San Antonio | Waco |                   |     |
| PFC* (@ 20k)         | -                            | -      | 11.5        | 6.5  | 9.0               | 39% |
| SMA (@ 20k)          | 3.8                          | 5.5    | 6.8         | 7.6  | 5.9               | 28% |
| Type C (@ 15k)       | 14.5                         | -      | -           | -    | 14.5              |     |
| ¾-inch SFHMA (@ 20k) | 12.7                         | 6.0    | 8.4         | 7.5  | 9.0               | 38% |
| Type B (@ 10k)       | 13.2                         | -      | -           | -    | 13.2              |     |
| 1-inch SFHMA (@ 20k) | 5.5                          | 5.5    | 9.7         | 4.2  | 6.2               | 38% |
| RBL (@ 10k)          | 12.5                         | 11.9   | 12.6        | 13.4 | 12.6              | 5%  |
| Threshold            | Rut depth ≤ 12.5 mm          |        |             |      |                   |     |

\*Note: In Texas, the Hamburg is generally not run for PFC mixes.

Legend: k stands for x1000, i.e., 20k = 20 000 HWTT load passes.

**Table 4-8. District Average Overlay Results.**

| HMA Mix            | Average Number of OT Cycles to Failure |        |             |      | Overall Average | COV |
|--------------------|--|--------|-------------|------|-----------------|-----|
|                    | Fort Worth                             | Laredo | San Antonio | Waco |                 |     |
| PFC                | -                                      | -      | 175         | 119  | 147             | 27% |
| SMA*               | 300                                    | 300    | 300         | 300  | 300             |     |
| Type C             | 324                                    |        |             |      | 324             |     |
| ¾-inch SFHMA       | 153                                    | 150    | 71          | 155  | 132             | 31% |
| Type B             | 175                                    |        |             |      | 175             |     |
| 1-inch SFHMA       | 108                                    | 16     | 58          | 125  | 77              | 64% |
| RBL*               | 900                                    | 900    | 900         | 900  | 900             |     |
| Benchmark utilized | OT cycles $\geq$ 300                   |        |             |      |                 |     |

\*Note: OT tests were terminated at 300 cycles for the SMA and 900 cycles for the RBL.

In general, greater statistical variability in the laboratory test results was experienced with the SFHMA mixes (followed by the PFC mixes), particularly in the Overlay test. A COV value as high as 64 percent was recorded for the 1-inch SFHMA mixes in the Overlay test. Poor workability, compactability problems, and poor AV distribution/honeycombing attributed to the coarse aggregate gradation were largely seen as some of the contributing factors.

Results were least statistically variable for the RBL mixes and were fairly consistent. Looking at [Tables 4-6](#) and [4-7](#), the COV for the RBL is a one-digit number, averaging 6 percent. The RBL mix with a finer and denser aggregate gradation generally yielded a more uniformly distributed AV structure that minimizes statistical variability both in the AV content and the laboratory physical test results. Figuratively speaking, these results are indicative that coarse-graded mixes are more prone to laboratory test variability compared to dense-graded mixes.

### **Project Comparison and Laboratory Performance Ranking**

[Tables 4-9](#) through [4-11](#) are comparative listings of the laboratory performance results for the field cores from all the Texas PP projects. The comparison includes modulus, Hamburg rutting, and Overlay cracking, respectively.

**Table 4-9. Moduli Comparison – Field Cores.**

| Project | Avg. Modulus @ 77 °F, 10 Hz (ksi) |       |        |          |        |          |       |
|---------|-----------------------------------|-------|--------|----------|--------|----------|-------|
|         | PFC                               | SMA   | Type C | ¾" SFHMA | Type B | 1" SFHMA | RBL   |
| #1      |                                   | 503   |        | 603      |        | 805      | 406   |
| #2      |                                   | 791   |        | 1081     |        | 2013     | 635   |
| #3      |                                   | 1114  |        | 1573     |        | 2213     | 837   |
| #4      |                                   | 886   |        | 1007     |        | 915      | 721   |
| #5      | 384                               | 661   |        | 710      |        | 1310     | 520   |
| #6      | 384                               | 661   |        | 655      |        | 1064     | 516   |
| #7      | 412                               | 650   |        | 669      |        | 1222     | 575   |
| #8      | 395                               | 760   |        | 747      |        | 1221     | 840   |
| #9      |                                   | 578   |        | 601      |        | 1346     | 508   |
| #10     |                                   | 578   | 704    |          | 1063   |          | 468   |
| Avg.    | 394                               | 718   | 704    | 850      | 1063   | 1345     | 603   |
| COV     | 3.4%                              | 24.9% |        | 37.8%    |        | 35.1%    | 25.2% |

**Project legend:** #1 = Price, #2 = Zumwalt02 (ZMW02), #3 = Gilbert, #4 = Zumwalt01 (ZMW01), #5 = San Antonio, #6 = New Braunfels, #7 = McLennan, #8 = Hillsboro, #9 = Fort Worth 01, & #10 = Fort Worth 02.

**Table 4-10. Hamburg Rutting Performance Comparison – Field Cores.**

| Project | Hamburg Rutting Results (mm) (≤ 12.5 mm) |           |              |           |              |            |
|---------|--|-----------|--------------|-----------|--------------|------------|
|         | SMA                                      | Type C    | ¾-inch SFHMA | Type B    | 1-inch SFHMA | RBL        |
| #1      | 4.3 @ 20k*                               |           | 3.9 @ 20k    |           | 3.1 @ 20k    | 12.4 @ 15k |
| #2      | 8.7 @ 20k                                |           | 6.1 @ 20k    |           | 10.0 @ 20k   | 12.5 @ 5k  |
| #3      | 3.4 @ 20k                                |           | 1.5 @ 20k    |           | 10.5 @ 20k   | 13.4 @ 9k  |
| #4      | 2.0 @ 20k                                |           | 2.3 @ 20k    |           | 3.8 @ 20k    | 8.0 @ 10k  |
| #5      |  |           | 9.8 @ 20k    |           | 4.7 @ 20k    | 12.6 @ 10k |
| #6      |  |           | 11.8 @ 20k   |           | 12.7 @ 18k   | 13.1 @ 10k |
| #7      | 5.8 @ 20k                                |           | 6.2 @ 20k    |           | 2.3 @ 20k    | 5.9 @ 10k  |
| #8      |  |           | 7.1 @ 20k    |           | 5.9 @ 20k    | 13.3 @ 8 k |
| #9      |  |           | 13.4 @ 12k   |           | 7.8 @ 20k    | 13.2 @ 3k  |
| #10     |  | 12.3 @ 9k |              | 12.5 @ 7k |              | 14.5 @ 10k |

**Project legend:** #1 = Price, #2 = Zumwalt02 (ZMW02), #3 = Gilbert, #4 = Zumwalt01 (ZMW01), #5 = San Antonio, #6 = New Braunfels, #7 = McLennan, #8 = Hillsboro, #9 = Fort Worth 01, & #10 = Fort Worth 02.

\*Note: k stands for x1000, i.e., 20k = 20 000 HWTT load passes.

**Table 4-11. Overlay Cracking Performance Comparison – Field Cores.**

| Project   | Number of OT Cycles to Failure ( $\geq 300$ ) |        |                |        |              |      |
|---|---|--------|----------------|--------|--------------|------|
|   | SMA   | Type C | 3/4-inch SFHMA | Type B | 1-inch SFHMA | RBL  |
| #1  | 300   |        | 300            |        | 31           | 1701 |
| #2  | 47  |        | 11             |        | 14           | 227  |
| #3  | 8   |        | 9              |        | 2            | 1500 |
| #4  | 300   |        | 300            |        | 31           | 1500 |
| #5  |   |        | 21             |        | 5            | 480  |
| #6  |   |        | 25             |        | 8            | 520  |
| #7  | 235   |        | 135            |        | 82           | 900  |
| #8  |   |        | 16             |        | 356          | 585  |
| #9  |   |        | 206            |        | 74           | 652  |
| #10   |   | 106    |                | 122    |              | 550  |
| Average   | 178   | 106    | 114            | 122    | 67           | 862  |
| Project legend: #1 = Price, #2 = Zumwalt02 (ZMW02), #3 = Gilbert, #4 = Zumwalt01 (ZMW01), #5 = San Antonio, #6 = New Braunfels, #7 = McLennan, #8 = Hillsboro, #9 = Fort Worth 01, & #10 = Fort Worth 02. |   |        |                |        |              |      |

Table 4-9 shows the highest moduli values for the SFHMA cores ( $> 800$  ksi) and the lowest for the RBL (603 ksi average) and PFC (394 ksi average) cores, as would be expected. With the exception of the New Braunfels cores at an average rut depth of 12.7 mm after 18,000 load passes, the results are generally consistent with the expected Hamburg rutting performance. The stiff SFHMA and SMA cores passed the Hamburg rutting criteria while all the RBL cores failed, with rut depths exceeding 12.5 mm. Again, this is not considered a performance issue because of the RBL’s location in the structure. As expected, the RBL cores exhibited superior cracking performance in the OT test while the SFHMA cores were the worst. For all these tests, variability in the results among the different projects appears to be on the high side. This was not unexpected as these are field cores and therefore, their laboratory performance is a function of the different mix-design characteristics confounded by construction quality.

### The 1-in SFHMA Lab Results

Tables 4-12 and 4-13 are comparative listings of the lab test results for the 1-inch SFHMA mixes/layers for selected projects.

**Table 4-12. Lab-Molded Samples and Plant-Mixes.**

| <b>Test Waco</b>         | <b>Fort Worth</b> | <b>Price</b> | <b>ZMW02</b> | <b>ZMW01</b> | <b>San Antonio</b> | <b>Gilbert</b> |      |
|--------------------------|-------------------|--------------|--------------|--------------|--------------------|----------------|------|
| Hamburg @ 20 k (mm)      | 4.2               | 3.1          | 1.5          | 5.3          | 5.0                | 6.8            | 8.5  |
| OT cycles                | 155               | 108          | 86           | 8            | 16                 | 16             | 28   |
| E*  @ 77 °F, 10 Hz (ksi) | 1001              | 1103         | 1664         | 1215         | 1152               | 990            | 1141 |

Legend: k stands for x1000, i.e., 20k = 20 000 HWTT load passes.

**Table 4-13. Field-Extracted Cores.**

| <b>Test Waco</b>         | <b>Fort Worth</b> | <b>Price</b> | <b>ZMW02</b> | <b>ZMW01</b> | <b>San Antonio</b> | <b>Gilbert</b> |      |
|--------------------------|-------------------|--------------|--------------|--------------|--------------------|----------------|------|
| Hamburg @ 20 k (mm)      | 4.1               | 7.8          | 3.1          | 10.0         | 3.8                | 12.7           | 2.6  |
| OT cycles                | 82                | 74           | 31           | 14           | 9                  | 8              | 2    |
| E*  @ 77 °F, 10 Hz (ksi) | 1221              | 1346         | 850          | 2013         | 915                | 1100           | 2213 |

Legend: k stands for x1000, i.e., 20k = 20 000 HWTT load passes.

In general, both the lab (Table 4-12) and field core (Table 4-13) result trends do not significantly differ statistically; the numbers obtained are fairly comparable. As expected by the design, the 1-inch SFHMA are very stiff mixes/layers with high moduli values in the range of 800 to 1500 ksi. The computed average for all the projects was 1286 ksi with a COV of 10 percent. Based on these results, recommendations were made to revise the SFHMA design moduli to a range of 800 to 1200 ksi. The initial TxDOT design proposal was 500 to 700 ksi, numbers that tended to yield conservative designs.

With the exception of the San Antonio cores at 12.7 mm and the ZMW02 cores at 10 mm, both Tables 4-12 and 4-13 indicate substantial resistance to rutting, with the laboratory measured rut magnitudes falling below 9 mm. As designed, this high rutting resistance in the Hamburg test was expected of these 1-inch SFHMA mixes. However, laboratory cracking resistance for these SFHMA mixes is very poor, with a range of only 2 to 155 OT cycles. Furthermore, the results show better OT performance for the lab-molded samples than for the field-extracted cores. Among other factors, this is assumed to be due to better quality control in the lab-molded samples in terms of both the OAC and the AVs than in the field where the core AVs varied significantly.



### |E\*| Master-Curves

From the DM test results, |E\*| master-curves were generated to graphically compare the stiffness and visco-elastic properties of the HMA mixes. The time-temperature superposition signomoidal model shown in Equation 4-1 was utilized to generate the |E\*| master-curves based on the sum of square error optimization technique (Pellinen and Witzczak, 2002):

$$\text{Log}(|E^*|) = \delta + \frac{\alpha}{1 + e^{\beta - \gamma(\log \zeta)}} \quad \text{Equation (4-1)}$$

Where, |E\*| is the dynamic modulus (psi);  $\zeta$  is the reduced frequency (Hz);  $\delta$  is the minimum modulus value (psi); and  $\alpha$ ,  $\beta$ , and  $\gamma$  are the model shape parameters. Figure 4-3 shows a comparative plot of the |E\*| master-curves for the SFHMA, Type B, and RBL (Layer 04) mixes at a reference temperature of 70 °F.

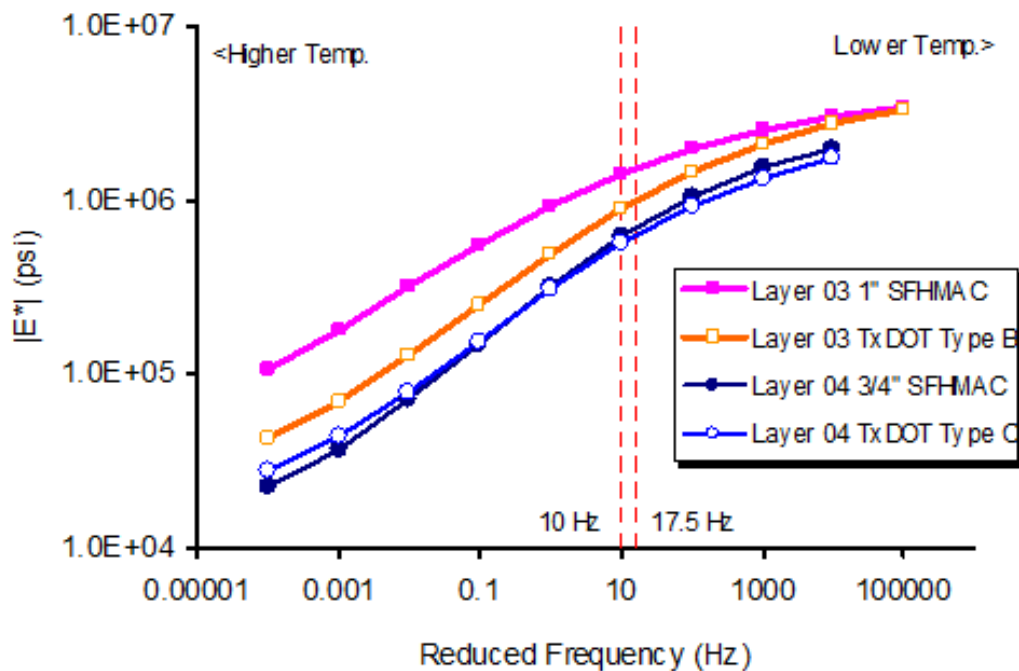


Figure 4-3. |E\*| Master-Curves (Reference Temperature = 70 °F).

The expected variation in stiffness between the SFHMA and RBL is clearly evident in [Figure 4-3](#) based on the higher and lower  $|E^*|$  magnitudes, respectively. As can be seen in [Figure 4-3](#), the high stiffness nature of the 1-inch SFHMA mixes with higher  $|E^*|$  values is particularly pronounced at the lower loading frequency (and high temperature domain), where rutting is often more critical. This response trend was theoretically expected and is consistent with the mix-design characteristics and visco-elastic nature of HMA mixes.

Notice also that as expected, the 1-inch SFHMA is considerably stiffer than the Type B mix, especially at the lower loading frequencies (i.e.,  $\leq 100$  Hz), which also corresponds to the higher temperature domain. However, the  $|E^*|$  magnitude is comparable at the higher loading frequencies that correspond to the lower temperature domain. Theoretically, this means that the visco-elastic response of both mixes would be indifferent at high loading frequencies (i.e., high vehicle speeds and shorter loading times) and lower temperatures (i.e., winter season). By contrast, significant differences in the visco-elastic response would be expected at high temperatures and under slow moving vehicles (i.e., lower loading frequency).

### **Permanent Deformation**

[Figure 4-4](#) is a plot of the permanent deformation results from RLPD testing at 104 °F under a repeated loading of 20 psi. The mixes in [Figure 4-4](#) were used on SH 114 in Fort Worth and shows that the 1-in SFHMA mix has superior resistance to permanent deformation and accumulated the lowest permanent strain after 5,000 load repetitions. These results are consistent with the Hamburg findings reported previously. By contrast, the RBL mixes exhibited the least resistance to permanent deformation, accumulating over two times the deformation of the 1-inch SFHMA mix, after just 1000 load repetitions.

Though not very significantly different, the SMA performed better than the  $\frac{3}{4}$ -inch SFHMA and Type B mixes. While the SMA and  $\frac{3}{4}$ -inch SFHMA used higher PG asphalt-binder grades (PG 70-28 and PG 76-22, respectively), the Type B mix utilized a PG 64-22 asphalt-binder. At such a relatively high temperature (104 °F), the binder PG grade definitely played a significant role in the permanent deformation performance of the mixes, particularly for the Type B mix.

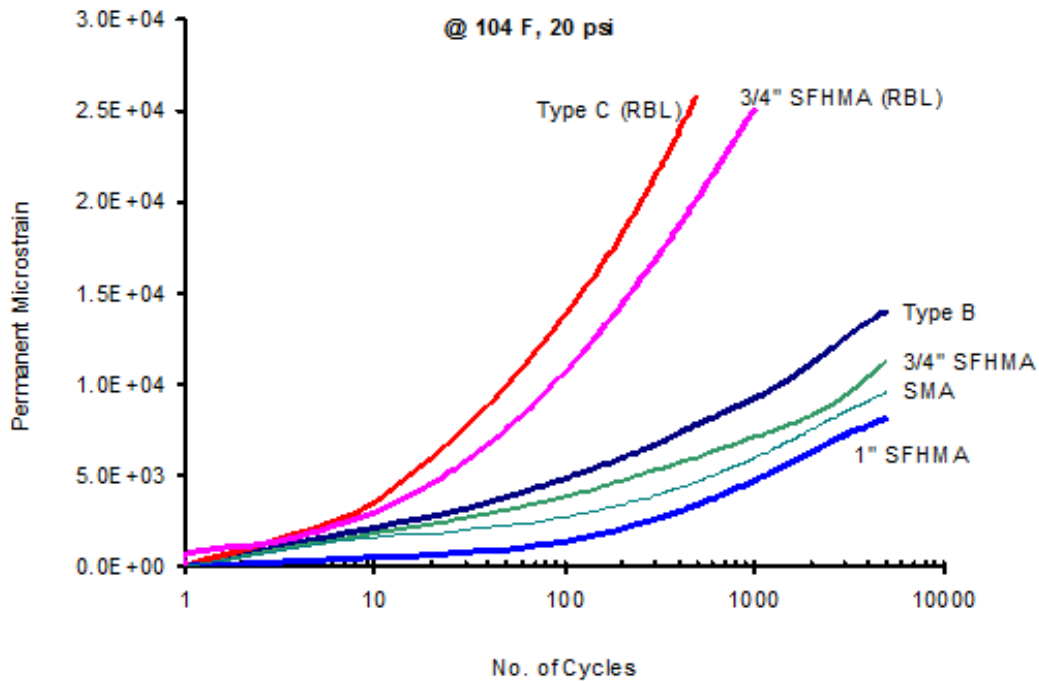


**Figure 4-4. Permanent Deformation Results.**

## X-RAY CT SCANNING AND AV CHARACTERIZATION

As discussed previously in [Chapter 3](#), X-ray CT scanning tests were also conducted to characterize the AV distribution of the field-extracted cores. The X-ray CT characterizes the AV distribution as a function of the core depth and therefore, also served as an indicative assessment of the potential for porosity and permeability problems. In general, the X-ray CT scanning results indicated high and non-uniform AV distribution for the SFHMA layers, with high potential for moisture entrapment, particularly if rain water infiltrates through the surface layers. This is particularly critical, especially since the RBL was found to be non-porous (low uniform AV distribution) and impermeable (see also [Table 4-4](#)).

[Figure 4-5](#) shows an example of the AV distribution as a function of depth for the 1-inch SFHMA and RBL layers from the IH 35 Price job in Laredo. While the AV distribution in the RBL is fairly uniform at around 4.8 percent, it is not in the 1-inch SFHMA layers. The AV distribution is non-uniform and very high in magnitude, particularly at the bottom of the lower lift, with a peak of about 13.5 percent. If rain water infiltrates through, it will obviously be trapped within the bottom zone of the 1-inch SFHMA layer. This is undesirable and a reflection of the unfavorable mix workability and constructability problems of the SFHMA mixes.

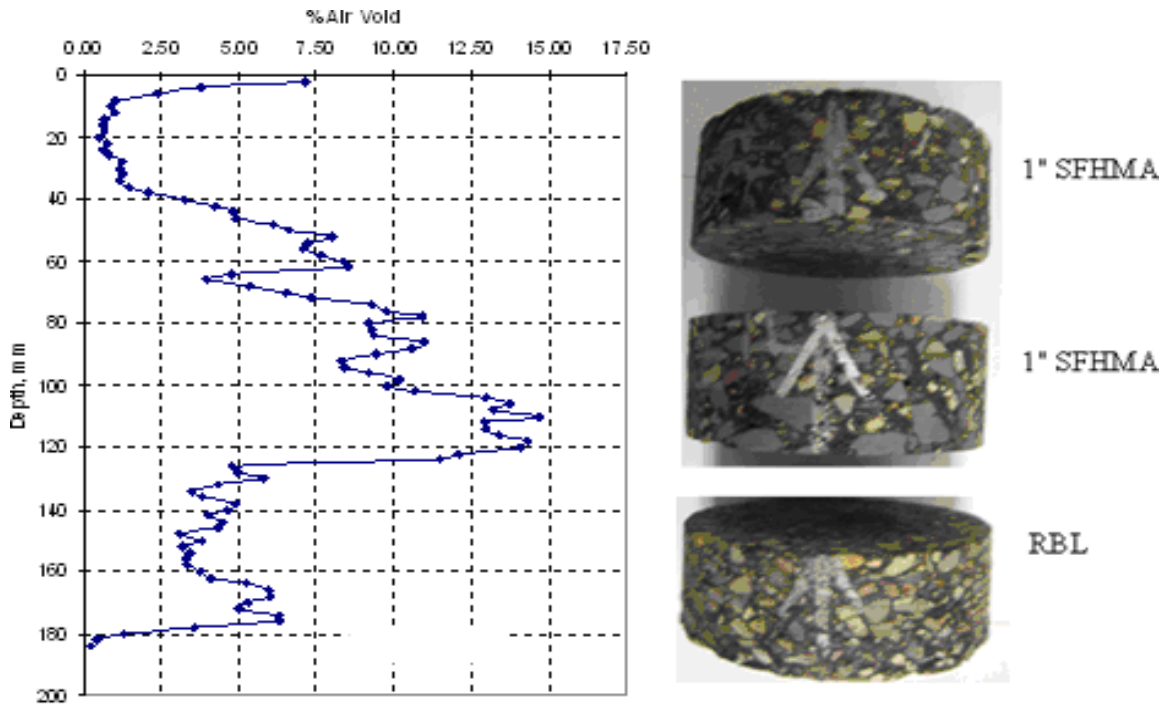


**Figure 4-5. X-Ray CT Results for IH 35 Laredo Cores (Price).**

Overall, the X-ray CT results were found to be consistent with the AV measurements discussed earlier in this chapter and the permeability results reported in [Table 4-4](#). The average laboratory measured core AVs were 8.9 and 6.7 percent for the SFHMA and RBL cores, respectively, with COVs values of 31 and 12 percent, respectively. Undoubtedly, a COV of 31 percent is indicative of high variability in the SFHMA core AV. As evident in [Table 4-4](#), the SFHMA and RBL show high (very porous) and zero (non-porous) permeability, respectively, which are fairly consistent with the X-ray CT AV distribution results. Thus, one of the solutions to mitigate the potential for moisture problems within the SFHMA layers, that could compromise the whole PP structural integrity, is to have well constructed impermeable surface layers.

During construction of the SH 114 project in 2006, the RBL and the clay backfill on the shoulder front slope created a “bathtub” with water retained within the 1-inch SFHMA layer ([Walubita and Scullion, 2007](#)). Provision of relief trenches and edge drains as well as application of a water proofing chip seal (on top of the 1-inch SFHMA layer) served to drain the water off and minimize future surface water ingress on this project. GPR measurements taken on this project later in summer 2009 showed no evidence of moisture presence within the PP structure, suggesting that the remedial measures were satisfactory.

## SUMMARY

The major findings from this chapter are summarized as follows:

- The SFHMA mixes were found to be stiffer with higher resistance to permanent deformation and rutting than other mixes used in PP structures. The average moduli values were substantially high, averaging about 1286 ksi at 77 °F with a range of 800 to 2500 ksi. The mixes satisfactorily passed the Hamburg criteria with rut depths below 9 mm after 20,000 load passes. Based on these findings, future SFHMA designs should consider using 800 to 1200 ksi as the design moduli range.
- In terms of cracking resistance, the SFHMA mixes performed poorly with an average number of OT cycles less than 100. However, resistance to cracking is a secondary consideration provided other aspects of construction are properly executed; these mixes will not encounter significant tensile forces because of their location within the PP structure. The SFHMA mixes were also found to be highly porous, with an average measured permeability value of  $1.42 \times 10^{-3}$ , very close to the measured PFC value of  $1.63 \times 10^{-3}$ . This is a cause for concern in terms of the potential for moisture damage, and this is attributed to the SFHMA coarse gradation and poor workability characteristics. Thus, it is imperative to have well constructed impermeable surface layers, particularly where the SFHMA mixes serve as the intermediate or bottom layers.
- Compared to other mixes, the SFHMA were associated with workability and compactability problems in the lab. Target AV attainment was very problematic and hardly uniform as evidenced by the X-ray CT scanning tests. Modifying the SFHMA mix-design by increasing the finer fractions content (i.e., sizes below the #8 sieve size) and/or increasing the design OAC is strongly recommended for improving the workability, compactability, cracking resistance, and impermeability properties of the SFHMA mixes. It should be noted that project specifications for these mixtures initially required SFHMA mixtures within 4 inches of the surface to be designed using the SP gyratory compactor with an  $N_{des}$  of 125 gyrations, and mixtures lower in the structure at an  $N_{des}$  of 100. Current (2004) specifications leave the  $N_{des}$  up to the engineer and generally these values have decreased; one expected result is higher AC contents.

- As designed, the RBL mixes were found to have superior cracking resistance and impermeability properties, but poor resistance to permanent deformation and rutting; majority failed at 10,000 load passes in the Hamburg rutting test. However, resistance to rutting is a secondary consideration because of the deep location of these mixes with the PP structure. The average measured number of cycles to failure in the Overlay test was over 600, more than 10 times the SFHMA mixes. The RBL mixes were found to be very workable, easily compactable (more uniform AV distribution) and highly impermeable mixes. In the lab, no water flow was measured through these mixes in the permeability test, i.e., zero permeability.
- Laboratory performance for the PFC and the SMA mixes was as expected. The PFC mixes were found to be of low structural value and very porous, with an average measured permeability value of  $1.63 \times 10^{-3}$ . However, while the SMA exhibited high laboratory resistance to rutting based on the Hamburg test, OT cracking resistance performance was variable and poor, particularly for the field-extracted cores. Some SMA cores had as few as only eight OT cycles to failure. This was primarily attributed to construction quality issues.
- On a comparative note, the Laredo mixes were generally found to be stiffer with higher moduli values and higher resistance to permanent deformation. However, they exhibited the poorest cracking resistance in the Overlay test, particularly for the field cores.
- In terms of statistical variability, higher variability in the laboratory test results, measured in terms of the coefficient of variation, was observed for the coarse-graded SFHMA, the SMA, and the PFC mixes. Test results were least variable for the dense-graded RBL mixes. This finding is considered to be attributed to better workability and compactability properties of the RBL mixes that allow for attainment of a consistent and uniform AV distribution.
- The asphalt binder content and aggregate extraction tests based on the Troxler ignition oven indicated non-compliance with the TxDOT operational tolerances on some projects, particularly for the SFHMA layers. Construction deficiencies and possible asphalt binder absorption by absorptive aggregates (especially certain limestones) were factored as the probable causes. Nonetheless, these results emphasize the need for tighter quality control in future SFHMA construction projects. By contrast, the RBL and most of the dense-graded (Type B and C) mixes/layers were generally compliant with the TxDOT operational tolerances, both in terms of the asphalt binder content and aggregate gradations.

## **CHAPTER 5**

### **FIELD TESTING AND PERFORMANCE EVALUATION**

Numerous field tests were conducted periodically (i.e., every winter [for crack-related distresses] and summer [for rutting-related defects]) to monitor and evaluate the performance of the Texas PP sections. These field tests are discussed in this chapter and include visual surveys for surface defects and cracking, surface rut measurements, surface profile measurements, FWD testing, and forensic evaluations through the GPR measurements and coring. A summary is then provided at the end of the chapter to highlight the main findings and pertinent recommendations made thereof. Detailed results and findings of the Texas PP field performance tests are documented elsewhere ([Walubita et al., 2009](#)).

In general, performance has been very satisfactory to date (2009) with no visible or structural defects such as rutting or fatigue cracking; see photographs in [Appendix C](#). The existing PP structures were found to have sufficient strength and stiffness, with high in situ moduli values (> 1000 ksi) and low surface rutting (< 0.15-inches). Ride quality as of summer 2009 was excellent with an average IRI of 62 in/mi based on surface roughness measurements.

However, there were instances of poor construction joints and construction-related cracking on some projects. The GPR also indicated construction-related subsurface anomalies such as in-situ density variations and localized voided areas within the SFHMA layers. All these issues are discussed in this chapter.

#### **VISUAL SURVEYS**

No visual surface defects were observed except for the poorly constructed open longitudinal and transverse construction joints on some projects, notably IH 35 (Gilbert, Zumwalt 01 and 02) and SH 114 (Superpave). Photos of some of these open construction joints are shown in [Figure 5-1](#). Conjecture is that poor joint compaction techniques are responsible for these deficiencies. Moisture ingress through the open construction joints, particularly during the rainy season, could eventually impact the PP structural performance. Based on these visual observations, recommendations were subsequently made to strip seal all the open construction joints. Recommendations were also made for future jobs to rigidly enforce the joint construction and compaction specifications, as well as the QC/QA evaluation protocols.

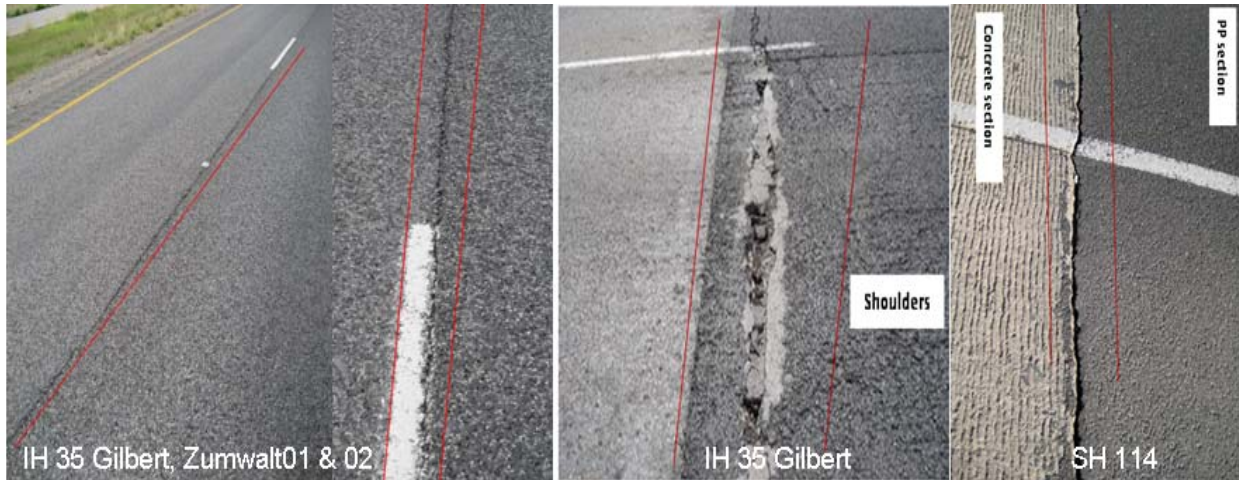


**Figure 5-1. Examples of Open Longitudinal and Transverse Construction Joints.**

As evident in [Figure 5-1](#), open longitudinal construction joints occurred at the interface between the main lanes, and is attributed to poor joint compaction, poor joint staggering, and the effects of trench construction. Open transverse construction joints occurred at the interface between the existing non-PP and PP sections, with particular severity at the transitioning point with adjoining concrete sections. Thus, better construction methods for transitioning between HMA and concrete pavements need to be used. The transverse joints were often more open in the shoulder areas.

## **CRACKING**

No fatigue-related cracking was observed; however, there are areas of construction-related longitudinal cracking on the IH 35 Gilbert project in the northbound lane between TRM 58+0.000 and 59+0.000. The cracking is believed to be surface initiated and is primarily related to the construction joint; it was apparent at this location that the joint was not adequately staggered with underlying mats. As shown in [Figure 5-2](#), the longitudinal cracking, which was about 400 ft long as of summer 2009, runs parallel to the construction joint at approximately 1 ft apart in the outside NB lane. From the core shown in [Figure 5-2](#), it is clear that the cracking initiated from the surface and is progressing downwards; the upper SMA and  $\frac{3}{4}$ -inch SFHMA layers disintegrated while the lower layers were relatively solid. In other areas however, the cracking had already progressed through the entire HMA including the RBL to the base; see the cores in [Figure 5-3](#).





**Figure 5-2. Longitudinal Cracking on IH 35 (Gilbert Job).**



**Figure 5-3. Coring along the Longitudinal Crack on IH 35 (Gilbert Job).**

Secondary causes of the longitudinal cracking on this section include traffic loading (bending effects due to the construction joint edge effect and proximity to the wheel path), poor construction practices (compaction technique/trench construction), poor bonding between lifts, and poor mix-design. All the HMA layers in this structure were found to be excessively stiff and brittle. As was discussed in [Chapter 4](#), the HMA mixes gave the poorest Overlay test performance of any of the Texas perpetual pavements in terms of laboratory cracking resistance, particularly for the field cores. As shown in [Figure 5-3](#) on the right-hand side core, the OT cycles (the numbers in parentheses) were in fact one-digit numbers for the top HMA layers, i.e., 8, 9, and 2 for the SMA,  $\frac{3}{4}$ -inch SFHMA, and 1-inch SFHMA, respectively.

With respect to the mix-design, the SMA and the 1-inch SFHMA layers had about 5.6 and 3.8 asphalt-binder content, respectively, from QC/QA ignition oven tests. The typical design OAC for the Texas SMA mixes is 6.0 percent; 5.6 percent, therefore, reflects a 7.0 percent deviation. For the 1-inch SFHMA layer, the design OAC was 4.3 percent while that derived from the ignition oven test was only 3.8 percent; see [Table 4-2](#) in [Chapter 4](#). Clearly, these QC/QA ignition oven-derived asphalt binder contents are out of the  $\pm 0.3$  percent operational tolerance. These low AC contents could have been a contributing factor to the poor cracking performance.

By contrast however, GPR measurements and further coring in the middle of the lane indicated that the adjacent areas away from the proximity of the construction joint were satisfactory. As shown in [Figure 5-4](#), coring from in-between and along the wheel paths indicated no evidence of cracking, suggesting that the longitudinal cracking is only occurring within the proximity of the construction joint and therefore, must be construction joint related. The core in [Figure 5-4](#) (away from the construction joint) is solidly intact compared to the badly deteriorated cores in [Figures 5-2](#) and [5-3](#) (along the crack and close to the construction joint).

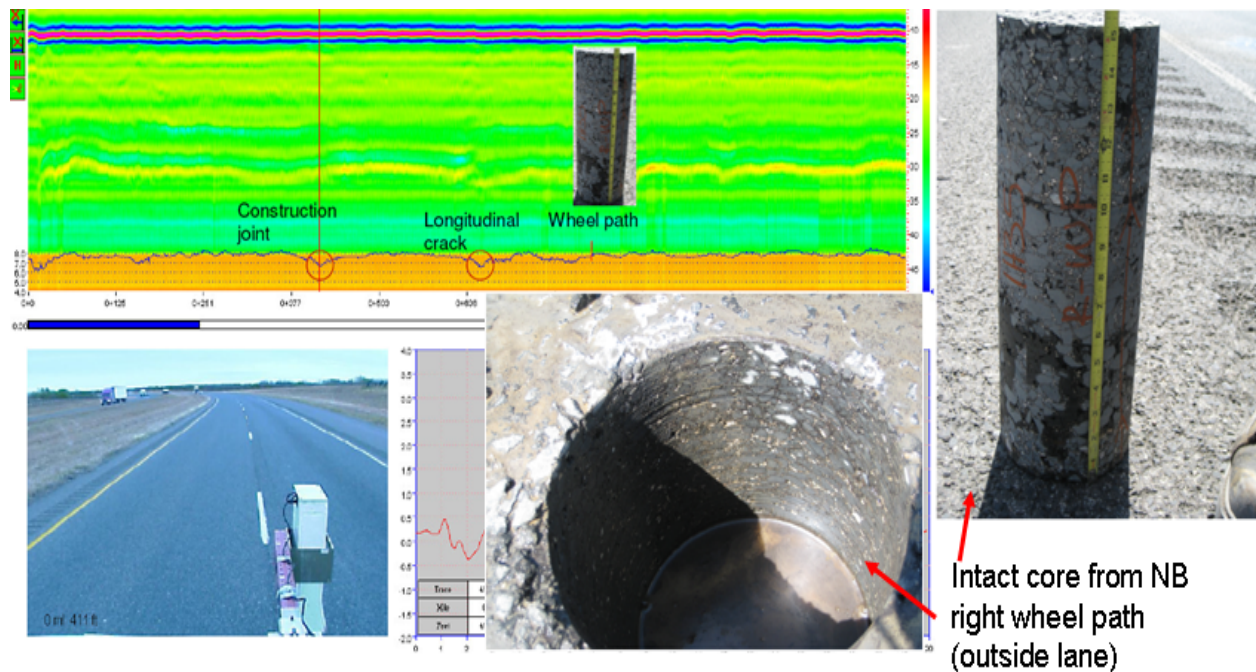


**Figure 5-4. GPR Measurements and Coring from the Wheel Path (IH 35 Gilbert Job).**

As a minimum, recommendations were made to strip seal all the longitudinal cracks and construction joints, so as to minimize moisture ingress and reduce further damage to the pavement structure. Continued performance monitoring of this section is also strongly recommended. In view of these observed problems, mitigation measures in future jobs should include the following:

- better enforcement of construction joint staggering,
- use of richer mix-designs (the comparative Overlay tester results are shown below),
- avoiding reductions to designed AC content,
- improvement of the construction processes—enforce the joint compaction specification; and
- avoiding trench-type construction practices that inherently limit joint staggering and proper edge compaction.

### SURFACE RUT MEASUREMENTS

A straightedge was used to measure the surface rut profiles along the PP sections at selected TRM and GPS locations in the wheel paths (both left and right). [Figure 5-5](#) shows an example of the summer 2009 surface rut measurements on the IH 35 Price project in Laredo. A summary of all the summer 2009 surface rut measurements is shown in [Figure 5-6](#).

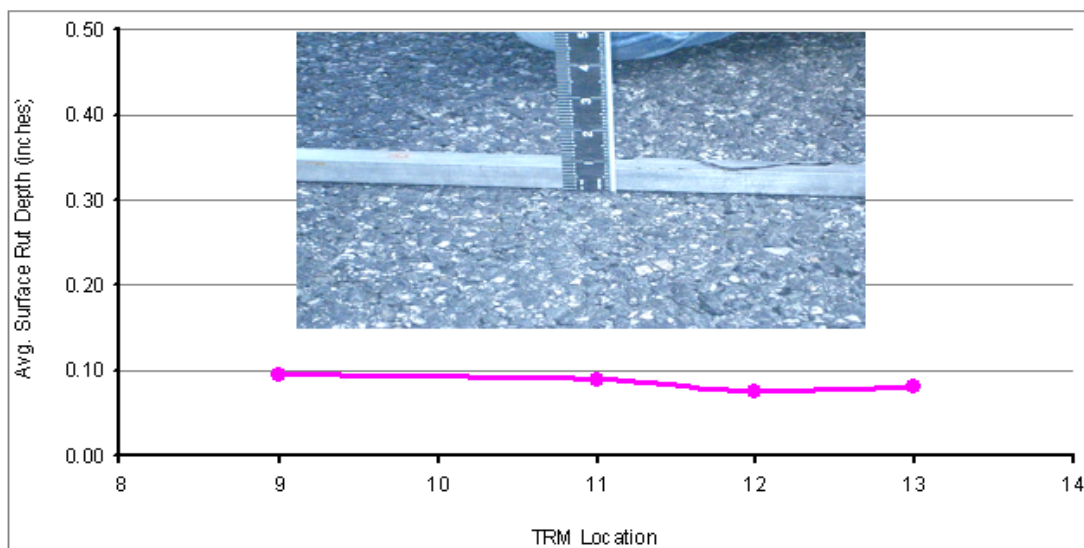


**Figure 5-5. Example of Summer 2009 Surface Rut Measurements on IH 35 (Price Job).**

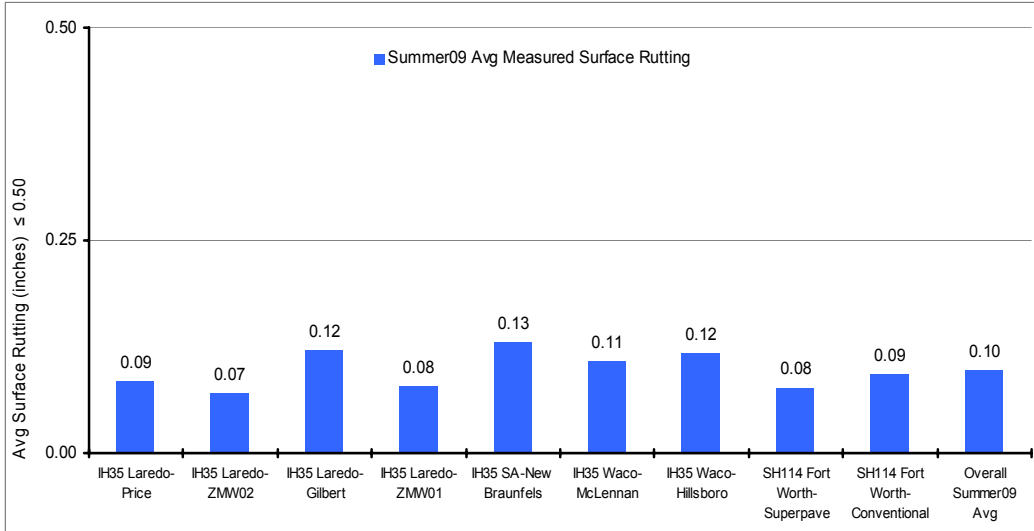


**Figure 5-6. Average Summer 2009 Surface Rut Measurements – All PP Projects.**

Both Figures 5-5 and 5-6 show negligible surface rutting of less than 0.15 inches. In fact, in the summer 2009, the overall average was only 0.10 inches. This is significantly marginal if 0.50 inches is utilized as the benchmark. Ultimately, these results indicate that the Texas PPs are very stiff rut-resistant structures as designed; needless to say that the majority of these PP sections had not been in-service for over 5 years at the time of this report and therefore some of the measured rutting could actually be due to HMA densification of the surface layers under traffic.

## **SURFACE PROFILES AND IRI MEASUREMENTS**

Profile measurements and IRI computations for surface roughness indicated that the PP structures had satisfactory ride quality. The average computed summer 2009 IRI was only 62 in/mi, which is significantly less than the MEPDG terminal limit of 172 in/mi. Again, the Texas PP structures are still relatively new and therefore continued long-term performance monitoring is still warranted.

Figures 5-7 and 5-8 show some examples of the IRI plots for SH 114 (Superpave) and IH 35 (Hillsboro) as a function of longitudinal mile offsets and year of profile measurements. The numbers represent an average of the left and right wheel paths for the outside lanes that are heavily trafficked (as compared to the inside lane). Examples of detailed left and right wheel path IRI plots are included in Appendix C.

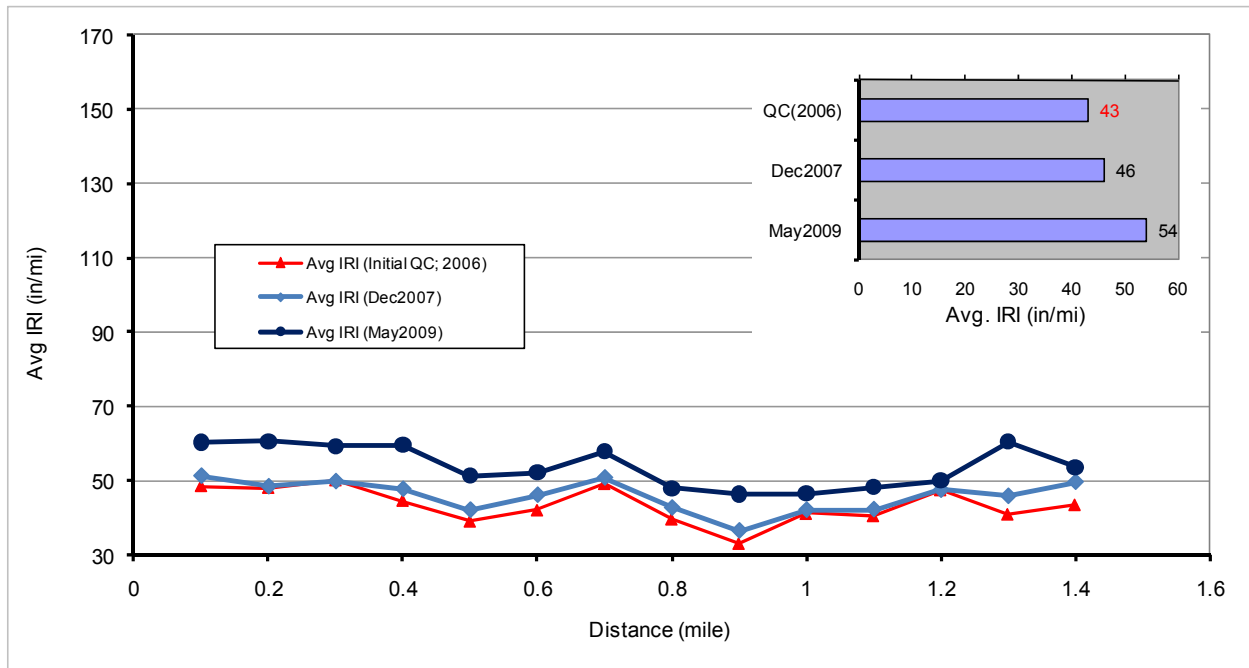


**Figure 5-7. Average IRI Plots for SH 114 (Superpave) – Outside EB Lane.**

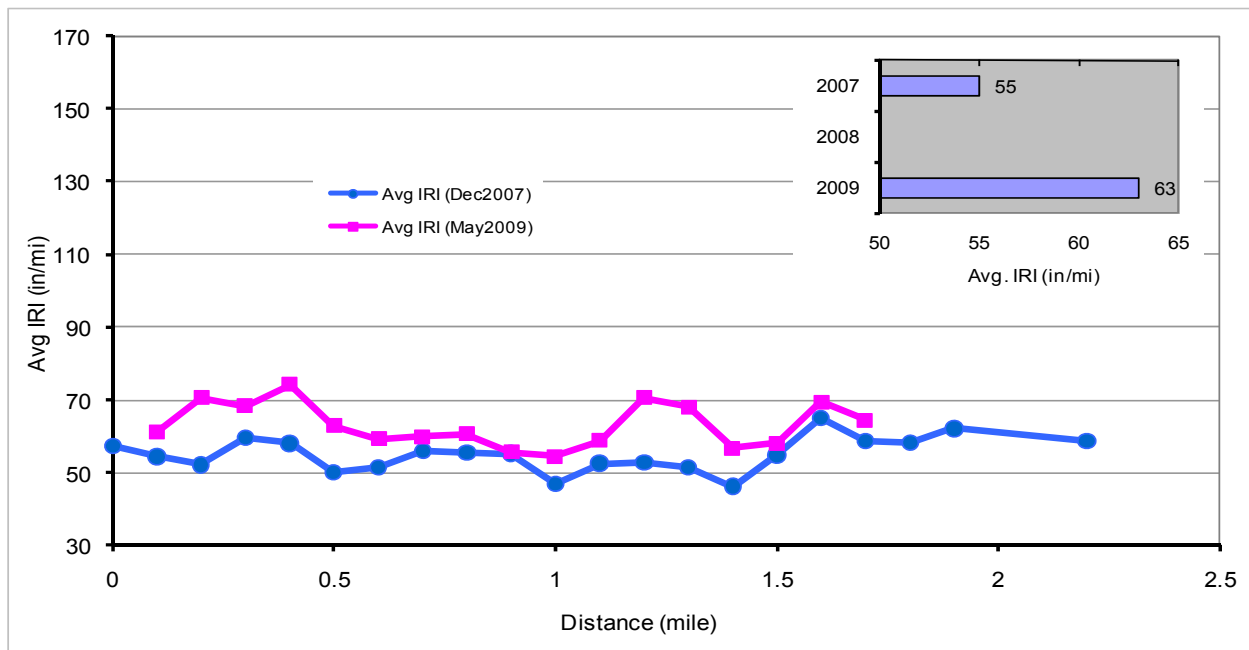


**Figure 5-8. Average IRI Plots for IH 35 (Hillsboro) – Outside NB Lane.**

As would be expected, both the above figures indicate a slight decline in ride quality based on the increasing IRI values in magnitude. [Table 5-1](#) shows a summary of the average IRI for all the Texas PP projects.

**Table 5-1. Average IRI Measurements (All PP Projects).**

| <b>Project</b>                | <b>QC/QA (2005/2006)</b> | <b>2007</b> | <b>2008</b> | <b>May 2009</b>    |
|-------------------------------|--------------------------|-------------|-------------|--------------------|
| IH35 Laredo-Price             |                          |             |             | 63                 |
| IH35 Laredo-ZMW02             | 55                       |             | 55          | 56                 |
| IH35 Laredo-Gilbert           |                          |             | 57          | 62                 |
| IH35 Laredo-ZMW01             | 70                       |             | 61          | 66                 |
| IH35 SA-New Braunfels         |                          |             |             | 68                 |
| IH35 Waco-McLennan            |                          |             |             | 67                 |
| IH35 Waco-Hillsboro           |                          | 55          |             | 63                 |
| SH114 Fort Worth-Superpave    | 43                       | 46          |             | 54                 |
| SH114 Fort Worth-Conventional | 40                       | 45          |             | 55                 |
| Overall average               | 52                       | 53          | 61          | 62                 |
| MEPG Threshold                | 63 (initial)             |             |             | 172 (after 20 yrs) |

As evident in [Table 5-1](#), the IRI results indicate acceptable surface roughness with scores placing sections in the good-to-very good ride quality categories. Though there is a marginal progressive increase in surface roughness as would be typically expected, the overall average IRI for summer 2009 is still less than 70 in/mi (versus the threshold of 172 in/mi). Based on the overall average IRIs in [Table 5-1](#) and if an exponential surface deterioration rate is subjectively considered, the extrapolated overall average IRI in 2025 (after 20 years of service) would be only 123 in/mi, which is still less than the 172 in/mi threshold; about 40 percent less. [Figure 5-9](#) demonstrates this extrapolative plot.

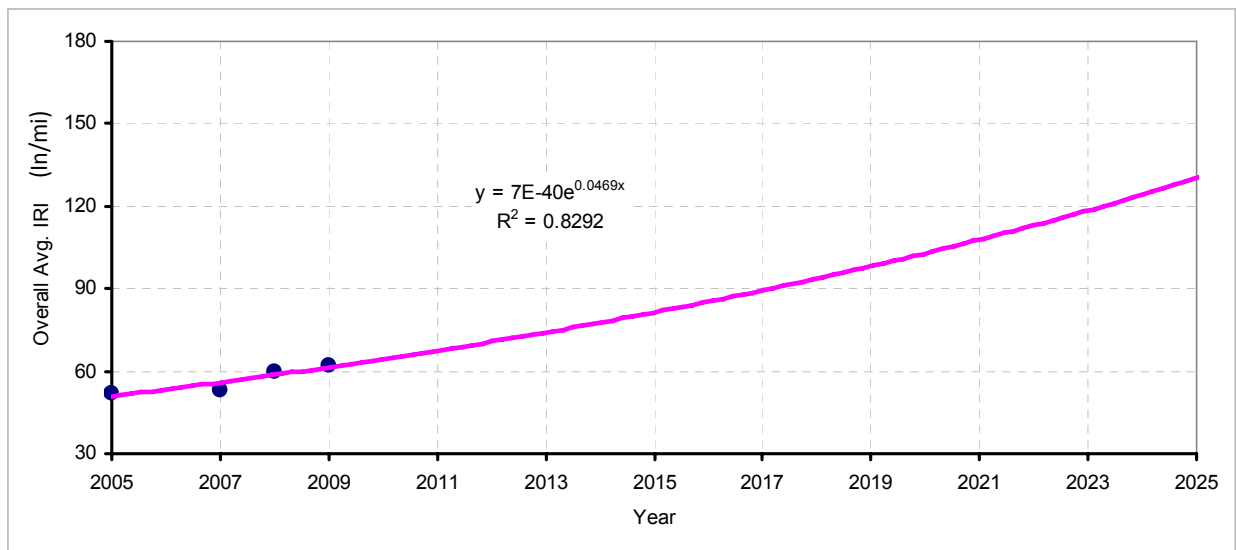


**Figure 5-9. Extrapolative Plot of the Overall Average IRI.**

With the exception of ZMW01, all jobs at their initial constructed state were well within the excellent category based on the Texas QC/QA IRI thresholds listed below:

- $30 \leq \text{QC/QA IRI} \leq 65$  in/mile:           excellent (\$600 bonus per mile)
- $75 \leq \text{QC/QA IRI} \leq 90$  in/mile:           poor (\$400 bonus per mile)
- QC/QA IRI  $> 90$  in/mile:                very poor (re-do)

The MEPDG suggests an initial IRI of 63 in/mi; therefore, these PP structures are satisfactory. Explanations for the high initial QC/QA IRI for ZMW01 were inconclusive as these measurements were not done by TTI but TxDOT. Nonetheless, possible causes were that the profile measurements were done on different locations compared to those done later. Another possible explanation is that the initial HMA densification under traffic could have evened out the roughness (bumps and dips) that existed in the initial IRI measurements just after construction.

## **FWD MEASUREMENTS**

During FWD testing, the impact load ranged from 9 kips (standard load) to 18 kips (particularly for the winter tests). The FWD tests were conducted intermittently along the PP section in the wheel paths. Pavement temperatures were also measured and recorded periodically during testing. Data from the FWD measurements were analyzed and grouped into three categories, namely: surface deflections, curvature indices, and moduli determination. The results and analyses are presented in this section. Detailed results can be found in [Walubita et al. \(2009\)](#).

### **FWD Surface Deflections**

Even under summer pavement temperatures of over 100 °F, the surface deflections were less than 10 mils. In fact, the overall average for summer 2009 was only 5.0 mils. As expected, the deflections were least in winter, with an overall average of only 2.2 mils. Evidently, these results re-affirm the fact that the Texas PPs are very stiff and non-temperature susceptible structures, with high potential for rutting resistance. Some examples of the FWD deflection results are shown in [Figure 5-10](#) for IH 35 (Laredo), while [Figure 5-11](#) shows the overall average for both winter and summer seasons.

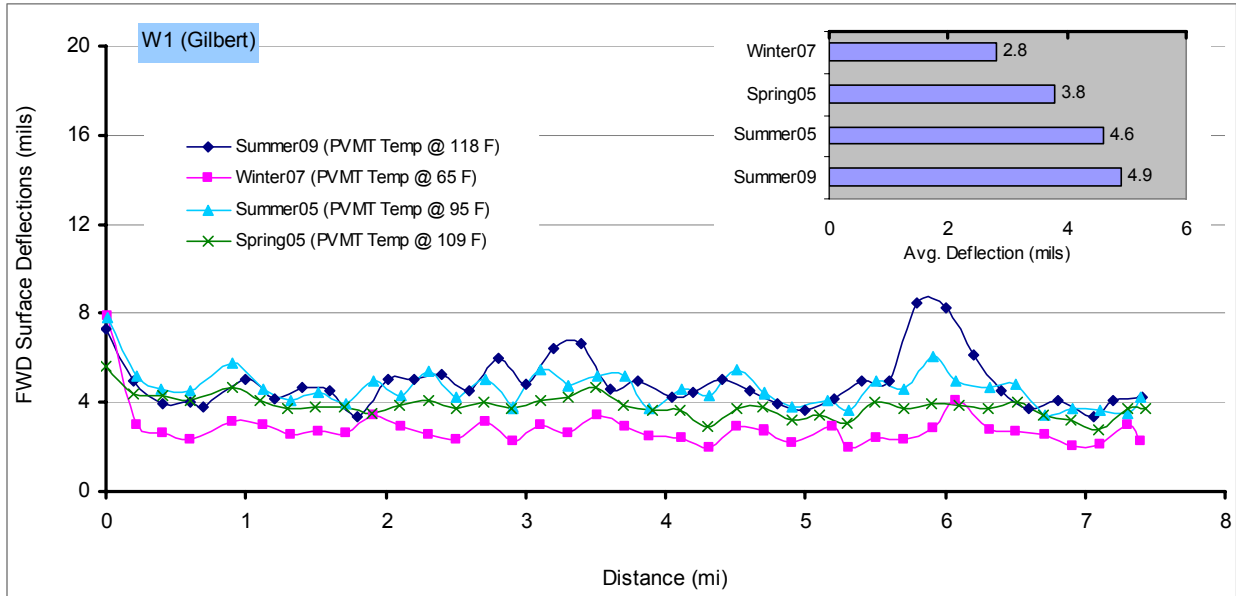


**Figure 5-10. Plot of FWD Deflections on IH 35 Gilbert (Laredo).**

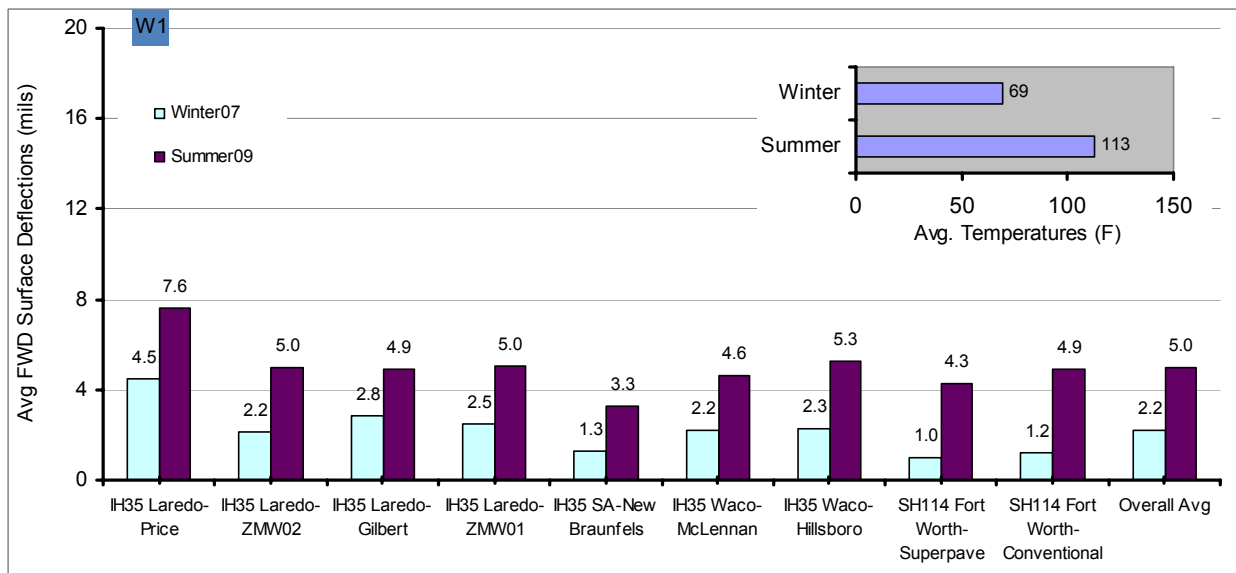


**Figure 5-11. Average FWD Surface Deflections (Winter and Summer).**

Both Figures 5-10 and 5-11 show considerable differences in the winter and summer deflections, believed to be almost wholly attributed to the pavement temperature differences, i.e., 69 versus 113 °F (Figure 5-11). Considering the visco-elastic nature of HMA, this temperature difference definitely played a role. For Figure 5-10, the summer deflections (2005 and 2009) are marginally indifferent especially if the pavement temperature differences are considered.



While [Figure 5-10](#) shows a peak of about 8.5 mils at 6 miles, [Figure 5-11](#) shows an average peak of 7.6 mils for the IH 35 Price project in Laredo. In fact, 8.5 mils was the maximum summer peak deflection measured on these PP projects. The overall summer 2009 average at an average pavement surface temperature of 113 °F was 5 mils.

### FWD Curvature Indices

In this project, the concept of the curvature index was also utilized to assess the structural strength of the PP structures. These curvature indices defined as surface curvature index (SCI) for the composite HMA layers, base curvature index (BCI) for the base, and subgrade curvature index ( $W_7$ ) for the subgrade were computed as follows ([Scullion, 2005](#)):

- Composite HMA layers;       $SCI = W_1 - W_2$  (SCI ≤ 4.0, good HMA)      (Equation 5-1)
- Base;       $BCI = W_2 - W_3$  (BCI ≤ 2.0, good base)      (Equation 5-2)
- Subgrade;       $W_7$  ( $W_7$  ≤ 2.0, good subgrade)      (Equation 5-3)

In [Equations 5-1](#) through [5-3](#),  $W_i$  is the average surface deflection measured from the  $i^{\text{th}}$  sensor of the FWD loading plate. In applying these equations and interpreting the results for PP structures, the following aspects should be considered ([Scullion, 2005](#)):

- The SCI only looks at a total depth of about 8 or so inches below the pavement surface. It therefore does not evaluate the entire HMA thickness in a PP structure, but only the top HMA layers up to approximately 8 inches deep.
- The BCI evaluates the structure from about 8 inches down to about 16 inches. In the case of Texas PP structures, this is actually the lower HMA layers and not necessarily the base or any material below the HMA.
- The subgrade index ( $W_7$ ) evaluates the deeper subgrade, from about 4 ft depth and lower. From an engineering point of view, this depth is usually not economically addressable in terms of improving the material properties.

With the above considerations, both the SCI and BCI were therefore interpreted in the context of the HMA layers in this analysis; top ( $\approx 8$  inches) and lower ( $\approx 8$  to 16 inches) HMA layers, respectively. An example of the curvature index results is shown in [Figure 5-12](#) for IH 35 Zumwalt01 project. Detailed plots are included in [Appendix C](#).

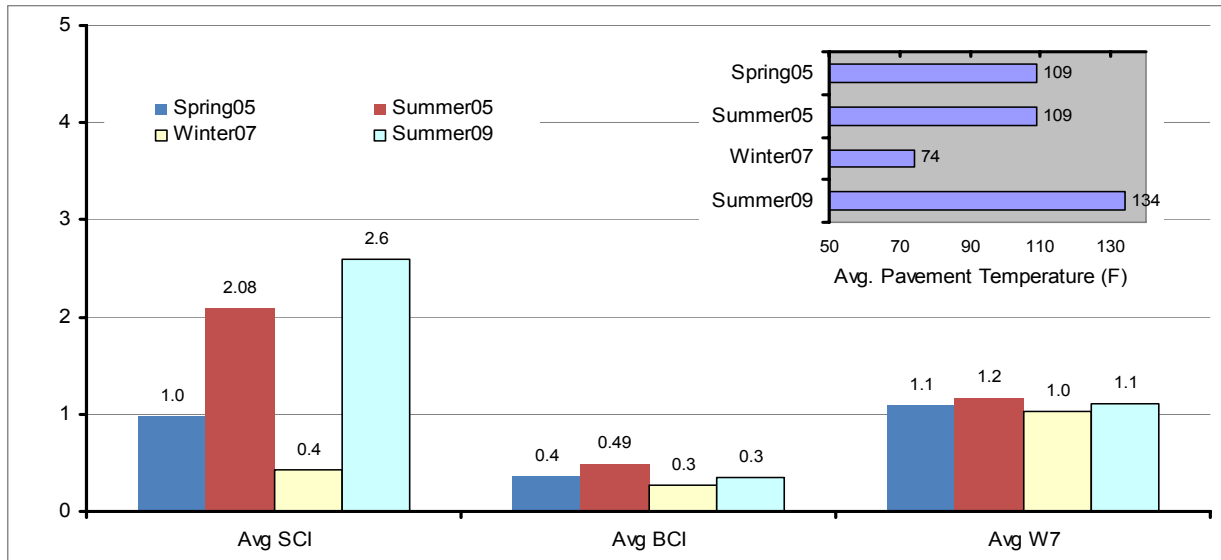


**Figure 5-12. Summary Curvature Index Results for IH 35 Zumwalt 01 Project (Laredo).**

Based on the thresholds indicated in [Equations 5-1](#) through [5-3](#), the IH 35 Zumwalt01 project like all the Texas PP structures, was found to have sufficient structural strength with very good stable HMA materials. In [Figure 5-12](#), all the curvature indices are less than 4, substantiating that the Texas PP structures have sufficient structural strength. This was not surprising considering the greater thickness and substantial stiffness (see modulus results in [Chapter 4](#)) of these Texas PP structures. [Figure 5-13](#) provides an overall summary of the curvatures indices for all the Texas PP structures, with the latest summer 2009 results as follows:

- Average SCI = 2.2                      Good condition and sufficient structural strength
- Average BCI = 0.6                    Good stable condition and sufficient structural strength
- Average  $W_7$  = 1.0                    Good stable condition and sufficient strength

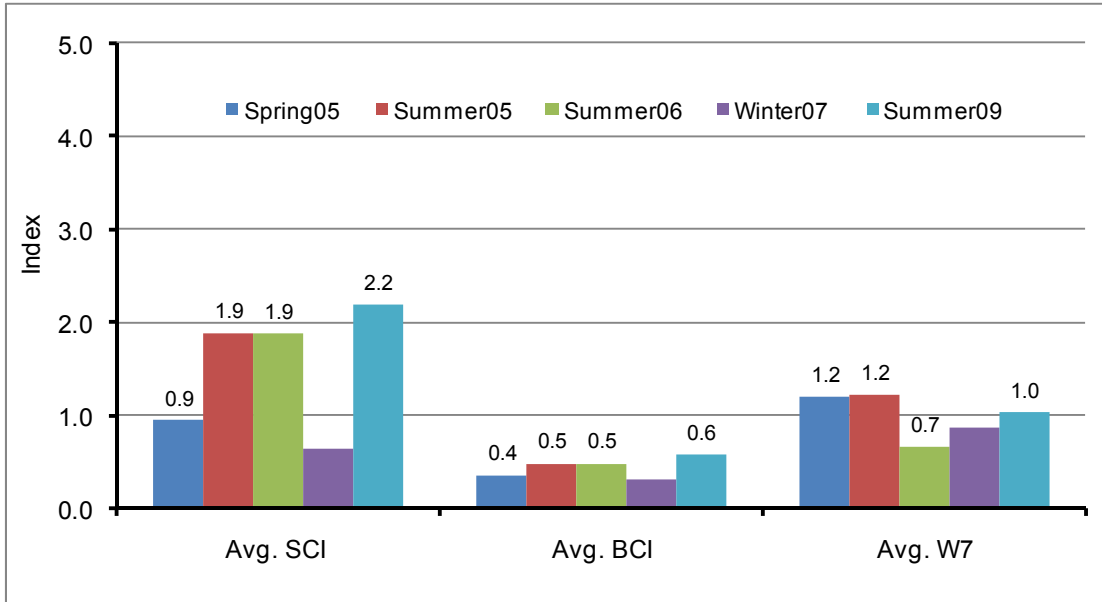


**Figure 5-13. Average Curvature Indices for All the PP Projects.**

Looking at [Figure 5-13](#) without considering temperature corrections for the summer measurements and excluding the winter measurements, both the SCI and BCI indicate an increase in magnitude with time, suggesting a gradual loss in strength with time as would be expected of any structure. Though highly subjective, the exponential extrapolation shown in [Figure 5-14](#) indicate that the Texas PP structures will still retain their structural strength even after 20 years of service.

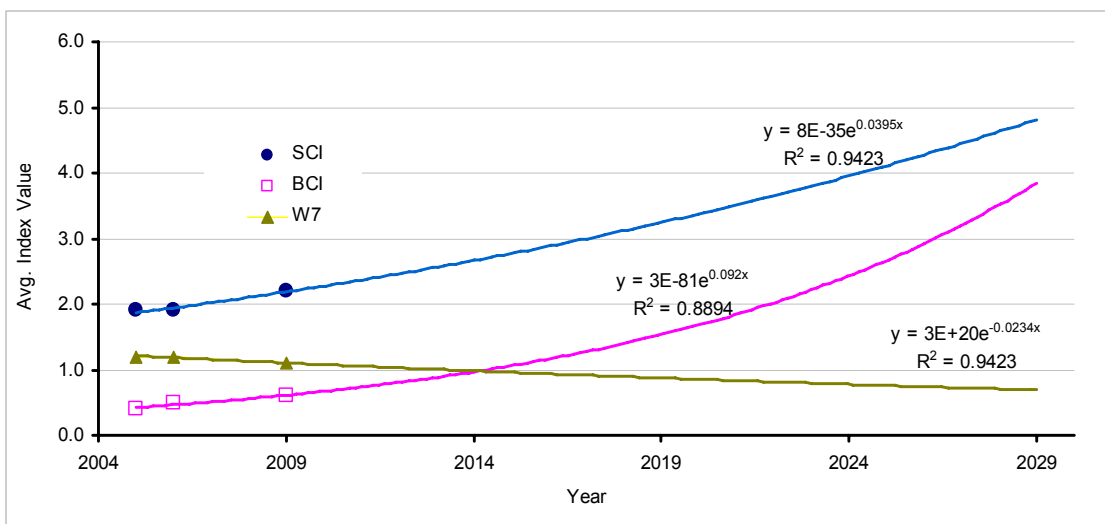


**Figure 5-14. Extrapolative Plot of the Curvature Indices.**

## **FWD Moduli Computations**

In general, it was problematic processing the FWD data to generate moduli values due to the thicker multi-layered nature of these PP structures and limitations of the back-calculation process in evaluating structures with more than four layers. Additionally, FWD moduli back-calculation is itself a very subjective process, and the results presented in this report are no exception. As was observed with laboratory testing, these pavements were found from FWD testing to be very stiff structures with high in-situ moduli values averaging about 1500 ksi, particularly for the SFHMA layers, which is indicative of a high potential for resistance to permanent deformation, as designed.

The average in-situ FWD modulus value for the 1-inch SFHMA layers was 1825 ksi at 77 °F, which is substantially higher than the values of 500 to 700 ksi submitted in the original design proposals. The other HMA layers ranged from 500 to 1500 ksi. The base and the subgrade had FWD back-calculated moduli values greater than 30 and 15 ksi, respectively. Some examples of FWD modulus plots are shown in [Figures 5-15](#) and [5-16](#). On a comparative note and in line with the laboratory test results, the Laredo structures were found to be the stiffest with the highest in-situ 1-inch SFHMA moduli values, averaging about 2100 ksi. A tabulation of the average district moduli values at 77 °F is shown subsequently in [Table 5-2](#). More detailed FWD moduli results including moduli plots and listing per project by layer are included in [Appendix C](#).

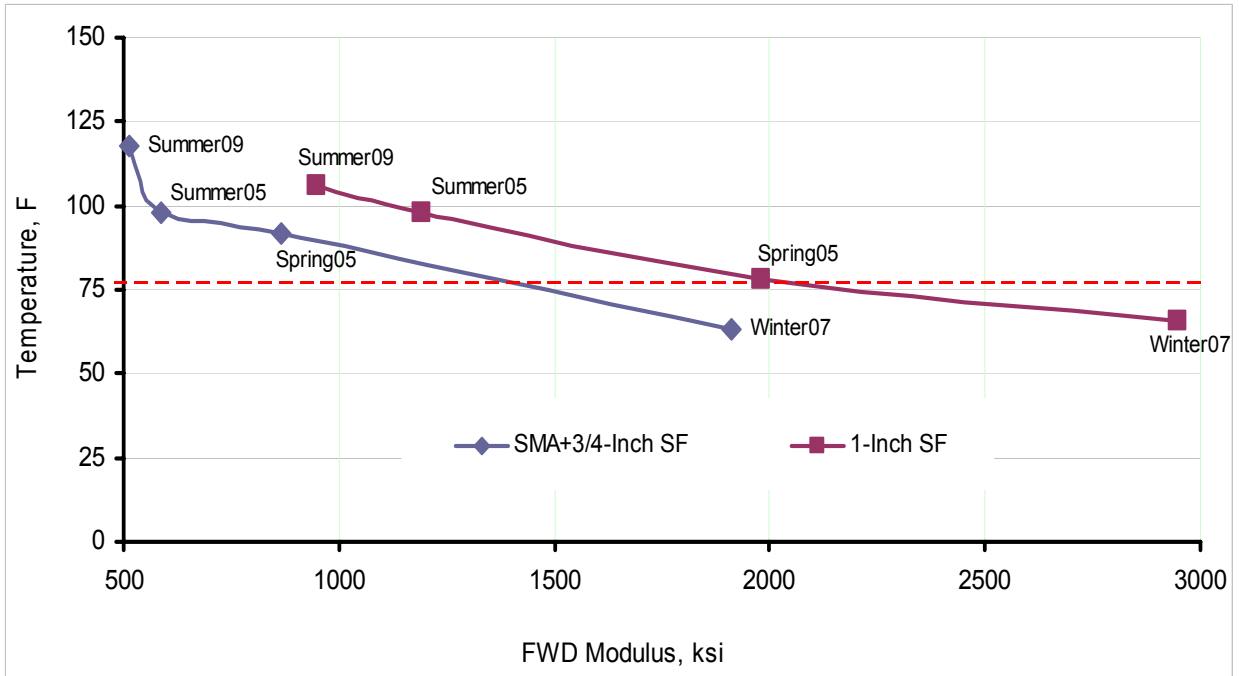


Figure 5-15. Example of FWD Moduli Plots (HMA Layers) for IH 35 Gilbert (Laredo).

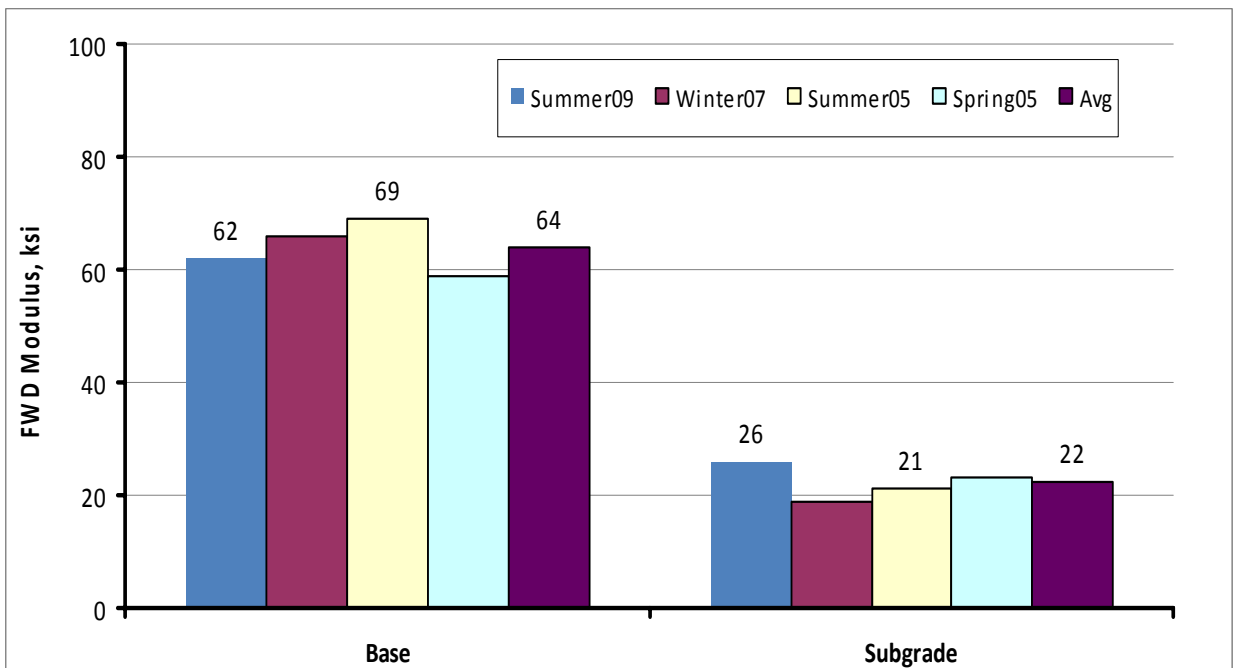


Figure 5-16. FWD Moduli Plots (Base and Subgrade) for IH 35 Gilbert (Laredo).

Based on [Figure 5-15](#), it is clear from interpolation that the 1-inch SFHMA modulus would be around 2100 ksi while that of the composite SMA and ¾-inch SFHMA would be about 1400 ksi at 77 °F, indicating the HMA layers of the Texas PP structures are substantially stiff. Even under summer temperatures of over 100 °F, [Figure 5-15](#) shows that the HMA layer moduli are still greater than 500 ksi, indicating that the HMA mixes used on this structure are only minimally temperature susceptible. The average modulus for the base and subgrade ([Figure 5-16](#)) is about 64 and 22 ksi, respectively, also exhibiting considerable strength with no indication of seasonal variation.

**Table 5-2. District Average In-Situ FWD Moduli Values at 77 °F.**

| Layer        | Average Modulus (ksi) |        |             |      | Overall Average (ksi) |
|--------------|-----------------------|--------|-------------|------|-----------------------|
|              | Fort Worth            | Laredo | San Antonio | Waco |                       |
| SMA          | 850                   | 1130   | 803         | 665  | 862                   |
| Type C       | 700                   | -      | -           | -    | 700                   |
| ¾-inch SFHMA | 850                   | 1127   | 803         | 680  | 865                   |
| Type B       | 1500                  | -      | -           | -    | 1500                  |
| 1-inch SFHMA | 1750                  | 2100   | 1655        | 1793 | 1825                  |
| RBL          | 500                   | 590    | 520         | 524  | 534                   |
| Base         | 74                    | 70     | 70          | 54   | 67                    |
| Subgrade     | 12                    | 22     | 29          | 23   | 22                    |

The HMA back-calculated moduli values in [Table 5-2](#) were normalized to 77 °F by applying a multiplicative temperature-correction factor given by [Equation 5-4](#) below:

$$TCF = T^{2.81} / 200,000 \quad \text{Equation (5-4)}$$

Where  $TCF$  is the asphalt modulus temperature correction factor to 77 °F, and  $T$  is the temperature of the HMA at the time the FWD data were collected. Clearly, [Table 5-2](#) shows the highest HMA moduli values were in the Laredo District. Coring from the Laredo projects had also indicated very stiff-brittle HMA layers. As evident in [Table 5-2](#), the base (at 67 ksi) and the subgrade (at 22 ksi) in all the districts appear to be stable with sound stiffness and no evidence to date of moisture susceptibility. On the IH 35 Zumwalt 02 project where cement treatment was used, the base was found to have an average modulus of 102 ksi and did not vary significantly as a function of season. [Figure 5-17](#) shows these results.

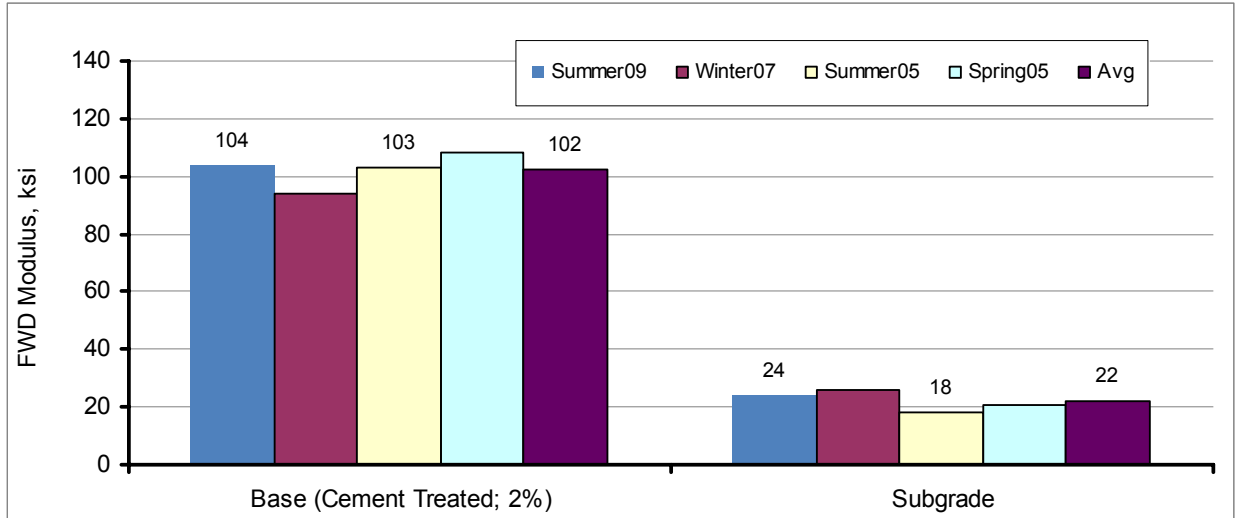


**Figure 5-17. Plot of Base and Subgrade FWD Moduli for IH 35 Zumwalt 02 (Laredo).**

### GPR MEASUREMENTS AND FORENSIC EVALUATIONS

With the exception of a few projects such as those in San Antonio, performance evaluation with the GPR did not detect any serious subsurface anomalies with the Texas PP structures. As evident in [Figure 5-18](#), the San Antonio structures exhibited evidence of density variations and localized voiding within the SFHMA layers, particularly at the lift interfaces. This is cause for concern particularly in terms of moisture and debonding-related problems. Subsequent coring from this section also indicated voiding and vertical segregation in the SFHMA layers. Minimization of moisture ingress through the surface HMA layers should thus be a priority on these projects.

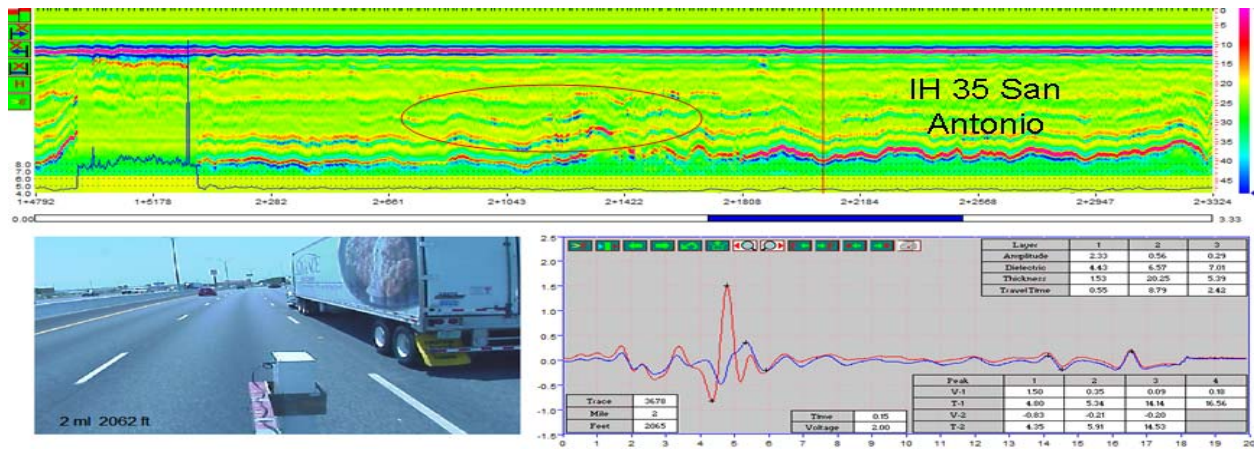
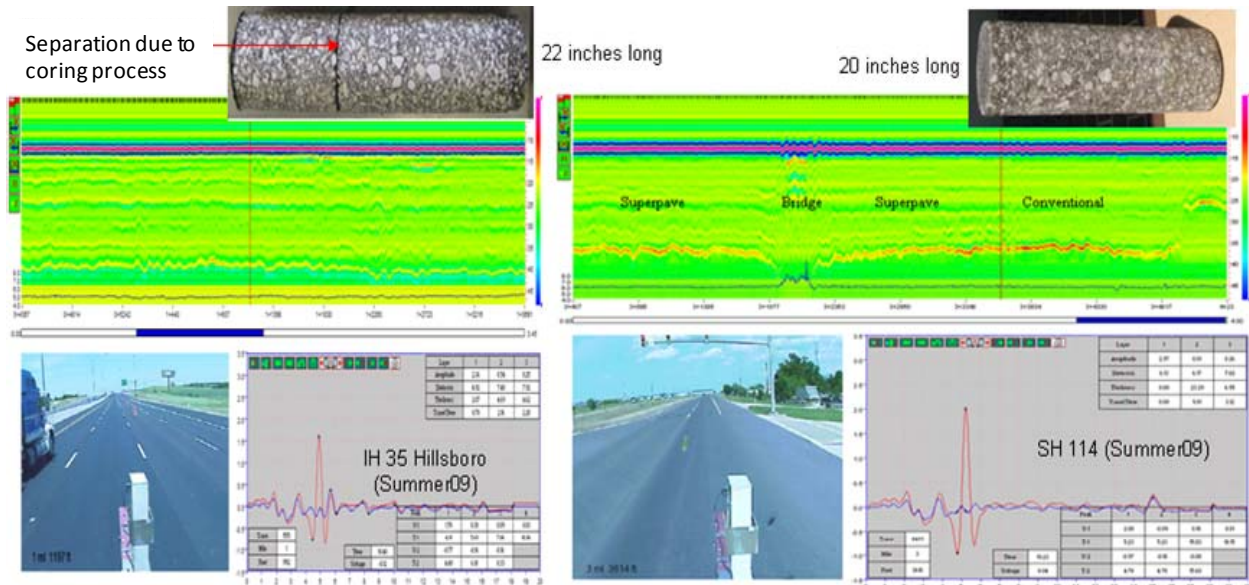


**Figure 5-18. Summer 2009 GPR Measurements on IH 35 (San Antonio).**

GPR measurements did not detect any evidence of subsurface defects on most of the other Texas PP structures. Examples are shown in Figure 5-19 for IH 35 (Hillsboro) and SH 114 (Fort Worth). The GPR readings are clean showing little definition at lift interfaces, and as indicated the cores extracted from these projects were intact full length with no visible defects.





- Surface rut measurements and FWD deflections also indicated that the Texas PP structures were substantially stiff and non-temperature susceptible. The measured surface rut depths were less than 0.15 inches (against the 0.5 inches threshold), while the FWD surface deflections were below 10 mils; all tests done in summer.
- Based on the curvature index concept, the HMA layers were found to have sufficient structural strength, with the computed indices substantially lower than the threshold. The average calculated SCI for the top HMA layers (up to approximately 8 inches deep) was 2.2 (versus the 5.0 threshold). Extrapolative analysis also indicated that the Texas PP sections have the potential to retain their structural strength even after 20 years of service.
- FWD back-calculated moduli results also indicated that both the base and subgrade were fairly stable with sufficient strength and no indication of moisture susceptibility. The average measured numbers were 67 and 22 ksi, respectively, and did not exhibit any significant seasonal variation in terms of the magnitude.
- The surface roughness, which is an indicator of the ride quality, is excellent with the average IRI being 62 in/mi. Extrapolative analysis indicated that the IRI would subjectively be around 123 in/mi after 20 years of service, which is reasonable and still below the 172 in/mi threshold. However, effects of weathering may dictate the need for a surface renewal before then. At an average of 52 in/mi, the measured QC/QA IRI values were also within the construction expectation.
- In the initial structural designs, trial and error lower moduli values were used and these resulted in conservative designs. In future Texas PP designs, recommendations are thus made to consider using the actual measured moduli values documented in this report. Use of these moduli will cost-effectively optimize the Texas PP structural designs.
- Visual surveys as well as GPR measurements and forensic evaluations indicated potential for moisture problems due to open construction joints, associated parallel longitudinal cracking, and SFHMA voiding on some projects. In future construction jobs, it is thus imperative to optimize the joint construction/compaction methods as well as ensuring that the surface HMA layers are impermeable.
- In view of the fact that a majority of these PP sections were just over 5 years in service at the time of this report, long-term performance monitoring is strongly recommended to further validate these findings, particularly the Gilbert project with longitudinal cracking.

- Overall, the GPR was found to be an effective and ideal NDT-tool for performance monitoring and detection of forensic defects. It should be incorporated in future Texas PP performance monitoring efforts.

## CHAPTER 6

### TRAFFIC WIM AND MDD RESPONSE MEASUREMENTS

As a means to validate the Texas PP design concept, WIM traffic and MDD response measurements were conducted on selected projects. The results and analysis of these measurements are discussed in this chapter. More detailed analyses and results are contained in the Texas PP database (Walubita et al., 2009). Traffic comparison evaluations of the initial design and actual traffic counts together with a re-design of the PP structures based on forecasted cumulative traffic loading projected from actual measured traffic data and actual material properties is also presented in this chapter. The chapter then concludes with a summary of major findings and recommendations.

#### WIM TRAFFIC MEASUREMENTS

As shown schematically in Figures 6-1 and 6-2, two WIM stations, designated as Station 531 and 527 were installed within the project limits on IH 35 (Zamwalt 02, Laredo) and SH 114 (Superpave, Fort Worth), respectively, for in-motion traffic counting and axle weight measurements.

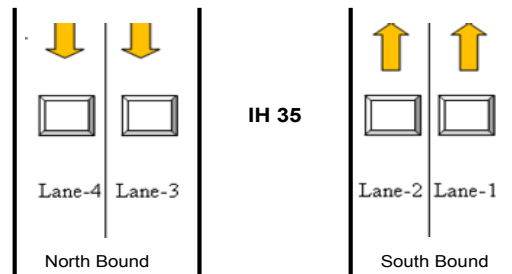


**Figure 6-1. WIM Station 531 – IH 35 Zumwalt02 (Laredo).**

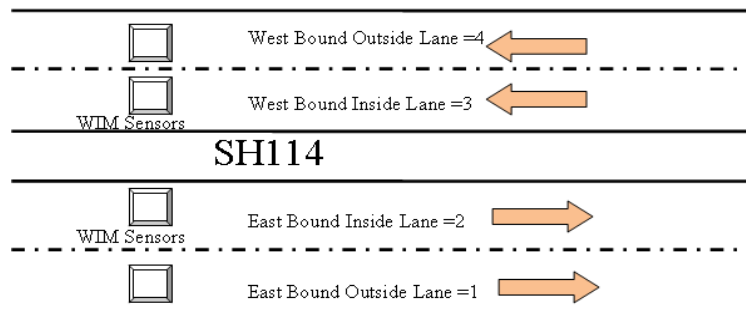


**Figure 6-2. WIM Station 527 – SH 114 Superpave (Fort Worth).**

Both IH 35 and SH 114 have four lanes. IH 35 runs in the north- and southbound (NB and SB) directions, with two lanes in either direction. SH 114 runs in the east- and westbound directions (EB and WB), with two lanes in each direction. On each highway section, WIM sensors were installed on all the lanes designated Lane 1 through 4 as shown in [Figures 6-1 and 6-2](#). The approximate GPS locations of these WIM stations are:

- Station 531 – N 28° 12.860', W 99° 18.236', and 483 ft elevation
- Station 527 – N 33° 02.203', W 97° 25.730', and 880 ft elevation

At the time of this report, only one year's worth of traffic data (2008) had been acquired from both stations despite the WIM stations being in operation since 2005 and 2006. In general, it is problematic acquiring traffic data from state WIM stations and what was acquired from these two stations was incomplete. For instance, up to 34 days' worth of traffic data (9.3 percent) were unavailable or missing for Station 531. Station 527 had 9 days worth of data missing (i.e., 2.5 percent). This means that only 331 and 356 days data were available for analysis for IH 35 and SH 114, respectively. Note that these traffic data were acquired through TxDOT. TTI researchers were not directly involved in the traffic data collection, and therefore, the authors of this report theorize that WIM system breakdown and/or servicing were probable reasons for the missing data.

Also, it was problematic reading and processing the raw traffic data due to differences and inconsistencies in the data formats, i.e., the data format for Station 531 was different from that of Station 527. Nonetheless, TTI researchers managed to develop software that automatically did the traffic analysis. However, due to incompleteness of the data (i.e., some months were missing) and inconsistencies in reporting data for some vehicles classes, only trucks were analyzed in this report. Also, since only one-year's traffic data were made available to the authors, no growth factors were computed in this report. Therefore, assumptions were made to allow for the 20-year traffic estimates.

### **Truck Weight Distributions**

[Figure 6-3](#) displays a plot of total truck weight distributions in kips from both Stations 531 and 527.

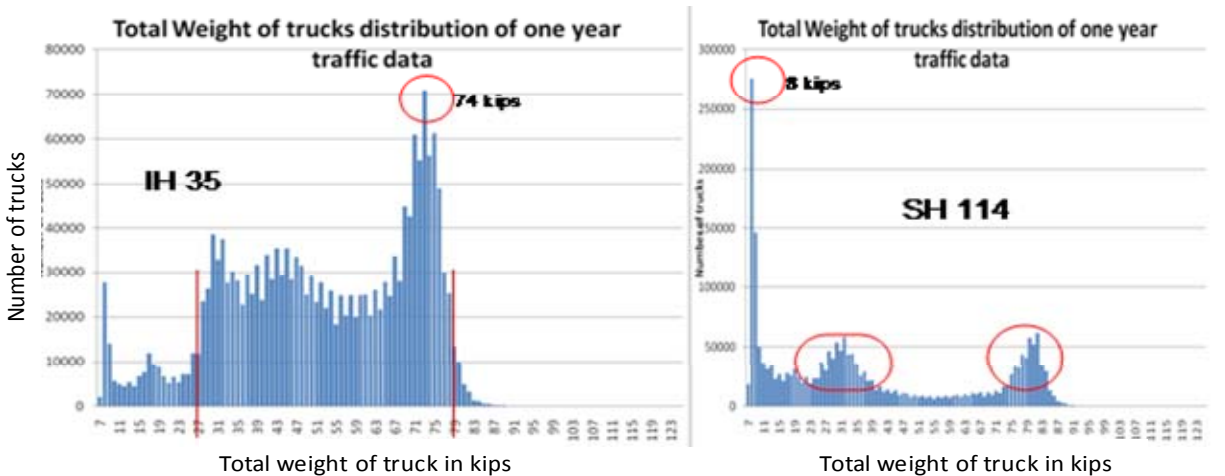


**Figure 6-3. Truck Gross-Vehicle Weight Distributions.**

Figure 6-3 shows two clear distinct distributions for IH 35 and SH 114, with IH 35 showing a peak at 74 kips while SH 114’s peak is at 8 kips. For IH 35, the majority of the trucks (over 80 percent) had gross-vehicle weight (GVW) between 28 and 79 kips. Very few were over 80 kips. In addition to 8 kips, SH 114 has two other peaks at 31 and 81 kips. Based on Figure 6-3, at least 5 percent of the trucks had over 80 kips weight on SH 114. Although marginally small, these results suggest the need for monitoring the 80-kip GVW on this highway. On a comparative note, however, the two 74 and 8 kips peaks suggest that there are more loaded trucks on IH 35 and empty trucks on SH 114. Comparing the vertical Y-axis on each figure, Figure 6-3 shows much higher truck counts on SH 114 compared to IH 35.

### Hourly 18 kip Distributions

Figure 6-4 shows the 18 kip hourly distributions calculated using the following equation for a 24-hour period:

$$\text{Log } Wt = 5.93 + 9.36 \text{ Log } (SN + 1) - 4.79 \text{ Log } (L1 + L2) + 4.33 \text{ Log } L2 + Gt/b \quad \text{Equation (6-1)}$$

Where  $W$  is the axle load applications of end of time  $t$ ;  $SN$  is the structural number;  $L_1$  is the load on one single or one tandem axle set in kips;  $L_2$  is the axle code (1 for single and 2 for tandem axle);  $G_t$  is a function of the change in PSI from initial to final PSI; and  $b$  is a function of design and load variables.

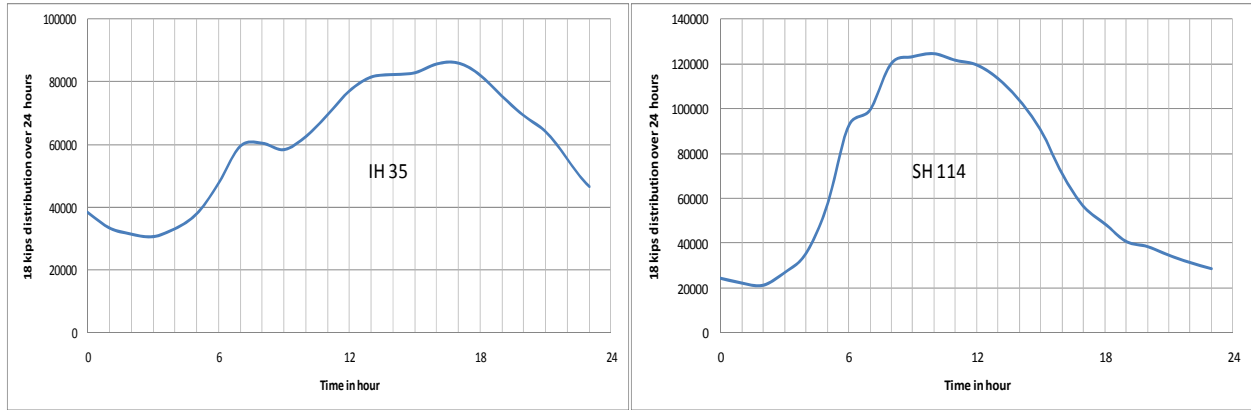


**Figure 6-4. Hourly 18 kips Distributions over 24 Hours.**

Like Figure 6-3, Figure 6-4 shows more 18-kip counts on SH 114. For IH 35, the majority of the truck loading occurs between 10:00 AM and 9:00 PM, with a peak at 5:00 PM, i.e., 85,000 18-kip counts. For the SH 114, majority of the truck traffic occurs between 5:00 AM and 5:00 PM, with a maximum peak at 10:00 AM for 125,000 counts.

### Monthly 18 kips Distributions

Figure 6-5 shows an example on the monthly 18 kips distribution (two-way directions) for the month of August 2008. Results show less traffic loading for the weekend, particularly for SH 114. This is indicative that most of truck traffic occurs during week days, with the weekend accounting only for about 17 percent. Intuitively, these results may also suggest that most of the truck traffic of these highways is commercial/business-related.

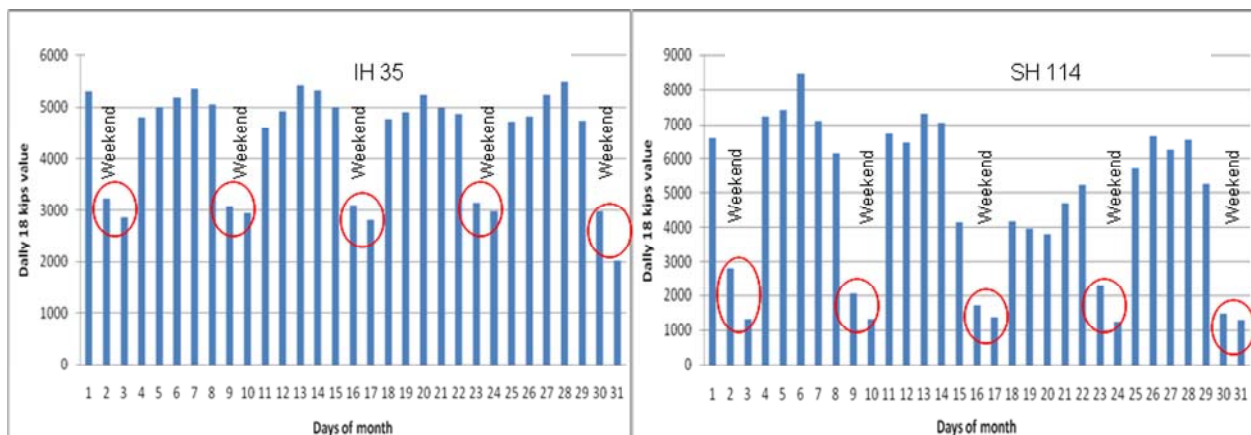


**Figure 6-5. Example of Monthly 18 kips Distributions for August 2008.**

## Axle Load Distributions

Figure 6-6 shows a comparative plot of the axle distributions and indicates that the majority (99.2 percent) of the axle distributions are single (22.8 percent) and tandem (77 percent) axles. Only about 0.2 percent are tridems, with loads ranging from 10 to 80 kips.

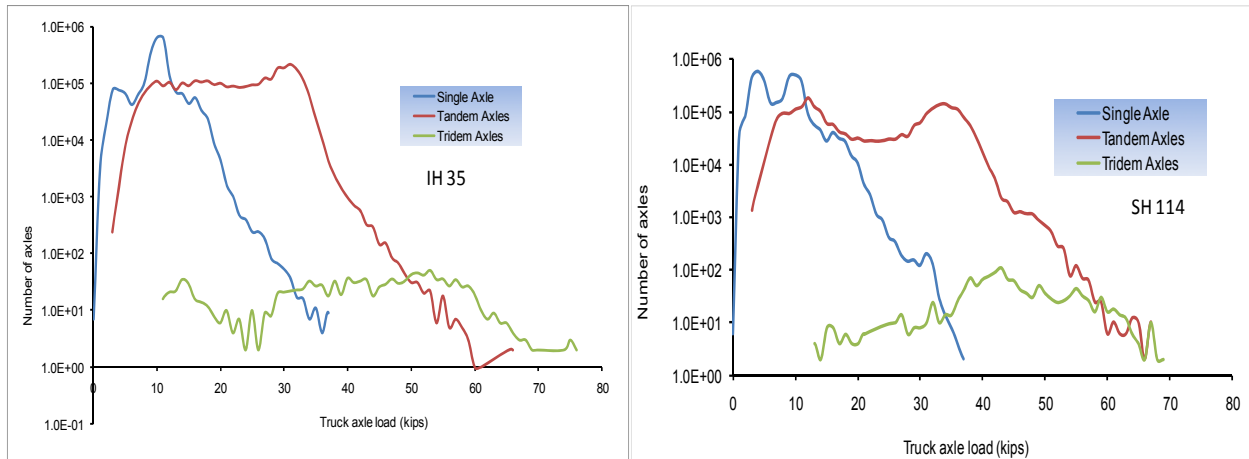


**Figure 6-6. Axle Load Distributions.**

## Lane and Directional Distributions

In general, results indicated more trucks in the outside lanes, as expected. The average numbers were 91 percent in the outside and 9 percent in the inside lane. Direction wise, IH 35 exhibited a similar distribution between the NB and SB lanes. On SH 114, the EB direction had more truck traffic than the WB direction, i.e., 70 versus 30 percent. One of the attributing factors for this uneven distribution is the fact that the trucks go loaded in the EB direction (i.e., to the city of Roanoke) and come back unloaded in the WB direction. These results are shown in Figure 6-7.

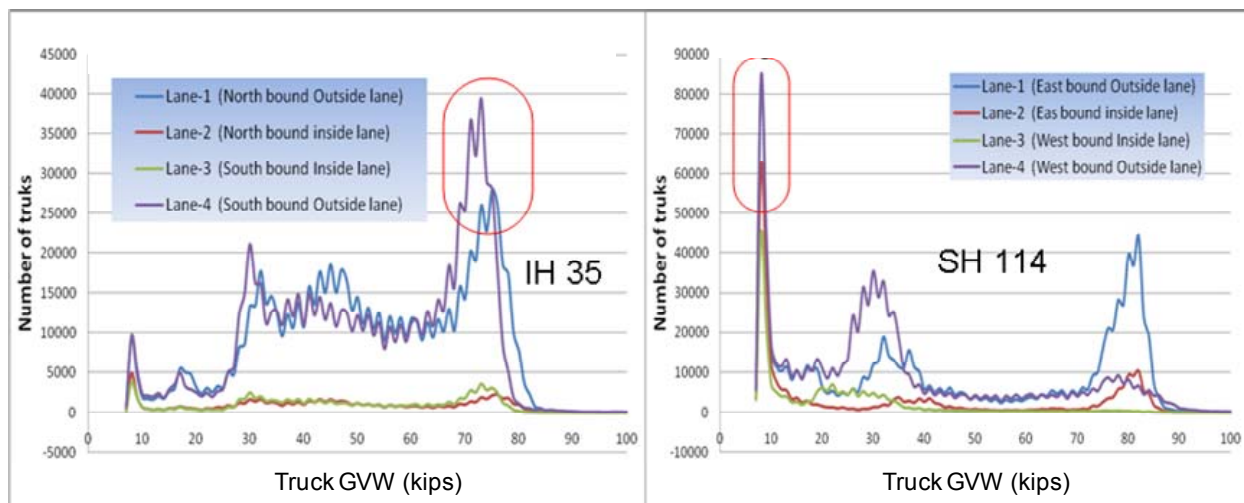


**Figure 6-7. Truck GVW Distribution by Lane.**

### Traffic Count Comparisons

Table 6-1 shows a summary listing of the WIM traffic analyses on IH 35 and SH 114. For 20-year traffic estimate calculations, a 5 percent growth rate was arbitrarily assumed on both sections.

**Table 6-1. WIM Traffic Counts.**

| Item                                      | IH 35 (NB+SB)                   | SH 114 (EB+WB)                  |
|---|---------------------------------|---------------------------------|
| Avg. hourly count                         | 182                             | 193                             |
| Avg. daily count                          | 4,377                           | 4,630                           |
| Avg. monthly count                        | 120,756                         | 137,110                         |
| Avg. weekend distribution                 | 12.1%                           | 22.2%                           |
| Avg. workday distribution                 | 87.9%                           | 77.8%                           |
| Avg. yearly count (million)               | 1 .58                           | 1.69                            |
| Assumed growth rate                       | 5.0%                            | 5.0%                            |
| 20-yr estimate (million)                  | 52.30                           | 55.76                           |
| Directional distribution                  | 49% NB & 51% SB                 | 70% EB & 30% WB                 |
| Actual directional distribution (million) | 25.63 NB + 26.67 SB             | 39.03 EB + 16.73 WB             |
| Lane distribution                         | 90% outside and 10% inside lane | 92% outside and 8% outside lane |
| Initial design ADT                        | 11,900                          | 7,500                           |
| Growth rate estimate (in initial design)  | 3.0%                            | 4.3%                            |
| Percent trucks (in initial design)        | 46.2%                           | 27.3%                           |
| Initial 20-yr design estimate             | 26.5                            | 37.2                            |



On both sections, [Table 6-1](#) shows that the initial traffic design estimates were reasonable and do not differ significantly from the actual WIM measurements and predictions. This validates the fact that the initial traffic design estimates were satisfactory.

## MDD RESPONSE MEASUREMENTS

As a means of validating the Texas PP structural response and design concept, MDDs were installed in the IH 35 structure (Zumwalt02, Laredo) to measure the vertical deflections and compressive strain responses of the PP structure under actual traffic loading. The MDDs were installed at approximately TRM 51+0.400 location (GPS location: N 28° 12.840', W 99° 18.271 ft, and 523 ft elevation) in the SB outside lane in the outside (right) wheel path. The outside lane was utilized because this is where heavy truck-traffic is predominantly concentrated. The MDD instrumentation set up and installation details are shown in [Figures 6-8a](#) and [b](#), respectively.

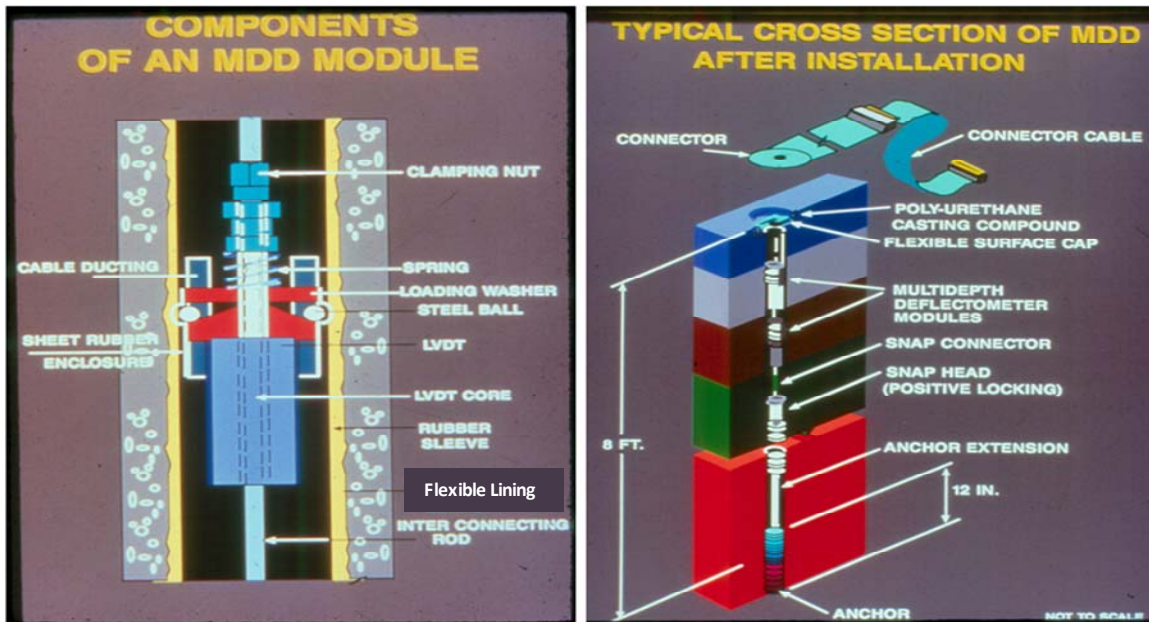


Figure 6-8a. MDD Instrumentation Set Up.



MDD connector, deflection module and anchor



MDD connector cables being buried for subsequent measurements

**Figure 6-8b. MDD Installation.**

As shown in [Figure 6-8b](#), the MDD connector cables were placed in cuts and sealed in the HMA up to the shoulder edges where a waterproof metal box was provided to house the main computer connection units. During measurements, the metal box would be un-buried and a portable laptop computer together with an integrated video system would be used to take the readings and automatically photograph the trucks as they pass over the MDDs.

The 25-inch thick PP structure at this section is comprised of 17 inches in total HMA thickness and an 8-inch thick base (stabilized subgrade) on natural subgrade. The MDDs were installed at four key depth locations to measure the total pavement surface deflections (at 0-inch depth), the deflection from the HMA layers (at 17-inch depth), deflection contributed by the base (at 25-inch depth), and deflection coming from the subgrade (at 33-inch depth) for each passing truck tire set in the right wheel path. [Figure 6-9](#) shows a diagrammatical layout of the MDD depth positions and the PP structural section.

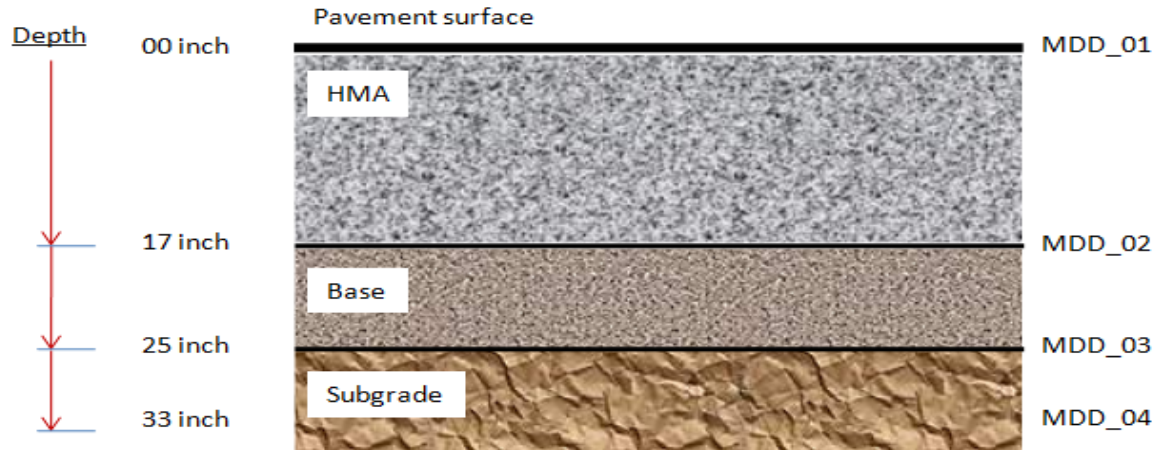


**Figure 6-9. MDD Depth Locations within the Zumwalt02 PP Structure.**

Note that the difference in deflection readings between MDD\_01 and MDD\_02 (i.e., MDD\_01 minus MDD\_02) constitutes the deflection from the HMA and that between MDD\_02 and MDD\_03 (i.e., MDD\_02 minus MDD\_03) is the deflection contribution from the base. The rest of the deflection would be considered to be coming from the subgrade. The difference in readings between MDD\_03 and MDD\_04 (i.e., MDD\_03 minus MDD\_04) constitute the deflection occurring in the top 8 inches of the subgrade. The readings from MDD\_01 at 0.0-inches depth constitute the total pavement deflection with the passage of truck traffic. Inadvertently, these MDD measurements also allowed for the vertical strain computations and percentage contribution of each respective layer. Note that horizontal strain gauges, because of their complex installation process, were not installed on any of the Texas PP sections. As such, no horizontal tensile strain measurements were conducted.

### **Vertical Deflections and Strain Measurements**

MDD measurements were conducted in the summer of 2006 while the pavement surface temperature was 108 °F. Summer (when the pavement temperatures are high and the HMA is considered more susceptible to deformation due to its visco-elastic nature) is considered the critical season for vertical deflection measurements under truck-traffic loading. The results of these measurements are shown in [Figures 6-10](#) through [6-13](#) and [Table 6-2](#). Other results are also included in [Appendix D](#) of this report.

The MDD vertical deflection response as a function of time under a typical passing 18-wheeler truck is shown in Figure 6-10. Four curves are evident in Figure 6-10 and are consistent with the MDD depth locations in Figure 6-9; the highest curve in each set represents readings from the pavement surface (MDD\_01), the second from MDD\_02 (bottom of HMA), the third from MDD\_03 (bottom of CTB), and the bottom curve represent readings from MDD\_04 (top 8 inch of the subgrade). Circled points 1, 2, and 3 represent the steering axle, drive tandem, and the trailer tandem axles, respectively.

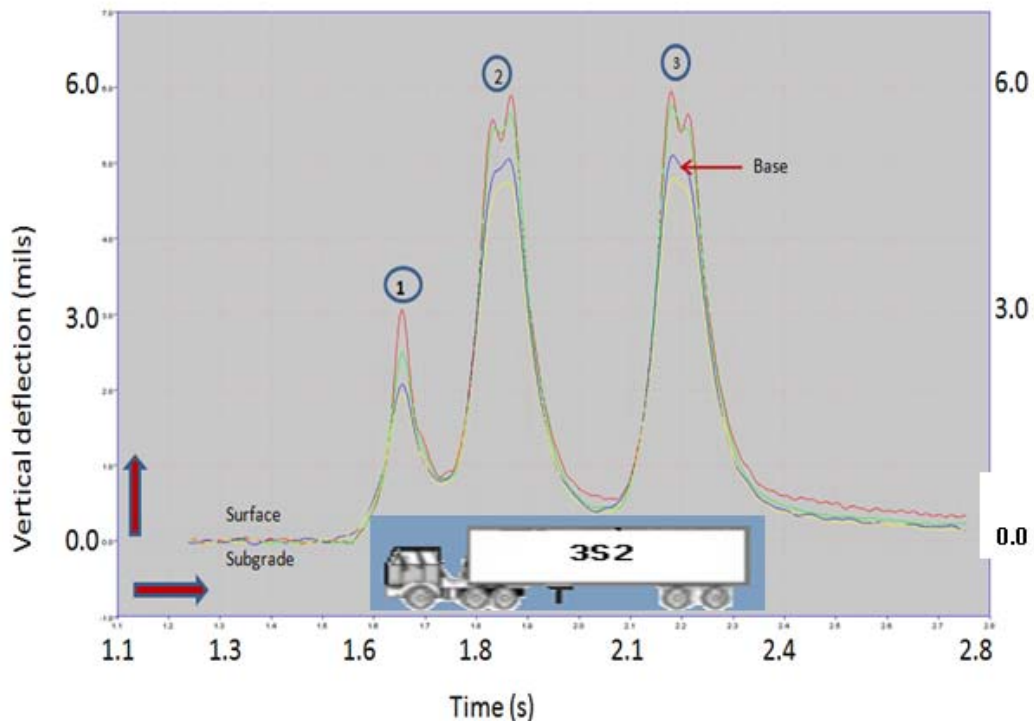


**Figure 6-10. Typical 18 Wheeler-Truck MDD Deflection Response with Time Passage.**

As would be expected, the impact of the steering axle is marginal (almost half in magnitude) compared to the rear axles; which are typically loaded. For this particular truck in Figure 6-10, the average peak vertical surface deflection recorded was 5.85 mils (0.00585 inches) by MDD\_01, with the deflection decreasing in magnitude from the surface through to the subgrade (bottom curve) with readings of 5.15 mils; see Figure 6-11. These results show the majority of the deflection occurred in the subgrade.

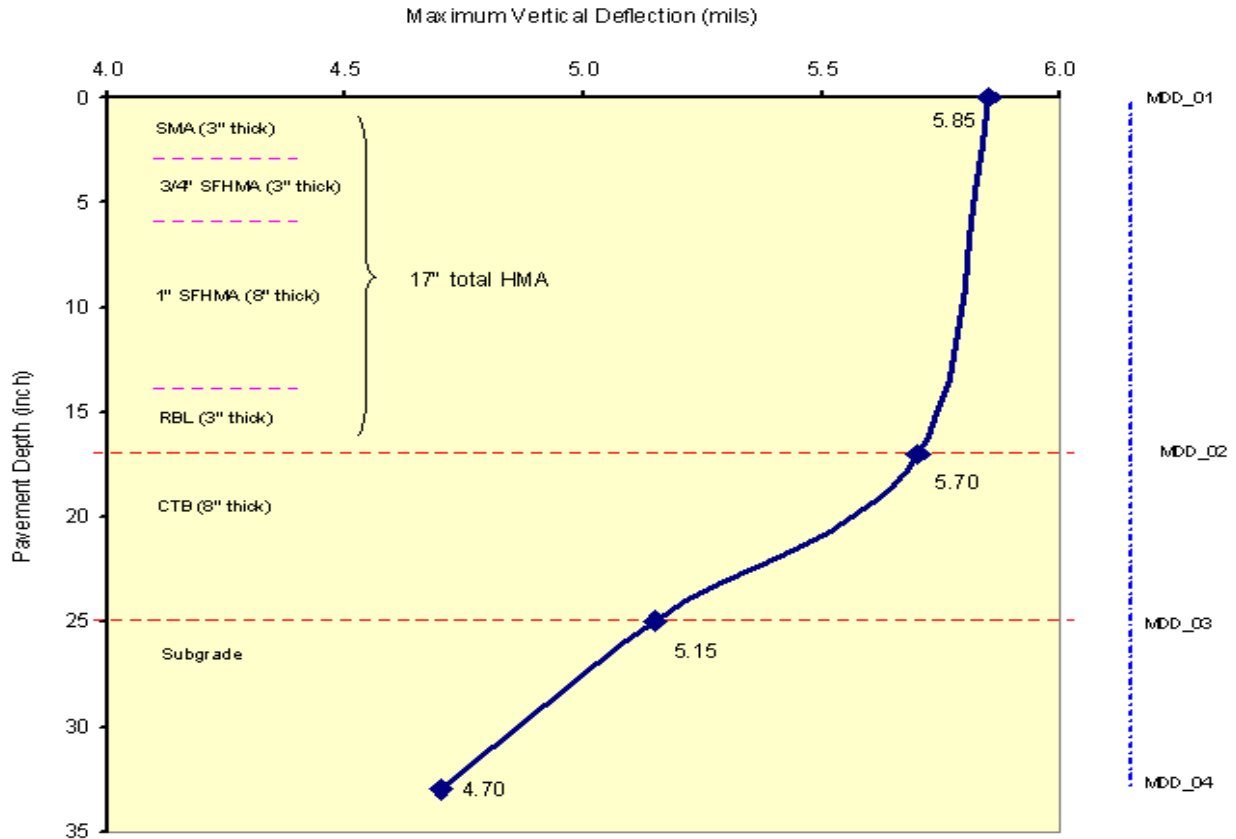


**Figure 6-11. Example MDD Deflection Measurements as a Function of Pavement Depth.**

Table 6-2 shows an example of the average layer peak vertical deflections and strain computations for the 18-wheeler truck shown in Figure 6-10.

**Table 6-2. Peak Vertical Deflections and Strain Computations.**

| MDD#   | Vertical Deflections |         | Layer Deflections<br>inches | Layer                  | Percent Contribution | Vertical Strain ( $\mu\epsilon$ ) |
|--------|----------------------|---------|-----------------------------|------------------------|----------------------|-----------------------------------|
|        | mils                 | inches  |                             |                        |                      |                                   |
| MDD_01 | 5.85                 | 0.00585 |                             |                        |                      |                                   |
| MDD_02 | 5.70                 | 0.00570 | 0.00015                     | 17-inch HMA            | 2.56%                | 9                                 |
| MDD_03 | 5.15                 | 0.00515 | 0.00055                     | 8-inch base            | 9.40%                | 69                                |
| MDD_04 | 4.70                 | 0.00470 | 0.00045                     | Top 8-inch<br>subgrade | 7.69%                | 56                                |
|        |                      | 0.00470 |                             | Subgrade ( $\infty$ )  | 80.34%               | 00                                |

The total average peak surface deflection recorded by MDD\_01 was 0.00585 inches, of which only about 3 percent was contributed by the HMA layers, 9 percent by the CTB, and the rest by the subgrade. These results are indicative that this PP structure was sufficiently designed, and the HMA layers are structurally able to efficiently transfer the traffic loading to the underlying layers, in particular to the subgrade.

Based on these MDD peak vertical deflection measurements, the average vertical compressive strains occurring in the top 8-inch zone of the subgrade for this particular truck was computed to be 56  $\mu\epsilon$  (see [Table 6-2](#)). This is substantially lower than the prescribed 200  $\mu\epsilon$  M-E threshold, i.e., about 70 percent below the threshold. Thus, this PP structure is considered to be structurally sufficient in terms of meeting the M-E design criterion for PP vertical strain responses to mitigate full-depth permanent deformation and rutting. [Figure 6-12](#) shows a graphical representation of the cumulative frequency vertical strain plots for various traffic and MDD measurements.

Clearly, [Figure 6-12c](#) shows that the vertical compressive strain is well below the 200  $\mu\epsilon$  M-E limit in the subgrade. In fact, the maximum computed strain on top of the subgrade was 60  $\mu\epsilon$ , with the majority being in the 40  $\mu\epsilon$  range. The actual measured summer average was 38  $\mu\epsilon$  with a COV of 44 percent.

In the base ([Figure 6-12b](#)), the frequency plot shows the majority of the compressive strains being between 50 and 90  $\mu\epsilon$ , also considerably lower than the subgrade threshold of 200  $\mu\epsilon$ . The least deformation appears to be occurring in the HMA layers; with a majority of the compressive strains falling in the 28 to 42  $\mu\epsilon$  range ([Figure 6-12a](#)). [Figure 6-13](#) shows the relationship between surface deflections and the vertical strain responses in the top 8 inches of the subgrade.

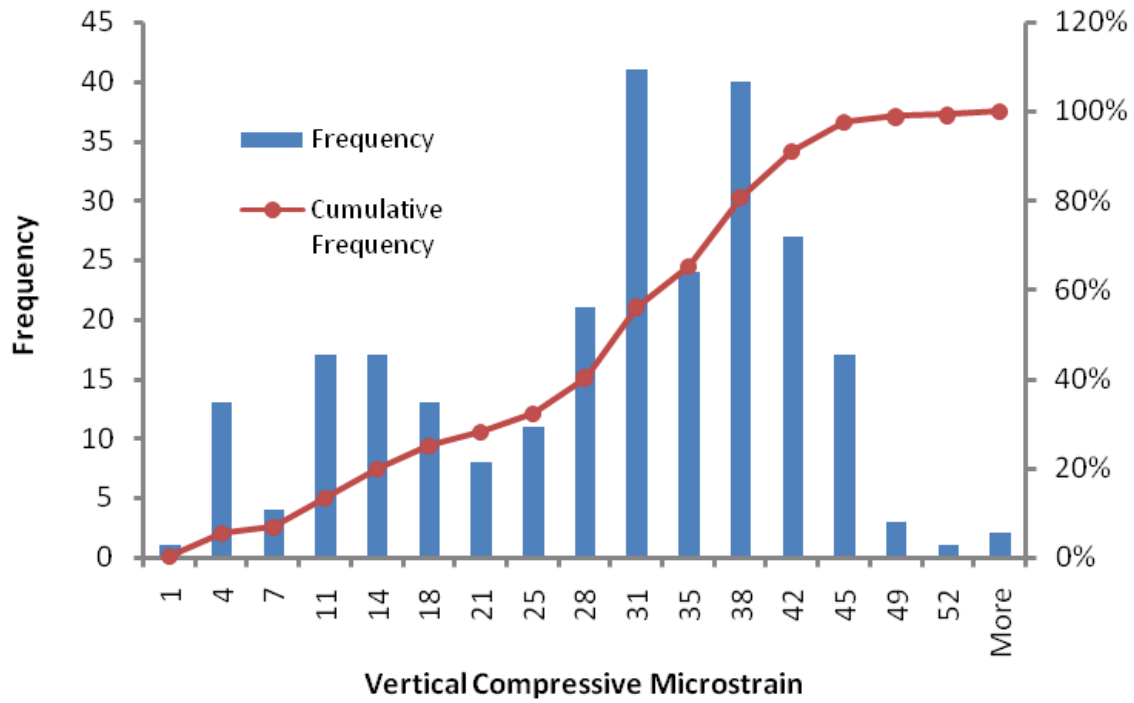


Figure 6-12a. Vertical Strain Plot for the HMA Layers.

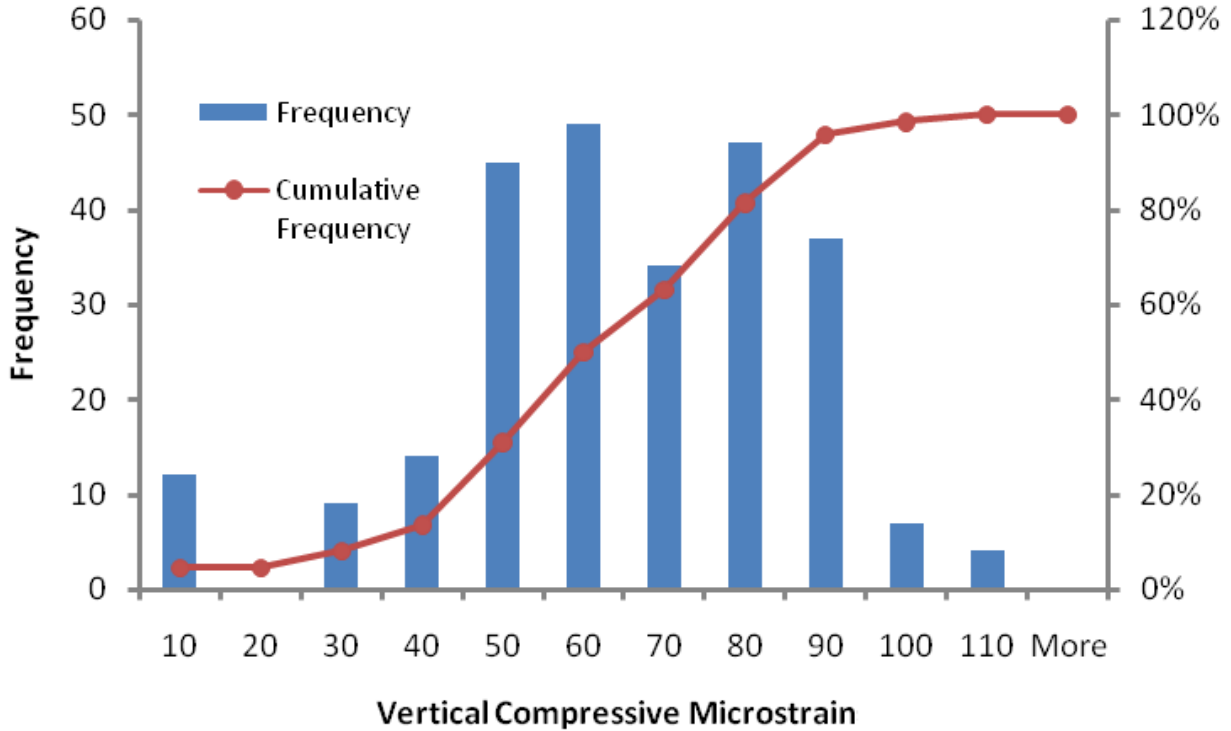
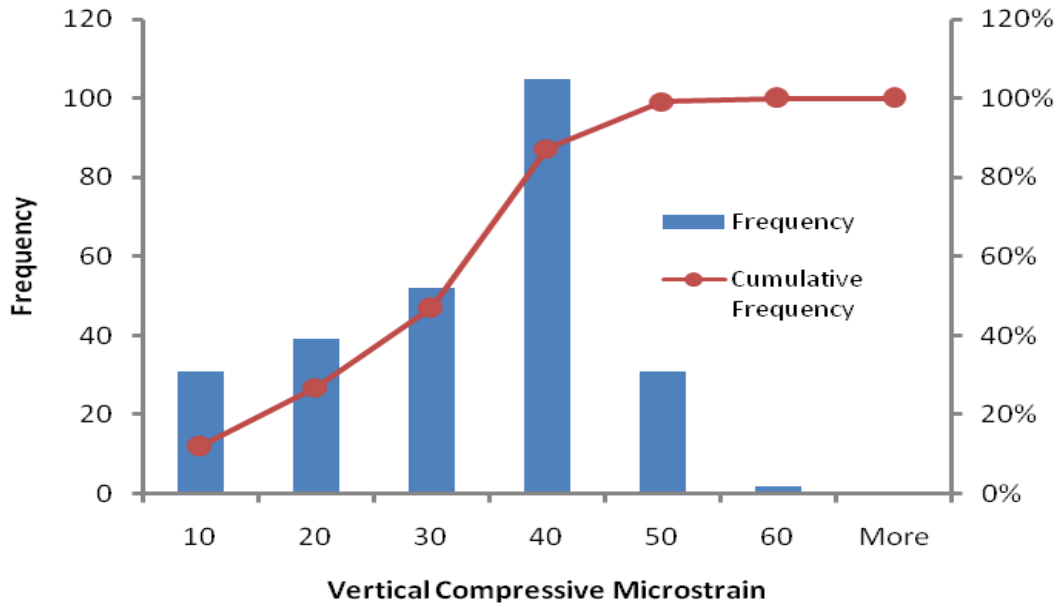
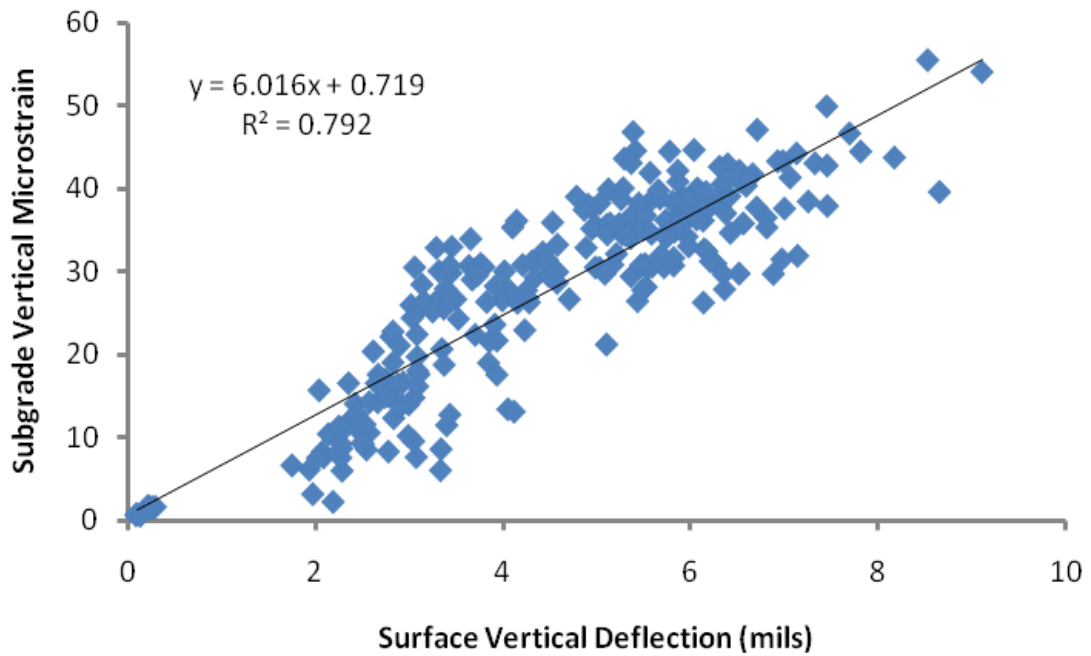


Figure 6-12b. Vertical Strain Plot for the Base.



**Figure 6-12c. Vertical Strain Plot in the Subgrade Top 8 inches.**



**Figure 6-13. Surface Deflection versus Subgrade Microstrains in the Top 8 inches.**



With a moderately low coefficient of variation, the scatter plot in [Figure 6-13](#) exhibits a near linear trend. This is suggestive that the subgrade strain response is consistent with the pavement surface deflections, thus further reinforcing the fact that there is an efficient load transfer mechanism in the upper PP structural layers to the subgrade. Considering the strain magnitudes, [Figure 6-13](#) is further evidence that the upper PP layers are substantially limiting the strains transferred to the top of the subgrade. As discussed in [Chapter 5](#) and consistent with these MDD measurements, the FWD vertical surface deflections have also remained substantially low (5.0 mils in summer 2009), less than 10 mils even under summer pavement temperatures of over 100 °F. To date, after more than four years of service, no structural defects such as cracking or rutting have been observed on this PP section or on any of the other Texas PP sections.

### Strain Computations Using the FPS Software

Using the actual FWD moduli values reported in [Chapter 5](#) and the traffic data in this chapter, vertical compressive strain computations at the top of the subgrade were predicted for both single and tandem axle loadings. As was shown in [Figure 6-6](#), the majority of axle load distributions on these highways are single and tandem, and hence, their use as a basis for the strain computations in the subgrade. The results of these FPS strain computations are shown in [Table 6-3](#).

**Table 6-3. FPS Strain Computations in the Subgrade.**

| Item   | Axle Loading                | Vertical Compressive Strain |
|--|-----------------------------|-----------------------------|
| FPS computation  | Single ( $\approx$ 18 kips) | 54 $\mu\epsilon$            |
| FPS computation  | Tandem ( $\approx$ 34 kips) | 61 $\mu\epsilon$            |
| Actual maximum measured from MDDs  |                             | 60 $\mu\epsilon$            |
| In-situ PP structure = 3-inches SMA + 3 inches ( $\frac{3}{4}$ -inch SFHMA) + 8 inches (1-inch SFHMA) + 3 inches RBL + 8-inches cement treated based & the subgrade                            |                             |                             |
| In-situ FWD moduli values = 600 ksi for the SMA, 1400 ksi for the $\frac{3}{4}$ -inch SFHMA, 2400 ksi for 1-inch SFHMA, 500 ksi for the RBL, 102 ksi for the base, and 22 ksi for the subgrade |                             |                             |

[Table 6-3](#) shows that both the FPS computational predictions and the actual measured strains are comparable and significantly less than the M-E design limit of 200  $\mu\epsilon$ . Thus, the PP section is structurally sufficient with respect to full depth rutting. Note that the actual in-situ PP structure and back-calculated FWD layer moduli values ([Appendix C](#)) were used for the FPS analyses.

## PP Re-Designs with the FPS Software

Using cumulative loading projections based on actual measured traffic data and material properties, the IH 35 (Zumwalat02, Laredo) and SH 114 (Fort Worth) were redesigned using the FPS software. Results of these computational modeling are presented in [Table 6-3](#).

The results in [Table 6-3](#) indicate that the PP structures could be optimized down to about 12 to 14 inches in total HMA thickness, without compromising the PP structural integrity. The computed strain responses are satisfactorily within the M-E threshold, and the predicted performance life is over 20 years. Both the structures indicate a minimum RBL thickness of 2 inches. Performance predictions with the MEPDG also indicated a service life of about 20 years with the IRI as the critical limiting distress.

[Table 6-4](#) also shows that the material properties had greater influence in the initial design of these PP structures. There is much more reduction in the total HMA when the actual measured material properties (i.e., the measured moduli values in [Chapters 4 and 5](#)) are used as compared to the influence of traffic loading. This is not surprising because as was shown in [Table 6-1](#), the initial traffic design assumptions were fairly consistent with the actual measured traffic.

However, the much lower moduli values used in the initial designs ultimately resulted in conservative designs in all currently existing PP structures; see [Table 6-4](#). Clearly, there is a significant difference in the moduli values in [Table 6-4](#) between the actual measured (lab and field) and the initial design values. Thus, there is no doubt that these low initial design moduli values contributed to the conservatism of the SH 114 PP structures. This observation also stresses the significance of using the proper material properties (moduli values) in the PP structural designs.

**Table 6-4. PP Re-Designs with FPS 21W and Actual Measured Input Data.**

| <b>Item</b>                                    | <b>Initial Design</b>   | <b>With Actual Traffic Only</b>                                 | <b>With Actual Materials Only</b>                               | <b>Actual Traffic &amp; Materials</b>                           |
|--|---|---|---|---|
| <b>IH 35 (Laredo)</b>                          |   |   |   |   |
| PP structure                                   | 3-inch SMA + 3-inch (¾") SFHMA + 8-inch (1") SFHMA + 3-inch RBL | 2-inch SMA + 2-inch (¾") SFHMA + 8-inch (1") SFHMA + 2-inch RBL | 2-inch SMA + 2-inch (¾") SFHMA + 6-inch (1") SFHMA + 2-inch RBL | 2-inch SMA + 2-inch (¾") SFHMA + 6-inch (1") SFHMA + 2-inch RBL |
| Total HMA thickness                            | 17 inches   | 14 inches   | 12 inches   | 12 inches   |
| Tensile strains ( $\leq 70 \mu\epsilon$ )      | 34 $\mu\epsilon$  | 58 $\mu\epsilon$  | 29 $\mu\epsilon$  | 29 $\mu\epsilon$  |
| Compressive strains ( $\leq 200 \mu\epsilon$ ) | 103 $\mu\epsilon$   | 155 $\mu\epsilon$   | 83 $\mu\epsilon$  | 93 $\mu\epsilon$  |
| Life prediction                                | 31 years  | 27 years  | 30 years  | 36 years  |
| HMA saving                                     |   | 3 inches  | 5 inches  | 5 inches  |
| <b>SH 114 (Fort Worth)</b>                     |   |   |   |   |
| PP structure                                   | 2-inch SMA + 3-inch Type C + 13-inch Type B + 4-inch RBL        | 3-inch SMA + 3-inch Type C + 8-inch Type B + 3-inch RBL         | 2-inch SMA + 3-inch Type C + 8-inch Type B + 2-inch RBL         | 2-inch SMA + 2-inch Type C + 8-inch Type B + 2-inch RBL         |
| Total HMA thickness                            | 22 inches   | 17 inches   | 15 inches   | 12 inches   |
| Tensile strains ( $\leq 70 \mu\epsilon$ )      | 23 $\mu\epsilon$  | 52 $\mu\epsilon$  | 35 $\mu\epsilon$  | 32 $\mu\epsilon$  |
| Compressive strains ( $\leq 200 \mu\epsilon$ ) | 57 $\mu\epsilon$  | 149 $\mu\epsilon$   | 104 $\mu\epsilon$   | 101 $\mu\epsilon$   |
| Life prediction                                | 32 years  | 31 years  | 26 years  | 29 years  |
| HMA saving                                     |   | 5 inches  | 7 inches  | 8 inches  |

**Table 6-5. Example Comparison of Moduli Values for SH 114.**

| <b>Layer/Material</b>                 | <b>Modulus at 77 °F (ksi)</b> |                            |                                  | <b>Poisson's Ratio</b> |
|---------------------------------------|-------------------------------|----------------------------|----------------------------------|------------------------|
|                                       | <b>Initial Design</b>         | <b>Actual Lab Measured</b> | <b>Actual Field FWD Measured</b> |                        |
| SMA                                   | 500                           | 640                        | 850                              | 0.35                   |
| ¾" SFHMA                              | 500                           | 825                        | 850                              | 0.35                   |
| 1" SFHMA (rut-resistant layer)        | 750                           | 1275                       | 1750                             | 0.35                   |
| RBL (fatigue-resistant layer)         | 17                            | 565                        | 500                              | 0.35                   |
| Base – lime treated subgrade material | 17                            | 66                         | 74                               | 0.45                   |
| Subgrade                              | 9.1                           | N/A                        | 12                               | 0.45                   |

## SUMMARY

Significant findings and recommendations from this chapter are summarized as follows:

- The initial traffic design estimates were fairly reasonable and did not deviate significantly from projections based on the actual measured traffic data. Indications are that the underestimation of the layer moduli, particularly for the SFHMA mixes, is what resulted in exceptionally conservative designs for the currently existing Texas PP structures. Thus, it is very imperative to use the moduli values recommended in the report for the future designs of Texas PP structures.
- The current PP structures are satisfactory and sufficiently meet the M-E criterion for full depth rutting mitigation. Both the actual measured and predicted subgrade strains were substantially lower than the 200  $\mu\epsilon$  threshold. The average actual measured compressive strain was 33  $\mu\epsilon$  while those computed from the FPS software with FWD moduli values were 54 and 61  $\mu\epsilon$  under single ( $\approx$  18 kips) and tandem ( $\approx$  34 kips) axle loading (1.0ESAL), respectively.
- FPS analyses indicated that the current Texas PP design concept is conservative and has potential for much optimization down to about 12 to 14 inches in total HMA thickness. Compared to the current Texas PP design concept, this transition will result in over 6 inches HMA cost savings.
- Future requests for WIM data should always be stated in terms of “Classification and Weight Tables,” a recognized reporting standard. Data should be verified for completeness. Furthermore, it is recommended that at least 2 to 3 years’ traffic data be used for analyses of this nature. As an example it is not feasible to accurately predict or estimate the traffic growth with only one year’s data.
- Traffic WIM measurements indicated that about 90 percent of the truck-traffic uses the outside lanes while only about 17 percent of the truck loading (18 kips) occurs on weekends. Thus, it can be intuitively assumed that a majority of the truck-traffic on these highways is commercial/business related.

## CHAPTER 7

### COMPUTATIONAL MODELING AND SOFTWARE EVALUATION

As discussed in [Chapter 1](#), one of the objectives of this research was to evaluate and recommend suitable software for the design and modeling of the future Texas PP structures. Four software packages namely FPS, PerRoad, Vesys, and the MEPDG, were evaluated. Results of these evaluations and computational modeling including analytical validation of the Texas PP design concept are presented in this chapter. A list of important findings and recommendations is then presented to summarize the chapter.

#### VALIDATION OF THE TEXAS PP DESIGN CONCEPT

Computational modeling based on all the four software (FPS, PerRoad, Vesys, and MEPDG) indicated that the Texas PP structural design concept was analytically valid with additional potential for further optimization. As shown in [Table 7-1](#), the average predicted strain responses considering all the Texas PP structures were significantly less than the 70 and 200  $\mu\epsilon$  thresholds, thus meeting the M-E strain response criteria for perpetual pavements.

**Table 7-1. Summary Results of Computational Modeling.**

| <b>Item</b>  | <b>Average Number (All Texas PP Structures)</b> |
|--|---|
| Average predicted tensile strains at bottom of lowest HMA layer ( $< 70 \mu\epsilon$ )         | 31 $\mu\epsilon$                                |
| Average predicted compressive strains on top of the subgrade ( $< 200 \mu\epsilon$ )           | 88 $\mu\epsilon$                                |
| Average service life prior to first surface renewal or overlay (typical expectation is 20 yrs) | 26 yrs  |
| Average predicted structural life  | $> 20$ yrs                                      |
| Rutting and bottom-up fatigue cracking   | none  |

In all the Texas PP structures, no major structural distresses such as rutting or fatigue cracking were predicted. In fact, all the software indicated zero probability for fatigue cracking occurrence and only a 14 percent probability of total rutting exceeding the 0.75-inch MEPDG threshold. The predicted average service life prior to a first surface renewal or an overlay was 26 years, which is extraordinarily longer than the typical expectation of 10 to 12 years for Texas flexible HMA pavements.

Both the Vesys and MEPDG software indicated that surface roughness measured in terms of IRI would be the critical distress governing the Texas PP service life and the ultimate need for a surface renewal or an overlay. At 95 percent confidence level, 66 percent of the designs run failed to stay below the MEPDG 20-year IRI threshold of 172 in/mi while it was less than 10 percent for the other distress criteria.





However, the MEPDG analyses also indicated the need to switch to higher PG asphalt-binder grades or improvements in the surface HMA mix-designs to limit permanent deformation in the upper HMA layers. At 95 percent reliability level, the MEPDG indicated high potential for HMA permanent deformation in the PP structures utilizing PG 64-22 asphalt binders in the intermediate and/or upper HMA layers (particularly SH 114). On average, the MEPDG predicted about 30 percent probability of the HMA permanent deformation exceeding the 0.5-inch threshold at 95 percent reliability level. The potential for permanent deformation tends to negatively impact the IRI score.

As was demonstrated in [Chapter 6](#), using load projections based on the actual traffic data and measured material properties indicated that the Texas PP structures were conservatively designed. The results indicated that the total HMA thickness can be satisfactorily reduced to about 12 to 14 inches, resulting in an over 6-inch HMA cost-savings from the current 22 inches. With the currently designed greater total HMA thicknesses, the results also indicated that the RBL was structurally unnecessary. However, the RBL may still optionally be required for durability and impermeability characteristics.

## **COMPARATIVE SOFTWARE EVALUATION**

A comprehensive comparative evaluation of the software was completed, and the Texas PP sections on SH 114 were used as demonstration examples for modeling purposes. Results of these modeling analyses are documented in [Walubita and Scullion \(2007\)](#). [Table 7-2](#) summarizes the comparisons of the software. More details of these software packages, details including instructions on how to use them, are documented in the Texas PP database ([Walubita et al., 2009](#)).

**Table 7-2. Software Comparisons.**

| Item FPS                       | 21W   | PerRoad3.2  | Vesys5.0  | MEPDG1.0  |
|--------------------------------|---|---|---|---|
| Icon                           |  |  |  |  |
| Thickness design               | Yes   | No  | No  | No  |
| Alternative thickness designs  | Yes   | No  | No  | No  |
| Layers                         | ≤ 7   | ≤ 5   | ≤ 7   | > 7 with a maximum of 4 HMA layers  |
| Input data                     | Simple  | Comprehensive   | Comprehensive   | Comprehensive   |
| Output data                    | Alternative designs, performance life, & extensive structural analyses            | Performance life & structural (strain) analyses                                   | Extensive performance analyses in time plots  | Extensive performance analysis as function of time                                  |
| Climatic consideration         | Simple  | Moderate  | Comprehensive   | Comprehensive   |
| Analysis period                | > 20 yrs  | > 20 yrs  | 20 yrs  | > 20 yrs  |
| Stress-strain check            | Yes   | Yes   | No  | No  |
| Performance analysis           | Simple  | Simple  | Comprehensive   | Comprehensive   |
| Extensive lab testing required | No (uses FWD data)  | Yes (DM tests)  | Yes (RLPD tests)  | Yes (DSR/DM tests), but has Level 3 option with no testing required                 |
| Calibration necessary          | No  | Yes   | No  | Yes   |
| Running time                   | < 5 mins  | < 5 mins  | > 5 mins  | > 25 mins   |
| User-friendliness              | Excellent   | Moderate  | Moderate  | Moderate  |
| Applicability                  | HMA structures  | PP structures only  | Not ideal for PP structures   | HMA & concrete structures, but not ideal for thin HMA surfaces (i.e., < 2 inches)   |

In consideration of [Table 7-2](#) and the extensive computational analyses presented in [Walubita and Scullion \(2007\)](#), the FPS and MEPDG were recommended for the design and modeling of future Texas PP structures, namely:

- FPS – PP structural thickness design, M-E response analysis, and strain check; and
- MEPDG – PP design verification and performance prediction.

### THE FPS 21W SOFTWARE

The FPS is mechanistic-empirical (M-E) based software routinely used by TxDOT for: (1) pavement structural (thickness) design, (2) overlay design, (3) stress-strain response analysis, and (4) pavement life prediction (rutting and cracking).

The design approach is based on a linear-elastic analysis system and the key material input is the back-calculated FWD modulus values of the pavement layers. The FPS design system itself is comprised of two fundamental processes: (1) trial pavement structure development and thickness design and (2) design checks including performance prediction. The FPS system has an embedded performance function relating the computed surface curvature index of the pavement to the loss in ride quality. The design check is principally based on either the mechanistic design concepts or the Texas Triaxial criteria.

The mechanistic design check basically computes and checks the sufficiency of the mechanistic responses in terms of maximum horizontal tensile strains at the bottom of the lowest HMA layer and the maximum vertical compressive strains on top of the subgrade not exceeding prescribed limits. The mechanistic design check is recommended for all pavements with HMA surfaces. However, the fatigue analysis is restricted to all pavements where the HMA thickness is greater than 1.5 inches, but should be run for informational purposes on all thin-surfaced HMA designs. The Texas Triaxial criterion checks the likelihood of shear failure in the subgrade soil under the heaviest wheel load anticipated for the pavement section.

TxDOT traditionally uses the FPS for conventional flexible HMA pavement design. For this project and in consideration of the multi-layered nature of the Texas PP structures, a prototype upgrade, FPS 21W, was used. The FPS 21W allows for up to seven layers to be considered and therefore can sufficiently accommodate perpetual pavements.

Figures 7-1 through 7-4 show highlights of the FPS main screen, the FPS built-in layer options, and examples of the output data. The screen in Figure 7-2 allows the user to automatically select the materials and moduli of preference, thus making the software very user-friendly. As an example, the output data in Figure 7-3 can show up to 17 alternative designs, giving the user a very wide range of design options to choose from. For this SH 114 example, design 17 was selected, and the PP structure comprised of 12 inches of HMA and 8 inches of base yielded a performance life of 22 years. The predicted strains were 52 and 144  $\mu\epsilon$ , respectively, lower than the 70 and 200  $\mu\epsilon$  thresholds, respectively. As shown in Figures 7-3 and 7-4, the actual designed structure is highly optimized with 10 inches less HMA thickness than the initial design, i.e., the designed PP structure = 2 inches of SMA + 2 inches of  $\frac{3}{4}$ -inch SFHMA + 6 inches of 1-inch SFHMA + 2 inches RBL + 8 inches base. This again highlights the conservative nature of the initial Texas PP designs.



In these analyses, it would be prudent to note that no attempt was made to reduce or eliminate the “base” thickness because a stable/permanent foundation is deemed critical to the successful performance of a PP.

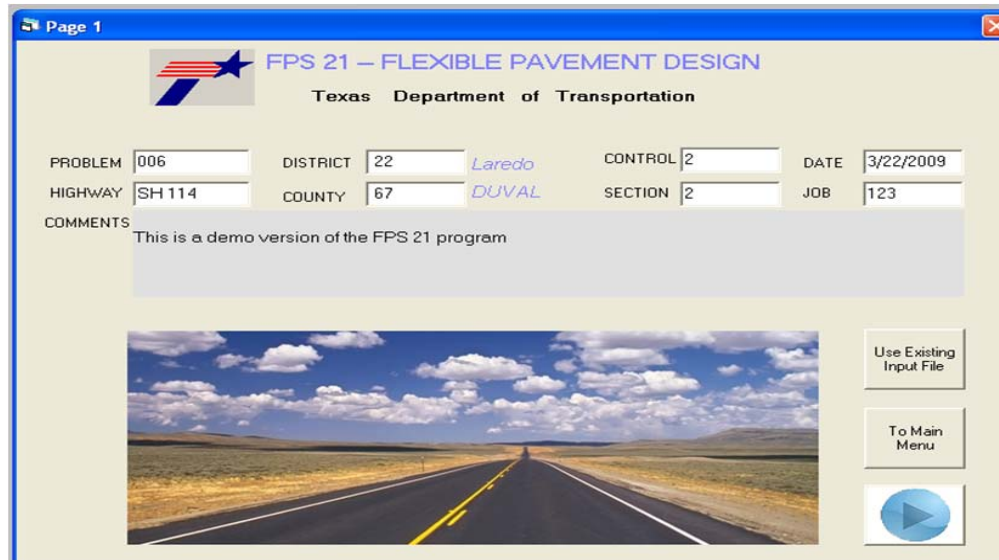


Figure 7-1. FPS 21W Main Screen.

| No | Material Type                 | 2004 Specificati | Design Modulus | Poisson' Ratio | Layer Type      |
|----|-------------------------------|------------------|----------------|----------------|-----------------|
| 1  | SURFACE TREATMENT             | Item 316, 318    | 200 ksi        | 0.35           | AC Layer        |
| 2  | DENSE-GRADED HMA Thin         | Item 340, 341    | 500 ksi        | 0.35           | AC Layer        |
| 3  | DENSE-GRADED HMA Thick        | Item 340, 341    | 650 ksi        | 0.35           | AC Layer        |
| 4  | PERMEABLE FRICTION COURSE     | Item 342         | 500 ksi        | 0.30           | AC Layer        |
| 5  | PERFORMANCE MX 3/4SF          | Item 344         | 650 ~ 950 ksi  | 0.35           | AC Layer        |
| 6  | PERFORMANCE MX 1 inch SF      | Item 344         | 650 ~ 950 ksi  | 0.35           | AC Layer        |
| 7  | STONE-MATRIX ASPHALT          | Item 346         | 650 ~ 850 ksi  | 0.35           | AC Layer        |
| 8  | LIMESTONE ROCK ASPH PVMT      | Item 330         | 200 ~ 350 ksi  | 0.35           | AC Layer        |
| 9  | HOT-MIX COLD-LAID ACP         | Item 334         | 300 ~ 400 ksi  | 0.35           | AC Layer        |
| 10 | RICH BOTTOM LAYER             | Item 344         | 400 ~ 600 ksi  | 0.35           | AC Layer        |
| 11 | FA or LFA STABILIZED          | Item 265         | 50 ~ 150 ksi   | 0.35           | Base Layer      |
| 12 | ASPHALT TREATED BASE          | Item 292         | 250 ~ 400 ksi  | 0.35           | Base Layer      |
| 13 | EMULSIFIED ASPH TRT BASE      | Item 314         | 50 ~ 100 ksi   | 0.35           | Base Layer      |
| 14 | FLEXIBLE BASE                 | Item 247         | 40 ~ 70 ksi    | 0.35           | Base Layer      |
| 15 | LIME STABILIZED BASE          | Item 260, 263    | 60 ~ 75 ksi    | 0.30 ~ 0.35    | Base Layer      |
| 16 | CEMENT STABILIZED BASE        | Item 275, 276    | 80 ~ 150 ksi   | 0.20 ~ 0.30    | Base Layer      |
| 17 | FLY ASH OR LIME-FLY ASH STABI | Item 265         | 60 ~ 75 ksi    | 0.30           | SubBase Layer   |
| 18 | LIME(CEMENT) STABILIZED SUBG  | Item 260, 275    | 30 ~ 45 ksi    | 0.30           | SubBase Layer   |
| 19 | EMULSIFIED ASPH TREAT SUBG    | Item 314         | 15 ~ 25 ksi    | 0.35           | SubBase Layer   |
| 20 | SUBGRADE                      |                  | 16 ksi         | 0.40 ~ 0.45    | Sub-Grade Layer |

Figure 7-2. FPS 21W Built-In Layer Options.

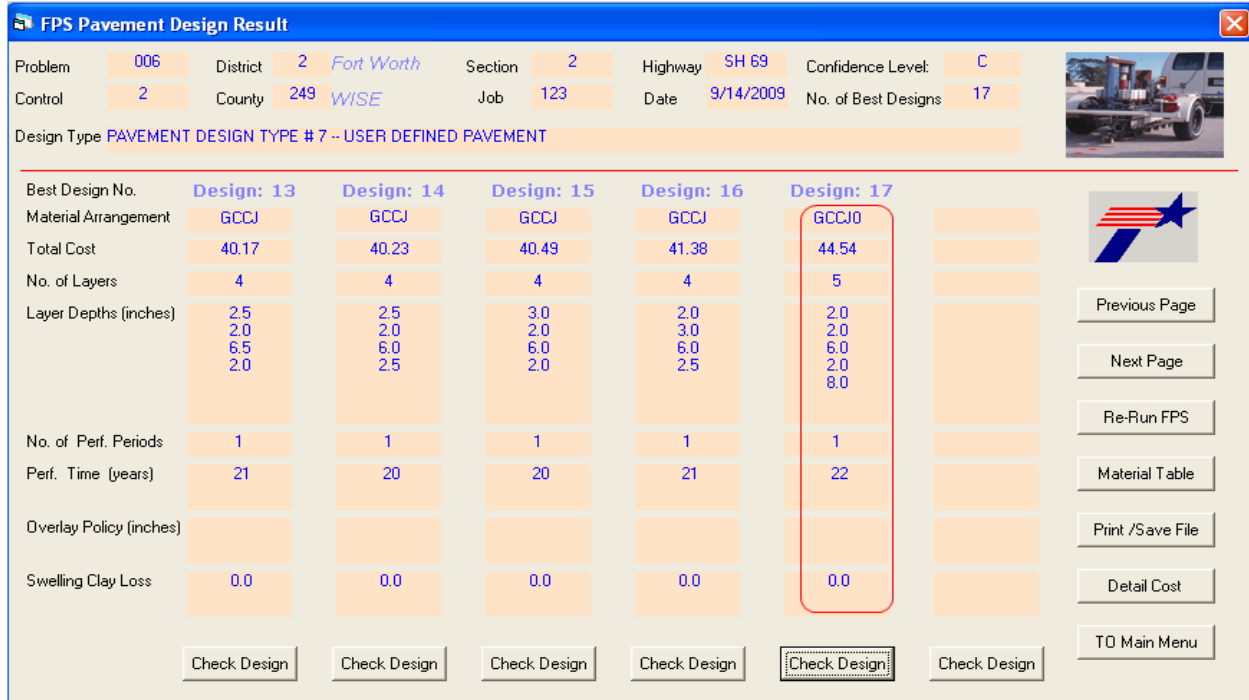


Figure 7-3. Example FPS 21W Design Output Data.

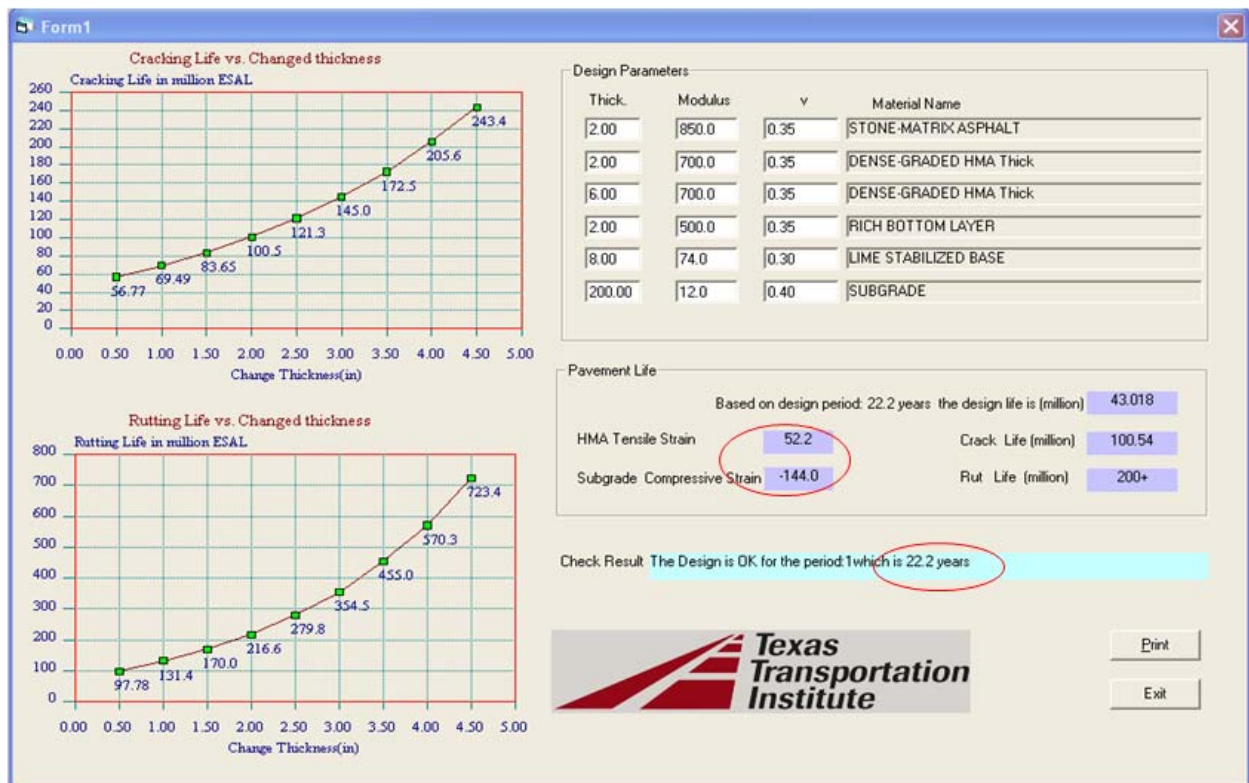


Figure 7-4. Example FPS 21W Mechanistic Analysis.

## THE MEPDG 1.00 SOFTWARE

The MEPDG is an M-E based analytical software for pavement structural design analysis and performance prediction, within a given service period (AASHTO, 2006). The MEPDG design procedure is primarily based on pavement performance predictions of increased levels of distress over time. However, unlike the FPS, the MEPDG does not directly generate pavement layer thickness designs. Instead trial pavement layer thicknesses/combinations are iteratively input into the software and the thicknesses/combinations that meet the prescribed performance criteria are selected as the final designs. The performance predictions include permanent deformation, rutting, cracking (bottom-up and top-down), thermal fracture, and surface roughness (IRI). The MEPDG adapts two major aspects of M-E based material characterization, pavement response properties and major distress/transfer functions as follows:

- Pavement response properties are required to predict states of stress, strain, and deformation within the pavement structure when subjected to external wheel loads and thermal stresses. The properties for assumed elastic material behavior are the elastic modulus and Poisson's ratio.
- The major MEPDG distress/transfer functions for asphalt pavements are load-related fatigue fracture, permanent deformation, rutting, and thermal cracking.

Because of its comprehensive performance analysis models, the MEPDG software was recommended for the future Texas PP design verification and performance analysis, with the actual PP thickness designs accomplished with the FPS software. However, application of the MEPDG to the Texas environmental zones and materials require local calibration. Using both the actual observed/measured Texas PP field performance data in Chapter 5 of this report and the performance data documented by Freeman et al. (2006) on other non-PP highways, a sensitivity analysis was conducted to establish some local calibration factors for Texas. An example of the sensitivity analysis based on the data by Freeman et al. (2006) is shown in Table 7-3. The data by Freeman et al. (2006) were incorporated in the sensitivity analyses because unlike the Texas PP structures that exhibited almost no structural defects, the highway sections in the Freeman et al. study exhibited appreciable structural distresses (rutting and cracking) that were considered ideal for sensitivity analyses.

**Table 7-3. Example of Sensitivity Analysis for Rutting.**

| Station Id | Measured<br>(inch) | Rut Depth (inch) Predicted by the MEPDG with                  |  |
|------------|--------------------|---|--|
|            |                    | $\beta_{s1}=0.6, \beta_{r1}=0.7, \text{ and } \beta_{r3}=1.0$ | $\beta_{s1}=0.6, \beta_{r1}=1.0, \text{ and } \beta_{r3}=0.94$ |
| 481060     | 0.35               | 0.37  | 0.36   |
| 481109     | 0.40               | 0.51  | 0.43   |
| 481169     | 0.45               | 0.47  | 0.46   |
| 481174     | 0.60               | 0.55  | 0.54   |
| 484749     | 0.50               | 0.51  | 0.49   |

Following this sensitivity analyses, some changes were made to some of the calibration factors in the MEPDG as follows:

- AC rutting:  $\beta_{r3}$ = from 1.0 to **0.94**
- Subgrade rutting:  $\beta_{s1}$ = from 1.0 to **0.6**
- AC cracking:  $C_1$  (bottom-up) = from 1.0 to **1.2**
- AC cracking:  $C_1$  (top-down) = from 7.0 to **9.0**

Although utilization of these proposed calibration factors yielded comparable results with observed field performance as shown in Table 7-3, these are to be considered only as preliminary and not final values. More sensitivity analysis is strongly recommended with long-term field performance data. As shown in Table 7-4, a re-run of the PP structure shown in Figure 7-4 yielded satisfactory performance results for a period of 20 years, which does not differ significantly from the 22 years prediction by the FPS.

**Table 7-4. MEPDG Distress Analysis (SH 114) at 95 percent Reliability Level.**

| Performance Criteria                                 | Distress Target | Predicted Distress | Reliability Predicted | Pass/Fail |
|--|-----------------|--------------------|-----------------------|-----------|
| 1 Terminal IRI (in/mi)                               | $\leq 172$      | 118                | 94.8%                 | Pass      |
| 2 AC Surface Down Cracking (Long. Cracking) (ft/500) | $\leq 1000$     | 0.0                | 99.9%                 | Pass      |
| 3 AC Bottom-Up Cracking (Alligator Cracking) (%)     | $\leq 25$       | 0.0                | 99.9%                 | Pass      |
| 4 AC Thermal Fracture (Transverse Cracking) (ft/mi)  | $\leq 1000$     | 1                  | 99.9%                 | Pass      |
| 5 Permanent Deformation (AC Only) (in)               | $\leq 0.50$     | 0.21               | 96.3%                 | Pass      |
| 6 Permanent Deformation (total pavement) (in)        | $\leq 0.75$     | 0.38               | 99.9%                 | Pass      |

Analysis period =20 yrs, Reliability threshold  $\geq 95\%$

Table 7-4 shows satisfactory performance with the IRI barely meeting the 95percent reliability threshold. Again these results indicate that IRI would likely be the governing distress criteria. Fatigue cracking is non-existent while the likelihood of the HMA permanent deformation exceeding the 0.5 inches threshold is only 3.7 percent. Similar performance results were obtained for all the other Texas PP structures.

## SUMMARY

The major findings from computational modeling and software evaluation as was presented in this chapter are summarized as follows:

- The Texas PP structural design concept is analytically valid:
  - 1) It meets the ME strain criteria with computed strains significantly less than the 70 and 200  $\mu\epsilon$  thresholds, respectively.
  - 2) No major structural distresses such as rutting or fatigue cracking were predicted.
  - 3) Life prediction to the first surface renewal or overlay was predicted to be over 20 years, with IRI as the controlling distress.
  - 4) To minimize the potential for HMA permanent deformation and surface roughness deterioration, the results indicated the need to use higher PG asphalt-binder grades or better rut-resistant mix-designs in the upper HMA layers of the PP structures.
- The Texas PP structures were conservatively designed with potential for further optimization:
  - 1) The total HMA thickness is analytically reducible to about 12 to 14 inches without compromising the structural integrity or performance expectations of the pavements. This leads to an over 6-inch HMA cost savings from the current 22-inch total HMA thickness.
  - 2) The RBL is structurally unnecessary but may optionally be required for durability and impermeability characteristics of the pavement. The greater HMA total layer thickness was analytically found to be structurally sufficient to mitigate the occurrence of bottom-up fatigue initiated cracking.

- The FPS and MEPDG were found to be the appropriate software tools for the future Texas PP designs, including M-E strains analysis/verification and performance analysis.

## **CHAPTER 8**

### **TEXAS PP PERFORMANCE COMPARISONS**

This chapter provides a performance comparison of some selected Texas PP sections with a focus on the main structural load-bearing (rut-resistant) layers. The comparison is based on the evaluation of the mix-designs and materials, PP structures, construction aspects, laboratory and field testing, traffic data, field performance evaluations, and computational modeling. A comparison was also made with some PP sections evaluated at the NCAT test track in Alabama. Results of these comparative analyses are also presented in this chapter. The chapter then ends with a summary of the major findings and recommendations.

#### **SH 114 (FORT WORTH) – SFHMA VERSUS TYPE B/C MIXES**

Two adjacent sections with the same structural thickness, but different mix-designs (one using SFHMA mixes and one using traditional dense-graded Type B/C mixes) were constructed on SH 114 in Fort Worth, designated herein as SH 114 Superpave and SH 114 Conventional, respectively. The SH 114 Conventional was primarily an experimental section constructed after the contractor experienced several constructability and permeability problems with the SFHMA mixes on the adjacent SH 114 Superpave section. The intent of the newer SH 114 Conventional section was to experimentally evaluate and compare the potential of using conventional dense-graded Type B/C mixes in the Texas PP structures, both in terms of constructability and performance.

[Figure 8-1](#) shows the pictorial location of the two sections. The actual in-situ PP structures are shown in [Figure 8-2](#). As shown in [Figure 8-2](#), both sections have the same PP structural design, 22 inches of total HMA layer thickness and 8 inches of lime-treated base (subgrade). The thickness of the main structural load-bearing (rut-resistant) layers (Layer 3) is the same for both sections, i.e., 13 inches of the 1-inch SFHMA or Type B. Both sections are located adjacently on SH 114 highway and are therefore subjected to the same traffic loading and environmental/climatic exposure. [Table 8-1](#) lists the results of the comparative evaluations and analyses.



**Figure 8-1. Pictorial Location of the SH 114 PP Sections.**

| SH 114 Superpave |                     |                                 |                    | SH 114 Conventional |                     |                                 |                    |
|------------------|---------------------|---------------------------------|--------------------|---------------------|---------------------|---------------------------------|--------------------|
| Layer            | Material            | Binder + Aggregate              | Thickness (inches) | Layer               | Material            | Binder + Aggregate              | Thickness (inches) |
| Layer 1          | ½" HDSMA            | 6.8% PG 70-28 + Igneous/Granite | 2                  | Layer 1             | ½" HDSMA            | 6.8% PG 70-28 + Igneous/Granite | 2                  |
| Layer 2          | ¾" SFHMAC           | 4.2% PG 76-22 + Limestone       | 3                  | Layer 2             | TxDOT Type C        | 4.4% PG 70-22 + Limestone       | 3                  |
| Layer 3          | 1" SFHMAC           | 4.0% PG 70-22 + Limestone       | 13                 | Layer 3             | TxDOT Type B        | 4.5% PG 64-22 + Limestone       | 13                 |
| Layer 4          | ¾" SFHMAC (RBL)     | 4.2% PG 64-22 + Limestone       | 4                  | Layer 4             | TxDOT Type C (RBL)  | 5.3% PG 64-22 + Limestone       | 4                  |
| Layer 5          | Stabilized Subgrade | 6% Lime Treated                 | 8                  | Layer 5             | Stabilized Subgrade | 6% Lime Treated                 | 8                  |
| Subgrade         |                     |                                 | ∞                  | Subgrade            |                     |                                 | ∞                  |

**Figure 8-2. SH 114 PP Structural Sections.**

In Figure 8-2, Layers 3 and 4 are the rut- and fatigue-resistant layers, respectively, all with the same thickness, but different mix-designs for each PP section. Both the surfacing SMA layer and the base have the same mix-design, materials, and structural thickness.



**Table 8-1. Comparative Evaluation of the SH 114 PP Sections.**

| <b>Item</b>   | <b>SH 114 Superpave</b>   | <b>SH 114 Conventional</b>                                    |
|---|---|---|
| Mix-design  | SFHMA mixes   | Type B and C mixes  |
| PP structure  | SMA + ¾-inch SFHMA + <b>1-inch SFHMA</b> + RBL + base + subgrade    | SMA + Type C + <b>Type B</b> + RBL + base + subgrade          |
| PP structure thickness  | 30 inches = 22-inches HMA + 8-inches base                           | 30 inches = 22-inches HMA + 8-inches base                     |
| RRL mix   | 13 inches 1-inch SFHMA  | 13 inches Type B  |
| RRL mix-design  | 4.0% PG 70-22 + limestone   | 4.5% PG 64-22 + limestone                                     |
| RRL gradation   | Coarse (1-inch NMAS)  | Dense to moderate coarse (¾-inch NMAS)                        |
| Constructability (workability & compactability)                     | Poor  | Good  |
| RRL QC asphalt-binder content                                       | 3.4%  | 4.5%  |
| Average RRL QC in-place AV  | 6.7%  | 9.8%  |
| Lab Hamburg rutting (field core) (≤ 12.5 mm)                        | 7.8 mm @ 20 k   | 12.5 mm @ 7 k   |
| Lab permanent micro-strain after 5 000 load repetitions (RLPD)      | 7,500 µε  | 14,000 µε   |
| Lab Overlay cracking (field core) (≥ 300)                           | 74  | 122   |
| Lab modulus at 77 °F (field core)                                   | 1346 ksi  | 1063 ksi  |
| Lab permeability (field core) (≤ 1.2 × 10 <sup>-3</sup> cm/sec)     | 1.52 × 10 <sup>-3</sup> cm/sec                                      | 0.57 × 10 <sup>-3</sup> cm/sec                                |
| Lab X-ray CT scanning (field core)                                  | High non-uniform AV distribution                                    | Uniform AV distribution                                       |
| Field surface rutting (summer09) (≤ 0.5-inches)                     | 0.09 inches   | 0.10 inches   |
| Field cracking (summer09)   | None  | None  |
| Field IRI (summer09) (≤ 172 in/mi)                                  | 54 in/mi  | 55 in/mi  |
| Field FWD surface deflections (summer 2009 at 113 °F) (≤ 20 mils)   | 4.3 mils  | 4.9 mils  |
| Field PP strength – SCI, BCI, W <sub>7</sub> (summer 2009)          | 2.3, 0.8, 0.5   | 2.0, 0.7, 1.0   |
| Field in-situ FWD modulus at 77 °F                                  | 1750 ksi  | 1500 ksi  |
| GPR & forensic evaluations  | Density variations, voided areas, vertical segregation, & debonding | None (clean GPR readings with solidly intact cores)           |
| Traffic - average daily 18 kip ESALs                                | 3,241   | 3,241   |
| Years in service at time of this report                             | 4.5   | 4.5   |
| FPS strain analyses (≤ 70 & 200 µε, respectively)                   | 35 µε (tensile) & 99 µε (compressive)                               | 29 µε (tensile) & 79 µε (compressive)                         |
| FPS service life prediction   | 27 yrs  | 23 yrs  |
| MEPDG performance prediction  | 23 yrs based on IRI distress (no rutting or fatigue cracking)       | 21 yrs based on IRI distress (no rutting or fatigue cracking) |
| MEPDG rutting prediction after 20 years of services (≤ 0.75 inches) | 0.38 inches   | 0.49 inches   |

Table 8-1 shows that the 1-inch SFHMA and Type B material properties and response performance are comparable and do not differ significantly; albeit the 1-inch SFHMA was found to be relatively stiffer (high moduli values) than the Type B mix as would be expected. Field performance is satisfactory for both sections, with no structural distresses or surface roughness problem (i.e., IRI is less than 60 in/mi). Surface rutting is less than 0.1 inch while no cracking was observed on either section. FWD results also indicated sufficient stiffness and strength, with summer surface deflections at about 113 °F pavement temperature barely reaching 5 mils under 9 kips FWD impact loading. Furthermore, both sections exhibited satisfactory performance predictions based on the FPS and MEPDG analyses. The predicted service life is around 20 years and the computed strain responses are all within the M-E limits of 70 and 200  $\mu\epsilon$ , respectively.

However, evaluations indicated constructability problems and forensic defects with high porosity and non-uniform AV distribution for the 1-inch SFHMA mix/layer. The 1-inch SFHMA measured permeability value of  $1.52 \times 10^{-3}$  cm/sec is exceptionally high and is indicative of the potential for moisture problems, particularly if rainwater infiltrates through the surface layers. As discussed previously in Chapter 3, the coarse gradation nature of these SFHMA mixes compounded with the low asphalt-binder content was seen as the primary contributor to constructability problems and forensic defects associated with these mixes. As shown in Figure 8-3, the GPR measurements, coring, and X-ray CT scanning all indicated forensic defects and high non-uniform AV distribution within the 1-inch SFHMA layers. By contrast, Figure 8-4 shows clean GPR readings with no indication of subsurface defects on the SH 114 Conventional section. Cores extracted from this section were completely intact with no visible defects and the AV distribution was considerably more uniform at around 7 percent compared to the SH 114 Superpave core, which had AV peaks as high as 13.5 percent in the 1-inch SFHMA layer.

Overall, these results support and validate the need to consider switching to the dense-graded Type B mix in the future Texas PP designs, particularly for the main structural load-bearing layers. As evident in Table 8-1 and Figure 8-4, the Type B mix is more workable with better compactability and constructability properties than the coarse-graded 1-inch SFHMA mix. The mix is less susceptible to forensic defects or moisture damage and has thus far exhibited satisfactory performance. However, the Hamburg, the RLPD, and MEPDG results in Table 8-1 indicate the need to consider using high asphalt-binder PG grades or more rut-resistant

mix-design for the Type B mix, i.e., the results indicate potential for HMA permanent deformation.

A point of consideration is that the Hamburg and RLPD tests do not consider that the Type B mix is protected by depth of cover of two or more lifts of more rut resistant mixtures.

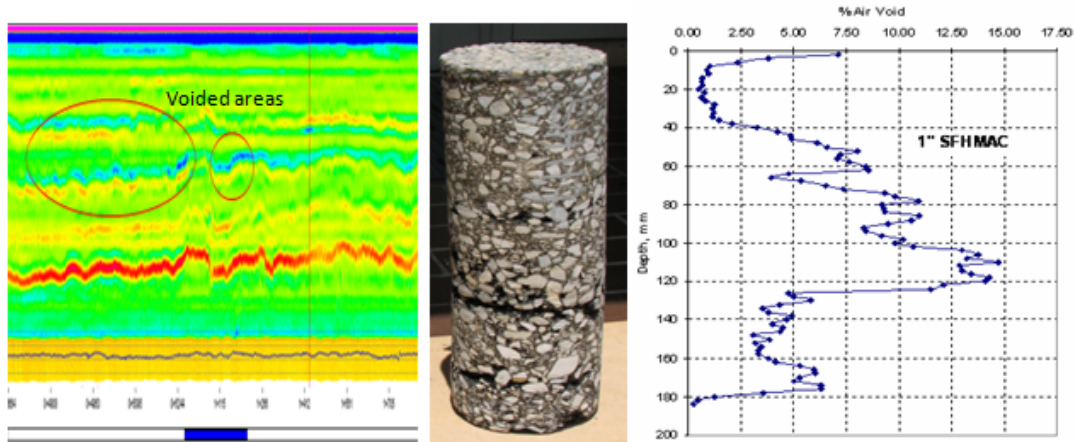


**Figure 8-3. Non-Ideal GPR Readings, Defective Core, and High Non-Uniform Core AV Distribution from SH 114 Superpave.**

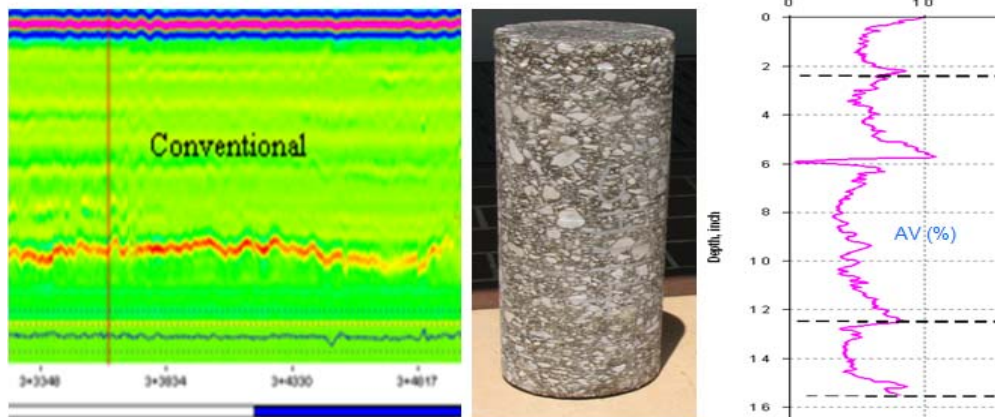


**Figure 8-4. Ideal GPR Readings, Non-Defective Intact Core, and Uniform AV Core Distribution from SH 114 Conventional.**

While the data presented in [Table 8-1](#) and [Figures 8-3](#) and [8-4](#) seem to favor switching to the Type B mix as the RRL in the future Texas PP designs, it should be emphasized that verification of long-term performance of these PP sections is still necessary. At the time of this report, these PP structures had been in service for not more than 5 years. Therefore, the findings and recommendations made herein are preliminary and warrant further verification over time. Furthermore, some optimization of the Type B mix design for rutting resistance improvement may be warranted as indicated by the Hamburg, RLPD, and MEPDG results in [Table 8-1](#).

## GENERAL TEXAS PP PERFORMANCE COMPARISON

Table 8-2 provides a comparative evaluation of some selected PP sections.

**Table 8-2. Comparative Evaluation of Selected PP Sections.**

| <b>Item SH</b>   | <b>114<br/>Superpave<br/>(Fort Worth)</b>                                 | <b>IH 35<br/>Zumwalt02<br/>(Laredo)</b>                                   | <b>IH 35 New<br/>Braunfels<br/>(San Antonio)</b>                                      | <b>IH 35<br/>Hillsboro<br/>(Waco)</b>   |
|--|---|---|---|---|
| Sectional length   | 2.20 mile   | 4.00 mile   | 1.30 mile   | 3.25 mile   |
| PP structure   | SMA + ¾-inch<br>SFHMA + <b>1-inch</b><br>SFHMA + RBL +<br>base + subgrade | SMA + ¾-inch<br>SFHMA + <b>1-inch</b><br>SFHMA + RBL +<br>base + subgrade | PFC + SMA + ¾-<br>inch SFHMA + <b>1-<br/>inch SFHMA</b> +<br>RBL + base +<br>subgrade | PF C + SMA +<br>¾-inch SFHMA<br>+ <b>1-inch</b><br>SFHMA + RBL<br>+ base + subgrade |
| PP structure thickness   | 30 inches = 22 inches<br>HMA + 8 inches base                              | 25 inches = 17-<br>inches HMA +<br>8 inches base                          | 29.5 inches = 21.5<br>inches HMA + 8<br>inches base                                   | 30.5 inches =<br>22.5 inches HMA<br>+ 8 inches base                                 |
| RRL thickness  | 13 inches   | 8 inches  | 12 inches   | 12 inches   |
| RRL mix-design   | 4.0% PG 70-22 +<br>limestone  | 4.1% PG 70-22 +<br>limestone + 1.5%<br>lime                               | 4.5% PG 70-22 +<br>limestone + 0.5%<br>anti-strip                                     | 4.1% PG 70-22 +<br>limestone + 1.0%<br>lime + 2% filler                             |
| RRL QC asphalt-binder<br>content                               | 3.4%  | 3.9%  | 4.1%  | 4.1%  |
| RRL construction quality                                       | Poor  | Good  | Very poor   | Good  |
| RRL average QC in-place<br>AV                                  | 9.8%  | 9.4%  | 11.6%   | 7.3%  |
| Base material (treated<br>subgrade)                            | 6% lime treatment   | 2% cement<br>treatment  | Lime treatment  | 6% lime<br>treatment  |
| RRL lab Hamburg rutting<br>(field core) ( $\leq 12.5$ mm)      | 7.8 mm @ 20 k   | 10.0 mm @ 20 k  | 12.7 mm @ 18 k  | 5.9 mm @ 20 k   |
| RRL lab Overlay cracking<br>(field core) ( $\geq 300$ )        | 74  | 14  | 8   | 356   |
| RRL lab modulus at 77 °F<br>(field core)                       | 1346 ksi  | 2013 ksi  | 1064 ksi  | 1221 ksi  |
| Field surface rutting<br>(summer 2009)<br>( $\leq 0.5$ inches) | 0.09 inches   | 0.07 inches   | 0.13 inches   | 0.12 inches   |
| Field cracking (summer<br>2009)                                | None  | None  | None  | None  |
| Field IRI (summer 2009)<br>( $\leq 172$ in/mi)                 | 54  | 56  | 68  | 63  |
| Field FWD surface<br>deflections (summer 2009)                 | 4.3 mils  | 5.0 mils  | 3.3 mils  | 5.3 mils  |
| RRL field in-situ FWD<br>modulus at 77 °F                      | 1750  | 2400  | 1560  | 1585  |
| Visual surface defects   | None  | Open construction<br>joints   | None  | None  |
| Forensic (subsurface)<br>defects                               | Yes   | None  | Yes   | None  |
| FPS performance life<br>( $\leq 70$ & 200 $\mu\epsilon$ )      | 27 yrs  | 31 yrs  | 28 yrs  | 34 yrs  |
| MEPDG performance<br>predictions                               | 23 yrs based on IRI   | 24 yrs based on IRI   | 29 yrs based on<br>IRI  | 29 yrs based on<br>IRI  |

Based on [Table 8-2](#), performance as of summer 2009 was satisfactory and comparable for all the Texas PP sections. No structural distresses were observed, and the 1-inch SFHMA material properties in [Table 8-2](#) are fairly comparable. By contrast however, the results indicate very high moduli values ( $> 2000$  ksi) for the IH 35 Zumwalt02 section in Laredo and the presence of open construction joints. As pointed out previously in both [Chapters 4](#) and [5](#), the Laredo mixes exhibited the greatest stiffness based on their higher moduli values, but poor resistance to cracking based on the Overlay test. As evident in [Table 8-2](#), the Laredo and San Antonio sections exhibited the poorest laboratory cracking performance based on their lower number of OT cycles to failure, 14 and 8, respectively, for field-extracted cores.

Note also in [Table 8-2](#) that as would be expected, the projects that were associated with poor construction quality also exhibited forensic and subsurface defects within the PP structures. This was particularly very critical for the San Antonio projects. These forensic defects (density variations, localized voiding, vertical segregation, and poor layer bonding) are undesirable and thus, it is imperative to improve the SFHMA construction methods in future projects.

Computational analyses based on the FPS and MEPDG software also indicated satisfactory performance predictions. The average predicted service life was greater than 20 years, and the computed strain responses were substantially lower than the M-E thresholds, i.e., less than 70 and 200  $\mu\epsilon$  tensile and compressive strains, respectively. Considering the greater thickness (i.e., average 22 inches HMA and 8 inches base) and high stiffness nature of these PP structures, these predictions were not unexpected and, in fact, indicated potential for further optimization of the Texas PP structural design concept.

## **TEXAS PP COMPARISON WITH NCAT TEST TRACK PP SECTIONS**

In an effort to further validate the Texas PP design concept, a comparison was also made with the PP sections constructed at the NCAT APT test track in Alabama. This section discusses comparative analyses of these NCAT PP sections with the Texas SH 114 Conventional section. The comparison included evaluation of the PP structures, materials and mix-designs, material properties, laboratory test data, field performance data, and computational analyses.

## Brief Description of the NCAT Test Track

The NCAT test track is a unique APT facility that brings together real-world full-scale pavement construction with live heavy truck-traffic for rapid testing and analysis of HMA pavements. The test track is funded and managed by NCAT in conjunction with Auburn University as a cooperative project among highway agencies and industry sponsors. The track is a 1.7-mile oval pavement test track that consists of 46 different 200-foot test sections. Test sections are sponsored on three-year cycles. Each sponsor has specific research objectives for their section(s) as well as shared objectives for the track as a whole.

NCAT operates a fleet of heavily loaded tractor-trailers to provide 10 million 18 kips ESALs during each cycle. Pavement performance is monitored on a continuous basis to evaluate rutting, fatigue cracking, roughness, texture, friction, and noise. Structural pavement research test sections have embedded strain and pressure sensors for analysis of pavement response to loads. These pavement response measurements aid in the evaluation and validation of M-E design procedures. All test sections are also equipped with temperature sensors throughout the pavement depth. [Figure 8-5](#) shows a pictorial and schematic of the NCAT test track.

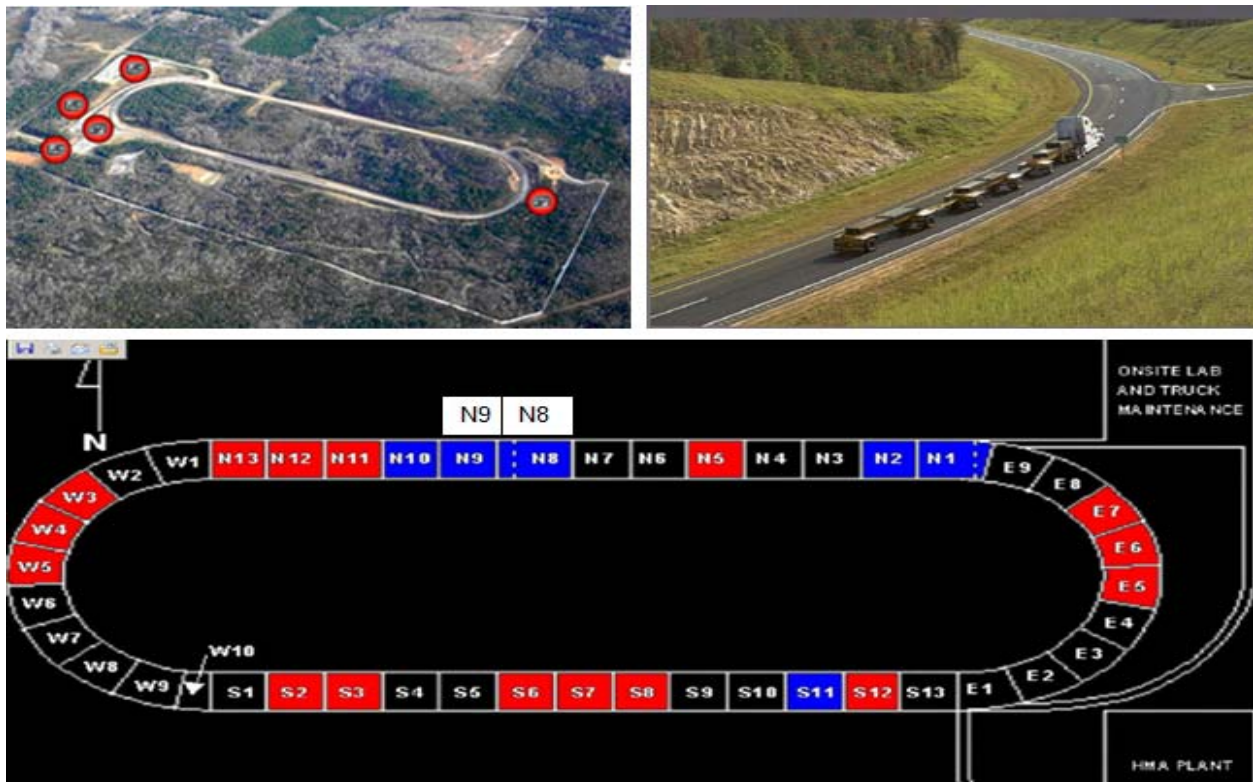


Figure 8-5. Overview of the NCAT Test Track.

In the 2006 test cycle, test sections N8 and N9 were designed and sponsored by the Oklahoma State Department of Transportation (ODOT) as perpetual pavements for M-E design evaluation and validation. These were the test sections utilized for comparisons with the Texas PP structure on SH 114 Conventional. The mix-designs of both N8 and N9 were comprised of dense-graded Superpave mixes and, therefore, it was found appropriate to only compare them with the Texas SH 114 Conventional section that also used dense-graded mixes.

In terms of structural design, N8 had 10 inches total HMA layer thickness while N9 had 14 inches, both supported on about 9-inch base material. The sections were subjected to 10 million 18 kips ESAL applications in a compressed time period of 2 years. NCAT monitored and recorded performance data periodically, ranging from a weekly to monthly basis depending on the data type.

### **Data Acquisition and Laboratory Testing**

In addition to accessing some of the NCAT performance data for these sections, TTI researchers had also obtained plant mixes and field cores (from in between the wheel paths) for laboratory testing and material property characterization. TTI researchers did the coring as well as conducted GPR measurements on the entire test track. Tests conducted in the TTI laboratory on both the NCAT plant mixes and the cores included the Hamburg (rutting resistance), Overlay (cracking resistance), and X-ray CT scanning (AV distribution characterization).

### **Texas SH 114 Conventional versus NCAT N8 and N9 Sections**

A summary of the comparative evaluation is listed in [Table 8-3](#). To facilitate first order comparisons with the Texas SH 114 Conventional section, only performance data at 5.32 million ESALs was utilized in the comparative analyses. This was necessary because the Texas SH 114 Conventional section had been subjected to only an estimated 5.32 million ESALs (18 kips) at the time of this report. This inevitably allowed for a fair first-order comparison.

**Table 8-3. SH 114 Comparison with NCAT N8 and N9 Sections.**

| <b>Item</b>   | <b>Texas SH 114<br/>Conventional</b>  | <b>NCAT N8<br/>(Alabama)</b>  | <b>NCAT N9<br/>(Alabama)</b>   |
|---|---|---|--|
| Sectional length (mile)                                 | 1.3 mile  | 200 ft  | 200 ft   |
| PP structure  | 2-inch SMA + 3-inch Type C + 13-inch <b>Type B</b> + 4-inch RBL + base + subgrade | 2-inch SMA + 6-inch <b>Superpave</b> + 2-inch RBL + base + subgrade | 2-inch SMA + 3-inch Superpave + 6-inch <b>Superpave</b> + 3-inch RBL + base + subgrade |
| PP structure thickness                                  | 30 inches = 22-inches HMA + 8-inches base   | 19 inches = 10-inches HMA + 9-inches base                           | 23 inches = 14-inches HMA + 9-inches base  |
| RRL thickness   | 13 inches   | 6 inches  | 6 inches   |
| RRL mix-type  | Type B  | ¾" Superpave  | ¾" Superpave   |
| RRL mix-design  | 4.5% PG 64-22 + limestone   | 4.3% PG 64-22 + granite   | 4.3% PG 64-22 + granite  |
| RRL gradation   | Dense to moderate coarse (⅞-inch NMAS)  | Dense (¾-inch NMAS)   | Dense (¾-inch NMAS)  |
| RRL QC asphalt-binder content                           | 4.5%  | 4.4%  | 4.8%   |
| RRL construction quality                                | Good  | Good  | Good   |
| Average QC in-place AV (RRL)                            | 6.7%  | 4.2%  | 4.1%   |
| Base material   | 6% lime treatment   | -   | -  |
| RRL lab Hamburg rutting (field core) ( $\leq 12.5$ mm)  | 12.5 mm @ 7 k   | 11.8 mm @ 20 k  | 9.6 mm @ 20 k  |
| RRL lab Overlay cracking (field core) ( $\geq 300$ )    | 122   | 82  | 290  |
| RRL lab modulus at 77 °F (field core)                   | 1063 ksi  | 1208 ksi  | 1310 ksi   |
| Field surface rutting (summer09) ( $\leq 0.5$ inches)   | 0.10 inches   | 0.20 inches   | 0.09 inches  |
| Field cracking (summer09)                               | None  | Yes (surface cracking)  | None   |
| Field IRI (summer09) ( $\leq 172$ in/mi)                | 55  | 125   | 125  |
| Field FWD surface deflections (winter)                  | 1.2 mils  | 1.6 mils  | 1.1 mils   |
| RRL field in-situ FWD modulus at 77 °F                  | 1750  | 1790  | 1830   |
| Visual surface defects                                  | None  | Surface cracking  | None   |
| Forensic (subsurface) defects                           | None (intact cores)   | None (intact cores)   | Yes (intact cores but with vertical segregation)                                       |
| X-ray CT scanning (RRL field core)                      | Uniform AV distribution   | Non-uniform AV distribution   | Non-uniform AV distribution  |
| Traffic (18 kips ESALs)                                 | 5.32 million  | 5.32 million  | 5.32 million   |
| FPS strain analyses ( $\leq 70$ & $200$ $\mu\epsilon$ ) | 29 $\mu\epsilon$ (tensile) & 79 $\mu\epsilon$ (compressive)                       | 63 $\mu\epsilon$ (tensile) & 189 $\mu\epsilon$ (compressive)        | 46 $\mu\epsilon$ (tensile) & 129 $\mu\epsilon$ (compressive)                           |
| FPS performance life                                    | 23 yrs  | 15 yrs  | 19 yrs   |
| MEPDG performance predictions                           | 21 yrs based on IRI   | 14 yrs based on rutting   | 19 yrs based on rutting  |



At equivalent traffic loading, [Table 8-3](#) shows that the Type B material properties and performance are fairly comparable to NCAT N9. Both sections exhibit no structural distresses with computed strain responses well within the M-E thresholds. Surface roughness was, however, very poor in the NCAT sections, averaging 125 in/mi just after 5.32 million ESAL applications. The MEPDG also predicted greater potential for rutting for the NCAT sections compared to SH 114. Compared to Type B, this was expected as the NCAT mixes used a much finer gradation; see [Figure 8-6](#) below. Nonetheless, these predictions together with the Hamburg test results suggest the need to consider mix design adjustments for rutting resistance optimization in future designs.

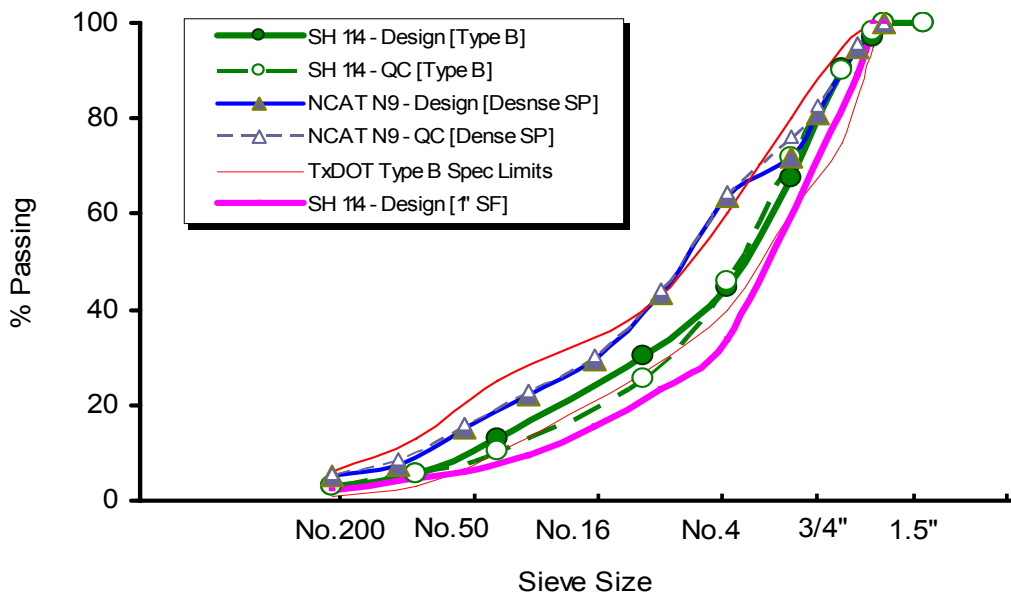


**Figure 8-6. Aggregate Gradation Comparisons.**

With respect to construction quality and forensic evaluations, the Texas SH 114 Conventional section exhibited superior performance, with NCAT N9 showing the poorest. Although cores from all the three sections were intact with no serious forensic defects, NCAT N9 exhibited visual evidence of vertical segregation and the AV distribution from X-ray CT scanning was hardly uniform. GPR readings were clean with no indication of significant in-situ density variations, low density spots, localized voided areas, or moisture presence in all three sections. These results are shown in [Figure 8-7](#).

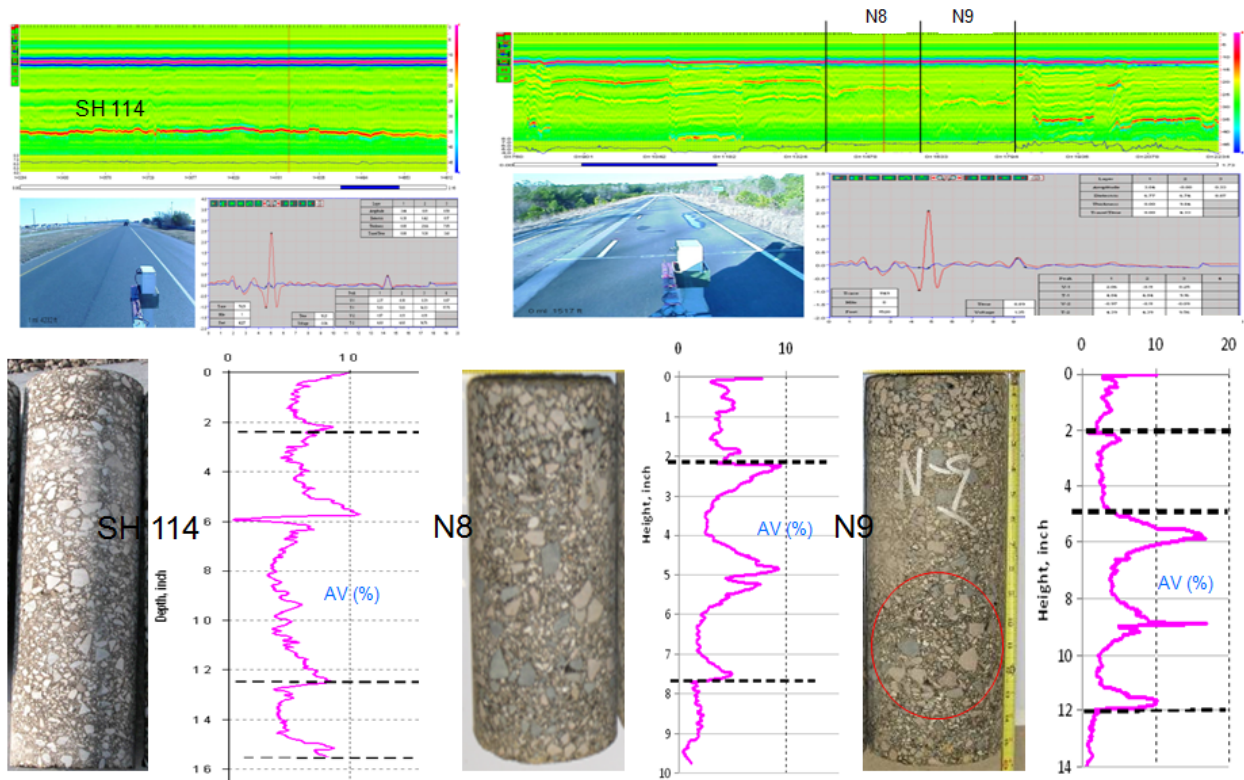


**Figure 8-7. Texas SH 114 vs. NCAT PP Sections (GPR, Cores, and AV Distribution).**

Clearly, [Figure 8-7](#) shows much higher AV variations in the NCAT cores, with N9 having AV peaks as high as 17 percent. However, both NCAT N8 and N9 indicate excellent AV distribution in both the top SMA layer and bottom RBL compared to the SH 114 Conventional section. This was in part attributed to the higher design asphalt binder contents in these layers; both had 7 percent while the SH 114 SMA and RBL had 6.8 and 5.2 percent, respectively. Note that high asphalt-binder content generally promotes mix compaction due to increased lubrication. Compared to N9, N8 exhibits higher AV distribution in the top 4 inches of the structure including the SMA and the upper portion of the RRL.

Due to performance data limitations, analyses of the surface cracking observed on NCAT N8 were inconclusive. However, speculative intuition suggests that the surface cracking on this section was related to construction, mix-designs, and possible debonding in the surface HMA layers. As shown in [Table 8-4](#), the field cores from this section including the SMA exhibited the poorest cracking resistance based on laboratory testing with the Overlay. This is indicative of poor mix-designs or possibly construction problems.

**Table 8-4. Comparison of OT Results – Field Cores (SH 114 vs. Alabama).**

| <b>Texas SH 114 Conventional</b> | <b>NCAT N8 (Alabama)</b> | <b>NCAT N9 (Alabama)</b> |
|----------------------------------|--------------------------|--------------------------|
| SMA= 300+                        | SMA= 197                 | SMA= 506                 |
| Type C= 106                      | N/A N/A                  | Superpave= 290           |
| Type B= 122                      | Superpave= 81            | Superpave= 290           |
| RBL= 550                         | RBL= 300+                | RBL= 300+                |

Overall, the results presented in this section substantiate the validity of the Texas PP design concept and, in fact, supports the transitioning to more optimal structures of about 14 inches in total HMA thickness. Performance of both the Texas SH 114 Conventional and NCAT N9 sections was satisfactory with the computed strain response equally meeting the M-E thresholds. Although field performance data still indicated satisfactory performance for NCAT N9 even after 10.0 million ESALs traffic loading, this does not repress the need for long-term performance monitoring of SH 114 to verify the findings reported herein.

## **SUMMARY**

The list below summarizes the major findings from this chapter:

- In the application as an RRL, both the material properties and performance of the Type B and 1-inch SFHMA were fairly comparable with no serious defects on either section. However, the Type B was found to be more workable with better compactability and constructability properties than the 1-inch SFHMA mix. The Type B mix exhibited a more uniform AV distributional structure with fewer density variations; it was less susceptible to forensic defects and moisture problems compared to the 1-inch SFHMA mix.
- While the SH 114 Conventional section exhibited better M-E response (largely due to thickness) and performance than NCAT N9, the material properties were fairly comparable and performance was satisfactory in both sections. However, the results indicated better constructability properties for the Type B mix than for NCAT N9 Superpave mix.
- While NCAT N9 provided supplementary data that the Texas PP design concept was sufficiently valid, the results also indicated potential for further optimization down to about 14 inches total HMA thickness. However, caution should be exercised when referencing the NCAT test sections as these were subjected to much less traffic (about one-third) compared to the minimum design 18-kip ESALs for the Texas PP structures.



## CHAPTER 9

### FUTURE TEXAS PP DESIGN AND RECOMMENDATIONS

This chapter provides a summation of the recommendations for the future design of Texas PP structures. A discussion of the construction, material testing, and field performance evaluations is also presented. A summary is then presented to wrap-up the chapter. Note that the recommendations and proposals made herein are based on all considerations of the entire research project including the work contained in reports 0-4822-1 and 0-4822-2 and the Texas PP database (Scullion, 2007; Walubita and Scullion, 2007; Walubita et al., 2009).

#### FUTURE PP STRUCTURAL AND MIX DESIGN PROPOSALS

Table 9-1 provides alternative structural designs as a function of three traffic levels, namely: (1) traffic ESALs  $\leq 30$  million, (2)  $30 \text{ million} < \text{Traffic ESALs} \leq 50$  million, and (3) traffic ESALs  $> 50$  million. These design proposals are based on the findings of Chapters 1 through 8 of this report and extensive computational analyses with the FPS and MEPDG software (using projections based on actual measured traffic data and measured layer moduli values). As a minimum, the proposal is for the future Texas PP design to have a structural thickness of 12 inches HMA and 6 inches treated base material for sections with traffic level of 30 million ESALs or less. For traffic greater than 50 million ESALs, the minimum should be 15 inches total HMA thickness and 8 inches treated base material.

#### Design and Analyses Software

Based on the software evaluations and computational modeling in Chapter 7 and report 0-4822-2 (Walubita and Scullion, 2007), FPS 21W and MEPDG 1.0 are the recommended software for the future design and modeling of Texas PP structures as follows:

- FPS 21W – PP structural thickness design, M-E response analysis, and strain check
- MEPDG 1.0 – PP design verification and performance analysis/predictions

For the MEPDG, the calibration factors listed in Chapter 7 should be used; namely  $\beta_{r3} = 0.94$ ,  $\beta_{s1} = 0.6$ ,  $C_1$  (bottom-up cracking) = 1.2, and  $C_1$  (top-down cracking) = 9.0.

**Table 9-1. Future Texas PP Design Proposals.**

| <b>Layer#</b>  | <b>Thickness<br/>(inches)</b> | <b>Mix Type</b>                  | <b>Designation</b>   | <b>2004 TxDOT<br/>Spec Item</b> | <b>Material</b>       |
|--|-------------------------------|----------------------------------|--|---------------------------------|-----------------------|
| <b>(a) Traffic ESALs ≤ 30 million</b>  |                               |                                  |  |                                 |                       |
| 1  | 2                             | SMA                              | Surfacing  | Item 346                        | PG 70-28<br>or better |
| 2  | 2                             | ¾-inch<br>Superpave              | Load transitional layer  | Item 344                        | PG 70-22<br>or better |
| 3  | ≥ 6                           | Type B                           | Main structural load-<br>carrying rut-resistant layer                    | Item 341                        | PG 64-22<br>or better |
| 4  | 2                             | Type C or<br>½-inch<br>Superpave | Rich bottom fatigue-<br>resistant layer (durability<br>& impermeability) | Item 341                        | PG 64-22              |
| 5  | ≥ 6                           | Base                             | Lime or cement treatment   | Items 260, 263, 275,<br>& 276   |                       |
| Subgrade (in-situ soil material)   |                               |                                  |  |                                 |                       |
| Minimum PP structure thickness = 18 inches (12 inches HMA and 6 inches base) |                               |                                  |  |                                 |                       |
| <b>(b) 30 million &lt; Traffic ESALs ≤ 50 million</b>                        |                               |                                  |  |                                 |                       |
| 1  | 2                             | SMA                              | Surfacing  | Item 346                        | PG 70-28<br>or better |
| 2  | 3                             | ¾-inch<br>Superpave              | Load transitional layer  | Item 344                        | PG 70-22<br>or better |
| 3  | ≥ 8                           | Type B                           | Main structural load-<br>carrying rut-resistant layer                    | Item 341                        | PG 64-22<br>or better |
| 4  | 2                             | Type C or ½-<br>inch Superpave   | Rich bottom fatigue-<br>resistant layer (durability<br>& impermeability) | Item 341                        | PG 64-22              |
| 5  | ≥ 6                           | Base                             | Lime or cement treatment   | Items 260, 263, 275,<br>& 276   |                       |
| Subgrade (in-situ soil material)   |                               |                                  |  |                                 |                       |
| Minimum PP structure thickness = 21 inches (15 inches HMA and 6 inches base) |                               |                                  |  |                                 |                       |
| <b>(c) Traffic ESALs &gt; 50 million</b>                                     |                               |                                  |  |                                 |                       |
| 1  | 2-3                           | SMA                              | Surfacing  | Item 346                        | PG 70-28<br>or better |
| 2  | ≥ 3                           | ¾-inch<br>Superpave              | Load transitional layer  | Item 344                        | PG 70-22<br>or better |
| 3  | ≥ 8                           | Type B                           | Main structural load-<br>carrying rut-resistant layer                    | Item 341                        | PG 70-22<br>or better |
| 4  | 2-4                           | Type C or ½-<br>inch Superpave   | Rich bottom fatigue-<br>resistant layer (durability<br>& impermeability) | Item 341                        | PG 64-22              |
| 5  | ≥ 8                           | Base                             | Lime or cement treatment   | Items 260, 263, 275,<br>& 276   |                       |
| Subgrade (in-situ soil material)   |                               |                                  |  |                                 |                       |
| Minimum PP structure thickness = 23 inches (15 inches HMA and 8 inches base) |                               |                                  |  |                                 |                       |

\*On top of the SMA, a PFC (TxDOT 2004 spec item 342) can be added as an “optional” surface moisture drainage, noise-reduction, and skid-resistant layer. Preferably, the PFC layer thickness should be 1.5 inches.

## **HMA Mix-Designs and Materials**

As seen in [Table 9-1](#), proposals are to use the Type B mix for the main structural load-carrying rut-resistant layer as opposed to the coarse-graded stone-filled HMA mixes in the current Texas PP design concept. This is because the stone-filled HMA mixes, as discussed previously in this report, exhibited undesirable constructability problems with high potential for moisture damage and other forensic defects. The Type B mix on other hand was found to be more workable with better compactability and constructability properties, attaining more uniform density with lower potential for moisture induced problems or forensic defects.

Performance wise, the Type B was comparable to the stone-filled HMA mixes and even superior in some instances, i.e., in terms of subsurface defects and anomalies. Although rutting tests and the MEPDG performance predictions had indicated potential for permanent deformation, particularly where PG 64-22 was used in the Type B mix, overall susceptibility to field rutting may be mitigated by its lower placement in the structure. As such, PG 64-22 should be used only as the minimum asphalt-binder PG grade in the Type B mix where it is used as the main structural load-carrying layers. Otherwise, recommendations are made herein to use higher PG grades such as PG 70-22 in future Texas PP designs. Alternatively, use of more rut-resistant mix-designs by modifying the aggregate type or gradations can be done.

## **The Base and Subgrade Materials**

The need to provide a structurally sound, permanent foundation cannot be overemphasized. History has shown that deep HMA structures placed on questionable foundations will still be influenced by soil movement and reflective cracking. Overall, this report has indicated that the base and subgrade materials currently used have performed satisfactorily, with sufficient stiffness and strength. The measured in-situ FWD moduli values were greater than 30 and 15 ksi for the base and subgrade, respectively. Seasonal moduli variations were also very marginal, thus, substantiating that both the base and subgrade material were relatively non-moisture susceptible. Therefore, the current TxDOT specifications for base and subgrade treatment should continue to be used. Lime stabilized subgrades should be designed according to Tex-Method 121 E part 1 and cement-treated subgrade and recycled layers as recommended in Tex Method 120 E.

As currently used in the Bryan District (Goehl, 2009), a cement content yielding a target unconfined compressive strength of 220 psi appears reasonable; the use of an 80 percent retained strength on capillary saturation should be enforced. Another successful technique, used in the Laredo District, applies microcracking on all bases where cement treatment is used to mitigate formation of shrinkage cracking that potentially could reflect to the surface. The minimum base treatment depth should be 6 inches. Furthermore, where lime is used as the stabilization agent, it should be applied in a liquid form as slurry.

### Layer Design Moduli

Based on the results in Chapters 4 and 5, the proposed layer design moduli values in the future Texas PP designs are listed in Table 9-2. These proposed moduli values are expected to yield optimal PP structural designs.

**Table 9-2. Proposed Future Design Moduli Values at 77 °F.**

| Layer/Material TxDOT            | 2004 Spec Item  | Proposed Design Modulus Value (ksi) | Recommended Design Modulus Range (ksi) | Poisson's Ratio |
|---------------------------------|-----------------|-------------------------------------|--|-----------------|
| PFC (optional)                  | Item 342        | 350                                 | 300-450                                | 0.30            |
| SMA                             | Item 346        | 650                                 | 500-850                                | 0.35            |
| ¾-inch Superpave                | Item 344        | 800                                 | 600-1200                               | 0.35            |
| RRL – Type B                    | Item 341        | 800                                 | 700-1300                               | 0.35            |
| RBL– Type C or ½-inch Superpave | Item 341        | 500                                 | 400-650                                | 0.35            |
| Base – lime treatment           | Items 260 & 263 | 60                                  | 50-75                                  | 0.30-0.35       |
| Base – cement treatment         | Items 275 & 276 | 100                                 | 80-150                                 | 0.20-0.30       |
| Subgrade                        |                 | 12                                  | 10-30                                  | 0.40-0.45       |

### M-E Design Criteria

Although, the tensile strain responses were not practically validated in the field, analytical indications based on the FPS and MEPDG modeling are that the structures are sufficient with respect to the M-E tensile strain criteria. On all the PP structures, the computed tensile strains were at least 25 percent lower than the 70  $\mu\epsilon$  threshold.



Considering the fact that field performance has generally been satisfactory with no structural defects as of the time of this report, the recommendation is that the 70 and 200  $\mu\epsilon$  maximum thresholds should continue to be used as the M-E response design criteria in the future Texas PP designs.

### Computational Validation of the Proposed Future PP Structural Designs

To assess the validity of the proposed PP structural designs in [Table 9-1](#), FPS and MEPDG analyses were conducted at the 95 percent reliability level. Traffic loading projections based on actual measured traffic parameters in [Chapter 6](#) and the moduli values in [Table 9-2](#) were utilized. [Table 9-3](#) shows results of these analyses.

**Table 9-3. Computational Validation of the Proposed PP Structural Designs.**

| <b>Item (a)</b>  | <b>Traffic ESALs <math>\leq</math> 30 million</b>  | <b>(b) 30 million &lt; Traffic ESALs <math>\leq</math> 50 million</b>                                      | <b>(c) Traffic ESALs &gt; 50 million</b>   |
|--|--|--|--|
| Traffic loading used in analysis   | 30 million   | 40 million   | 75 million   |
| Design life  | 20 yrs   | 20 yrs   | 20 yrs   |
| Environment  | Fort Worth   | Fort Worth   | Fort Worth   |
| PP structure   | 2-inch SMA + 2-inch ( $\frac{3}{4}$ -inch) Superpave + 6-inch Type B + 2-inch RBL + 6-inch base + subgrade | 2-inch SMA + 3-inch ( $\frac{3}{4}$ -inch) Superpave + 8-inch Type B + 2-inch RBL + 6-inch base + subgrade | 2-inch SMA + 3-inch ( $\frac{3}{4}$ -inch) Superpave + 8-inch Type B + 2-inch RBL + 8-inch base + subgrade |
| FPS tensile strains at bottom of lowest HMA layer ( $\leq 70\mu\epsilon$ ) | 54 $\mu\epsilon$   | 38 $\mu\epsilon$   | 37 $\mu\epsilon$   |
| FPS compressive strains on top of subgrade ( $\leq 200 \mu\epsilon$ )      | 143 $\mu\epsilon$  | 101 $\mu\epsilon$  | 94 $\mu\epsilon$   |
| FPS performance life prediction  | 17.9 yrs   | 19.7 yrs   | 17.5 yrs   |
| MEPDG IRI ( $\leq 172$ in/mi)  | 151 in/mi  | 138 in/mi  | 157 in/mi  |
| MEPDG rutting ( $\leq 0.75$ inches)  | 0.59 inches  | 0.53 inches  | 0.60 inches  |
| MEPDG cracking (should be zero percent)                                    | 0.00%  | 0.00%  | 0.00%  |
| MEPDG performance life prediction  | 18.5 yrs base on IRI   | 20 yrs based on IRI  | 18.1 yrs based on IRI  |

The results in [Table 9-3](#) indicate satisfactory performance predictions with a service life of close to 20 years prior to a surface renewal or an overlay, thus analytically validating the design proposals in [Table 9-1](#). Furthermore, the MEPDG performance predictions indicated IRI as the governing criteria for the surface renewal or an overlay.

## **FUTURE PP CONSTRUCTION**

The results presented in [Chapter 4](#) indicate the need for improved construction methods and as a minimum better enforcement of the QC/QA test protocols on future Texas PP construction jobs. This is necessary to optimize construction quality and minimize construction-related defects including subsurface anomalies within the PP structures. Some of the construction measures warranting improvements include the following:

- compaction rolling patterns/more rigorous application of control strips (Tex-207-F, Part IV);
- joint compaction specifications (i.e., test more than the minimum requirement until confidence is established in the contractor's performance);
- elimination of trench construction (where possible);
- enforcement of joint staggering at all levels within the pavement structure;
- transitioning techniques between concrete and HMA pavements;
- optimization of the compaction lift thickness based on mixture type and NMAAS;
- optimization of tack coat as a bonding material; and
- minimization of JMF changes that employ reductions in the AC content.

Based on the results of this report and the authors' field observations, it is proposed that 4 inches be specified as the maximum compaction lift-thickness for the Type B and  $\frac{3}{4}$ -inch Superpave mixes. This is particularly critical where the mixes are used as the structural load-bearing layers with a thickness greater than 4-inches in the PP structure. A 4-inch lift thickness is expected to significantly improve compaction and construction quality of the mix/layer.

As was discussed in [Chapter 4](#), IR thermal imaging and GPR measurements (supplemented with coring) proved very useful in monitoring the construction quality of these PP structures. These NDT tools were successfully utilized for HMA mat temperature measurements, layer thickness and compaction density measurements, and detection of subsurface anomalies such as density variations, localized voiding, vertical segregation, debonding, and moisture presence. Results from both IR thermal imaging and GPR measurements aided contractors in implementing construction changes on some projects that ultimately led to improved construction quality. It is therefore recommended that these NDT tools be incorporated in future Texas PP construction projects as a supplement to the current construction QC/QA test protocols.

### **FUTURE PP TESTING AND PERFORMANCE EVALUATION**

In addition to the traditional performance monitoring and evaluation tests such as the FWD typically used on flexible HMA pavements, the authors recommend incorporating GPR measurements on all future PP projects for forensics evaluations. In this research study, the GPR was found to be a very useful NDT tool for the structural evaluation of the perpetual pavements in terms of detecting forensic defects. The GPR has the potential to detect subsurface defects such as localized voiding, debonding, and moisture entrapment within the PP structures. This is particularly very critical in establishing pavement maintenance programs for the PP structures where it can beneficially lead to timely identification and treatment of the defects prior to terminal deterioration.

Because of their unique HMA structural thickness and the postulated superior performance compared to conventional flexible HMA pavements, it is also proposed that some performance thresholds be modified so as to provide a level basis of comparison. These performance thresholds are listed in [Table 9-4](#).

**Table 9-4. Comparison of Some Performance Thresholds.**

| <b>Item</b>                     | <b>Current Threshold for Good Performance</b> | <b>Proposal</b> |
|---------------------------------|---|-----------------|
| PP surface roughness            |   |                 |
| 1)QC IRI                        | 30 - 65 in/mi                                 | 30 - 65 in/mi   |
| 2)IRI after 20 yrs              | ≤ 172 in/mi                                   | ≤ 150 in/mi     |
| PP surface rutting after 20 yrs | ≤ 0.75 inches                                 | ≤ 0.60 inches   |
| Cracking after 20 yrs           | ≤ 25%   | ≤ 25%           |

The proposed thresholds in [Table 9-4](#) are largely based on the field results in [Chapter 5](#) and extrapolative analyses. Therefore, the numbers proposed should be treated as preliminary based on empirical data collect to date. Given that most of the Texas PP sections have barely been in service for 5 years, long-term performance evaluations are still necessary to validate these proposals.

## **SUMMARY**

This chapter summarized the recommendations for the design, construction, and performance evaluation of future Texas PP structures. Three structural design proposals categorized by three levels of traffic were proposed and analytically validated using the FPS and MEPDG software. The proposed PP structural designs are considerably more optimal compared to the design concept dating back to 2001 under which all the currently existing Texas PP structures were designed. Total HMA cost-savings in the proposed PP structural designs is over 6 inches. Recommendations were also made for the possible incorporation of IR thermal imaging and GPR measurements in future Texas PP construction and performance evaluation tasks. These NDT tools were very helpful in the current PP construction and structural performance monitoring.

## **CHAPTER 10**

### **SUMMARY AND CONCLUSIONS**

The major findings from this research project are summarized and listed as follows:

- 1) At the time of this report, field performance of all the Texas PP sections was satisfactory with no structural defects. However, the majority of these PP sections have been in service less than 5 years. Therefore long-term performance monitoring is strongly recommended to verify the findings reported herein. A sustained program of monitoring at 2-3 year intervals is recommended (rut, ride, deflection, GPR, visual).
  
- 2) Numerous construction problems (such as density variations, localized voiding, vertical segregation, and permeability issues) were associated with the existing PP structures, primarily due to the poor workability and compactability characteristics of the coarse-graded stone-filled HMA (SFHMA) mixes. In retrospective, however, this was not unexpected because it was the first time most Texas contractors had constructed perpetual pavements and used the stone-filled HMA mixes. Nonetheless, these problems highlighted the need for improved construction methods and adoption of increased frequency/tightening of the QC/QA test protocols. Accordingly, recommendations such as improving the compaction rolling patterns, increased frequency/enforcement of joint compaction specs and joint staggering provisions, eliminating trench construction (where possible), and optimizing the compaction lift-thickness were made in the report.
  
- 3) Laboratory testing and material property characterization, together with the back-calculated FWD moduli values, indicated that the PP structures were substantially stiffer (with high modulus values) and fairly non-temperature susceptible as compared to thinner HMA structures. Both the base and the subgrade were also found to have sufficient strength and have not shown moisture susceptibility. Furthermore, the results showed that the use of lower moduli values in the initial designs is what contributed to the conservative nature of the currently existing PP structures. Recommendations have

subsequently been made in this report to use more optimal moduli values in future Texas PP designs.

- 4) WIM traffic measurements on two selected PP sections indicated that the initial traffic loading projections were fairly consistent with projections based on actual traffic loading on the highways. Therefore, it was concluded that the initial traffic design estimates were valid and did not contribute significantly to the conservatism in the current PP designs. User of lower moduli values in the initial designs was the primary contributor.
- 5) From extensive computational modeling and software comparative evaluations, it was concluded that the FPS and MEPDG were the suitable software for modeling Texas PP structures. Consequently, recommendations have been made in this report to use these softwares in future Texas PP structural designs for layer thickness determination, M-E strain analyses, and performance predictions.
- 6) Both field MDD measurements and computational strain analyses have indicated that the current Texas PP design concept is conservatively valid, with potential for further optimization. Further computational analyses indicated the possible transitioning to an optimal PP structure in the range of 12 to 14 inches total HMA thickness which allows for at least 6-inch HMA cost-savings compared to the current design concept. This possible transitioning was successfully validated with the PP section at NCAT (Alabama) that had 14 inches total HMA and exhibited satisfactory field performance with no structural distresses after 10 million ESALs of APT trafficking.
- 7) In consideration of the conservative nature of the current design concept, three structural design proposals based on three levels of traffic categorization were proposed and analytically validated using the FPS and MEPDG software. These analyses resulted in a PP structure with a minimum thickness of 12 inches total HMA and a 6-inch base. In addition, a switch to mixtures with more dense-graded characteristics as opposed to the coarse-graded stone-filled HMA mixes was recommended for the main structural load-

bearing layers. This recommendation was necessitated by the need to circumvent the constructability problems associated with the stone-filled HMA mixes.

- 8) IR thermal imaging and GPR measurements (supplemented with coring) were found to be very helpful NDT tools in the current PP construction and structural performance-monitoring efforts. These NDT tools were successfully utilized for HMA mat temperature measurements, layer thickness and compaction density measurements, and detection of subsurface anomalies such as density variations, localized voiding, vertical segregation, debonding, and moisture presence. Proposals have, therefore, been made to incorporate these tools in future Texas PP projects.
  
- 9) Visual defects such as open joints (longitudinal and transverse) and longitudinal cracking were observed on some projects. These defects were construction related; attributed to poor joint compaction, poor joint staggering, and the effects of trench construction. Recommendations have subsequently been made in this report for improved construction quality control in future jobs. However, there is still a strong need to research better construction methods to transition between existing concrete pavement sections and a flexible (HMA) pavement. On most of the current PP sections, the transverse joints at the transitioning point between concrete and HMA pavements have become very open. These joints are likely to deteriorate further at an accelerated pace if not adequately sealed/repared. Moisture ingress through open joints or cracks is detrimental to PP structures, leading to further undesirable deterioration.
  
- 10) In view of the fact that the intermediate layers of the current Texas PP sections are composed of the highly permeable stone-filled HMA mixes with high potential for moisture damage and forensic defects, it is strongly recommended, as a minimum, that performance monitoring with GPR measurements be conducted yearly on these sections. Of particular importance is ensuring that the surface HMA layers remain impermeable so as to minimize moisture ingress into the subsurface layers.

11) On a comparative note, both the design and constructability of the RBL mixes were found to be satisfactory, with no indications of structural or forensic defects. The in-place density was fairly uniform. The RBL was found to be highly impermeable and crack-resistant as designed. Equally satisfactory were the dense-graded Type B/C mixes, the PFC, and the SMA. Consequently, no mix-design or construction modifications are recommended for these mixes/layers.



## REFERENCES

AASHTO. Pocket Facts: MEPDG Version 0.910, NCHRP 1-37A, “Guide for Mechanistic-Empirical Design of New and Rehabilitated Pavement Structures.” <http://www.trb.org/mepdg>, Accessed October 2006.

APA. “Asphalt Pavement Alliance: Perpetual Pavements – A Synthesis.” APA 101. Maryland, 2002.

AI – “Asphalt Institute. Superpave Mix Design – Superpave Series No. 2 (SP-2).” Lexington, Kentucky, 1996.

Degussa, E. Evaluation of Vestenamer and Ground Tire Rubber Blend In Hot Mix Asphalt. NCAT, Alabama, 2007.

Freeman, T. J., Uzan, J., Zollinger, D., and Park, E. Sensitivity Analysis of and Strategic Plan Development for the Implementation of the M-E Design Guide in TxDOT Operations. Technical Report FHWA/TX-05/0-4714-1. Texas Transportation Institute, College Station, Texas, 2006.

Goehl, D. Personal Communication. Bryan, TX, 2009.

Newcomb, D. E., Buncher, M., and Huddleston, I.J. “Concepts of Perpetual Pavements.” Transportation Research Circular Number 503. Perpetual Bituminous Pavements, Transportation Research Board (TRB), Washington D.C., December 2001, pp 4-11.

Pellinen, T. K. and Witzak, M. W. “Stress Dependent Master Curve Construction for Dynamic (Complex) Modulus.” *Annual Meeting of Asphalt Paving Technologist*, AAPT, Colorado Springs, Colorado, 2002.

Scullion, T. “Selecting Rehabilitation Options for Flexible Pavements: Training Classes and CDs.” Implementation Project 5-1712 Summary Report, Texas Transportation Institute, College Station, Texas, 2005.

Scullion, T. “Perpetual Pavements in Texas: The State of the Practice,” Report FHWA/TX-05/0-4822-1, Texas Transportation Institute, College Station, Texas, 2007.

Scullion, T. and Hilbrich, S. “Determining the Optimal Lime Content for the Lime Stabilized Subgrade on SH 114 in the Fort Worth District.” Study 4822 Internal Report, Texas Transportation Institute, College Station, Texas, July 2004.

Sidess, A. and Uzan, J. A. “Design method of perpetual flexible pavement in Israel.” International Journal of Pavement Engineering, Vol. 1(08), pp 1-9, 2008.

TxDOT. “Memorandum on Full-depth Asphalt Pavements, Flexible Pavement Design Task Force Implementation.” Texas Department of Transportation, Austin, Texas, April 23, 2001.

TxDOT. “*Standard Specifications for Construction and Maintenance of Highways, Streets, and Bridges.*” Austin, Texas, 2004.

Walubita, L. F and Scullion, T. “Perpetual Pavements in Texas: The Fort Worth SH 114 Perpetual Pavement in Wise County.” Technical Report FHWA/TX-05/0-4822-2, TTI, College Station, Texas, 2007.

Walubita, L. F, Hu, S, Umashankar, V., and Scullion, T. The Texas Perpetual Pavement Database – Users’ Manual. Draft Technical Report FHWA/TX-05/0-4822-2, TTI, College Station, Texas, USA, 2009.

Zhou, F., Hu, S., and Scullion, T. “Integrated Asphalt (Overlay) Mix Design with Balancing Both Rutting and Cracking Requirements.” Technical Report FHWA/TX-05/5123-1, TTI, College Station, Texas, 2006.

# APPENDIX A: EXISTING TEXAS PERPETUAL PAVEMENT SECTIONS

TPP Data Viewing System

## The Texas Perpetual Pavement (PP) Database

EXIT

- Introduction**
- The Texas PP Design Concept**
- Traffic Design Data**
- Climatic-Environmental Data**
- Construction Data**
- Existing In-Service PP Structures**  
Layer Thicknesses || Mix Types || Mix Design & Materials  
 RRL Mix-Design || RRL Gradation || RRL Compaction
- Lab Test Data & Material Properties**  
Asphalt-Binder DSR || Hamburg & Overlay || Permeability  
 Dynamic Modulus Data || Permanent Deformation  
 Modulus Prediction Template || IET Master Curve Template
- Field Tests & Performance Data**  
Visual Surveys || Surface Rutting || Surface Profiles  
 Traffic WIM Measurements || MDD Measurements  
 FWD Deflections || FWD Curvature Indices || FWD Modulus  
 GPR Data & Colormaps || Coring & Forensics  
 Cracking || IR Thermal Imaging
- Proposed Future Texas PP Design**

| Raw Data Files       |
|----------------------|
| Mix Design Sheets    |
| Profiles & Ride Data |
| FWD Data             |
| GPR Data             |
| Traffic WIM-MDD Data |

| MEPDG Data Files  |
|-------------------|
| Traffic           |
| Climate           |
| Level 1-PG Binder |
| Level 1-HMA       |
| Levels 2 & 3      |

| PP Design Software |
|--------------------|
| Training Manual    |
| FPS_Demo           |
| PerRoad_Demo       |
| MEPDG_Demo         |
| PaveCheck_Demo     |

**Summary - Modulus Data**

District Average for Each Mix-FWD @ 77F

District Average for Each Mix-LAB @ 77F

Moduli Design Recommendations @ 77F

District Comparison - Hamburg & Overlay

Figure A-1. Main Screen Shot for the Texas Perpetual Pavement Database.

**APPENDIX A: EXISTING TEXAS PERPETUAL PAVEMENT SECTIONS (CONTINUED)**

**Table A-1. PP Layer Thickness Details.**

| PERPETUAL PAVEMENT (PP) STRUCTURES - LAYER THICKNESSES |  |                   |                     |                   |                         |                       |                    |                     |                            |                               |
|--|--|-------------------|---------------------|-------------------|-------------------------|-----------------------|--------------------|---------------------|----------------------------|-------------------------------|
| PROJECT#   | 1  | 2                 | 3                   | 4                 | 5                       | 6                     | 7                  | 8                   | 9                          | 10                            |
| NO.  | IH35 Laredo-Price  | IH35 Laredo-ZMW02 | IH35 Laredo-Gilbert | IH35 Laredo-ZMW01 | IH35 SA-Old San Antonio | IH35 SA-New Braumfels | IH35 Waco-McLennan | IH35 Waco-Hillsboro | SH114 Fort Worth-Superpave | SH114 Fort Worth-Conventional |
| 1  | Layer 1<br>PFC (Inches)<br>(TXDOT Rec. Range = 1-1.5 inch)                     | -                 | -                   | -                 | 1.5                     | 1.5                   | 2                  | 1.5                 | -                          | -                             |
| 2  | Layer 2<br>SMA (Inches)<br>(TXDOT Rec. Range = 2 - 3 inch)                     | 3                 | 3                   | 3                 | 2                       | 2                     | 3                  | 2                   | 2                          | 2                             |
| 3  | Layer 3<br>¾" SFHMAC (Inches)<br>(TXDOT Rec. Range = 2 - 3 inch)               | 3                 | 3                   | 3                 | 2                       | 2                     | 3                  | 3                   | 3                          | 3                             |
| 4  | Layer 4<br>1" SFHMAC (Inches)<br>(TXDOT Rec. Range ≥ 8 inch)                   | 8                 | 12                  | 8                 | 12                      | 12                    | 10                 | 12                  | 13                         | 13                            |
| 5  | Layer 5<br>RBL (Inches)<br>(TXDOT Rec. Range = 2 - 3 inch)                     | 2                 | 2                   | 4                 | 4                       | 4                     | 4                  | 4                   | 4                          | 4                             |
| 6  | Layer 6<br>Base (Treated Subgrade) (Inches)<br>(TXDOT Rec. Range = 6 - 8 inch) | 8                 | 8                   | 8                 | 6                       | 8                     | 8                  | 14                  | 8                          | 8                             |
| Subgrade   | Natural Subgrade Material  | ∞                 | ∞                   | ∞                 | ∞                       | ∞                     | ∞                  | ∞                   | ∞                          | ∞                             |
| <b>Total HMA Thickness (Inches)</b>                    | <b>16</b>  | <b>17</b>         | <b>20</b>           | <b>18</b>         | <b>21.5</b>             | <b>21.5</b>           | <b>22</b>          | <b>22.5</b>         | <b>22</b>                  | <b>22</b>                     |
| <b>Total PP Structure Thickness (Inches)</b>           | <b>24</b>  | <b>25</b>         | <b>28</b>           | <b>26</b>         | <b>27.5</b>             | <b>29.5</b>           | <b>30</b>          | <b>36.5</b>         | <b>30</b>                  | <b>30</b>                     |
| <b>Average</b>   |  |                   |                     |                   |                         |                       |                    |                     |                            | <b>1.5</b>                    |
|  |  |                   |                     |                   |                         |                       |                    |                     |                            | <b>3</b>                      |
|  |  |                   |                     |                   |                         |                       |                    |                     |                            | <b>3</b>                      |
|  |  |                   |                     |                   |                         |                       |                    |                     |                            | <b>10.5</b>                   |
|  |  |                   |                     |                   |                         |                       |                    |                     |                            | <b>4</b>                      |
|  |  |                   |                     |                   |                         |                       |                    |                     |                            | <b>8</b>                      |
|  |  |                   |                     |                   |                         |                       |                    |                     |                            | <b>∞</b>                      |

Note: Complete data can be found in the Texas PP database.

# APPENDIX A: EXISTING TEXAS PERPETUAL PAVEMENT SECTIONS (CONTINUED)

Table A-2. Texas PP Location Details.

| Project# | Highway | CSJ#        | District    | County                  | TRM Location |                                    |   | Geographical                |                             |        | GPS Location |          |       | Elevation  |       |     | Section Length (mile) | Comment |
|----------|---------|-------------|-------------|-------------------------|--------------|------------------------------------|---|-----------------------------|-----------------------------|--------|--------------|----------|-------|--|-------|-----|-----------------------|---------|
|          |         |             |             |                         | Begin        | End                                | Limits  | Begin                       | End                         | Limits | Start        | End      | Start | End  | Start | End |                       |         |
| 1        | IH 35   | 0018-05-062 | Laredo      | Webb (Price)            | 08+0.403     | 13+0.828                           | From: 0.250 mi. N. of Milo Interchange<br>To: 0.500 mi. N. of Unroyal Rd                              | N 27° 37' 13" W 99° 29' 49" | N 27° 41' 42" W 99° 27' 58" |        | 498.0 ft     | 653.0 ft | 6,000 | Only the inside lanes were reconstructed as perpetual pavement (PP) structures. Starts just after Exit# 8 on NB lanes. PP sections actually end at bridge at Unroyal Rd just after TRM 13+0.000.   |       |     |                       |         |
| 2        | IH 35   | 0018-02-049 | Laredo      | La Salle (Zumwalt02)    | 49+0.431     | 53+0.427                           | From: 8.127 mi. N. of SH 44<br>To: 3.526 mi. S. of FM 133   | N 28° 11' 24" W 99° 16' 78" | N 28° 14' 62" W 99° 17' 72" |        | 528.0 ft     | 447.0 ft | 4,000 | NB has 1 mile of concrete section from TRM 51+0.000 to 52+0.000. WIM stations on both SB & NB lanes @ about TRM 51+0.600 (GPS: N 28° 12' 860". W 99° 18' 236". Elev. 483 ft). MDDs @ about TRM 51+0.600 on SB outside lane (right wheel path) (GPS: N 28° 12' 840". W 99° 18' 279". Elev. 523 ft). |       |     |                       |         |
| 3        | IH 35   | 0018-01-063 | Laredo      | La Salle (Gilbert)      | 58+0.000     | 65+0.362                           | From: 1.971 mi. N. of FM 133<br>To: 7.365 mi. N. of FM 133  | N 28° 18' 36" W 99° 16' 39" | N 28° 24' 57" W 99° 15' 26" |        | 492.0 ft     | 400.0 ft | 7,362 |  |       |     |                       |         |
| 4        | IH 35   | 0017-08-067 | Laredo      | La Salle (Zumwalt01)    | 69+0.439     | 74+0.003                           | From: 0.600 mi. N. of Gardendale<br>To: 1.670 mi. N. of FM 468  | N 28° 27' 70" W 99° 13' 93" | N 28° 31' 54" W 99° 12' 78" |        | 436.0 ft     | 559.0 ft | 5,442 | Only the NB lanes were rebuilt into a perpetual pavement. PP section starts just after Green Sign post written Pearsall 31 San Antonio 85.   |       |     |                       |         |
| 5        | IH 35   | 0016-04-091 | San Antonio | Comal (Old San Antonio) | 188+0.774    | 190+0.368                          | From: 0.8 km S. of SH 46<br>To: Kowald Rd   | N 29° 41' 85" W 98° 05' 84" | N 29° 44' 16" W 98° 04' 20" |        | 627.0 ft     | 687.0 ft | 1,740 |  |       |     |                       |         |
| 6        | IH 35   | 0016-04-094 | San Antonio | Comal (New Braumleys)   | 190+0.368    | 191+1.015                          | From: Kowald Rd<br>To: 0.48 km. N. of FM 306  | N 29° 43' 08" W 98° 05' 29" | N 29° 44' 16" W 98° 04' 20" |        | 687.0 ft     | 656.0 ft | 1,300 |  |       |     |                       |         |
| 7        | IH 35   | 0015-01-164 | Waco        | McLennan                | 340+0.052    | 342+0.622                          | From: 0.458 mi. S. of Craven Ave.<br>To: 0.241 mi. N. of BU 77-L<br>(Section ends exactly at start of | N 31° 37' 09" W 97° 05' 97" | N 33° 39' 01" W 97° 06' 03" |        | 465.0 ft     | 487.0 ft | 2,200 | Section ends exactly at start of bridge after Exit 342A  |       |     |                       |         |
| 8        | IH 35   | 0048-09-023 | Waco        | Hill                    | 368+0.724    | IH35E: 371+0.916<br>IH35W: 1+0.238 | From: Just N. of FM 286 in Hillisboro<br>To: N. of IH35 East/West split                               | N 32° 01' 15" W 97° 05' 72" | N 32° 03' 86" W 97° 05' 86" |        | 661.0 ft     | 656.0 ft | 3,250 |  |       |     |                       |         |
| 9        | SH 114  | 0353-01-026 | Fort Worth  | Wise                    | 580+0.804    | 583+0.500                          | From: 0.321 km E. of US 81/287 eastwards<br>To: Traffic lights  | N 33° 02' 20" W 97° 25' 73" | N 33° 02' 19" W 97° 23' 99" |        | 880.0 ft     | 761.5 ft | 2,200 | WIM station on this section at about TRM 580+0.950   |       |     |                       |         |
| 10       | SH 114  | 0353-01-026 | Fort Worth  | Wise                    | 583+0.500    | 586+0.200                          | From: Traffic lights eastwards<br>To: Denton County Line  | N 33° 02' 19" W 97° 23' 99" | N 33° 02' 16" W 97° 23' 54" |        | 761.5 ft     | 781.0 ft | 1,740 | Section starts at traffic lights   |       |     |                       |         |

Note: Complete data can be found in the Texas PP database.

**APPENDIX A: EXISTING TEXAS PERPETUAL PAVEMENT SECTIONS (CONTINUED)**

**Table A-2. Texas PP Traffic Design Details.**

| Project No. | Highway | CSJ#        | District    | County                  | ADT                                  |  | %Traffic Growth | % Trucks             | Σ ESALS (million)        | # Lanes        | Comment   |
|-------------|---------|-------------|-------------|-------------------------|--------------------------------------|--|-----------------|----------------------|--------------------------|----------------|---|
|             |         |             |             |                         | Begin                                | End                                    |                 |                      |                          |                |   |
| 1           | IH 35   | 0018-05-062 | Laredo      | Webb (Price)            | 18,900 (2001)                        | 34,800 (2024)                          | 3%              | 30.4                 | 18,508                   | 6 total        |   |
| 2           | IH 35   | 0018-02-049 | Laredo      | La Salle (Zumwalt02)    | 11,900 (2002)                        | 21,200 (2022)                          | 3%              | 46.2                 | 26,488                   | 4 total        |   |
| 3           | IH 35   | 0018-01-063 | Laredo      | La Salle (Gilbert)      | 12,400 (2001)                        | 23,100 (2021)                          | 3%              | 36.1                 | 24,097                   | 4 total        |   |
| 4           | IH 35   | 0017-08-067 | Laredo      | La Salle (Zumwalt01)    | NB only<br>6,600 (2001)              | NB only<br>11,200 (2021)               | 3%              | 42.2                 | 29,543                   | 2              | Only the NB lanes were rebuilt into a perpetual pavement. |
| 5           | IH 35   | 0016-04-091 | San Antonio | Comal (Old San Antonio) | 60,500 (2004)                        | 95,200 (2024)                          | 2%              | 16                   | 41,593                   | 6 to 8 total   |   |
| 6           | IH 35   | 0016-04-094 | San Antonio | Comal (New Braunfels)   | 60,500 (2004)                        | 95,200 (2024)                          | 2%              | 16                   | 41,593                   | 6 to 8 total   |   |
| 7           | IH 35   | 0015-01-164 | Waco        | McLennan                | 64,750                               | 112,300                                | 3%              | 17.7                 | 74,172                   | 6 total        |   |
| 8           | IH 35   | 0048-09-023 | Waco        | Hill                    | 41000                                | 70900                                  | 3%              | 27.5                 | 75,209                   | 8              |   |
| 9           | SH 114  | 0353-01-026 | Fort Worth  | Wise                    | EB: 7,500 (2004)<br>WB: 7,500 (2004) | EB: 15,000 (2024)<br>WB: 15,000 (2024) | 4%              | EB: 27.3<br>WB: 23.7 | EB: 37,242<br>WB: 13,086 | EB: 2<br>WB: 2 | WIM station on this section at about TRM 580+0.950.       |
| 10          | SH 114  | 0353-01-026 | Fort Worth  | Wise                    | EB: 7,500 (2004)<br>WB: 7,500 (2004) | EB: 15,000 (2024)<br>WB: 15,000 (2024) | 4%              | EB: 27.3<br>WB: 23.7 | EB: 37,242<br>WB: 13,086 | EB: 2<br>WB: 2 | Section starts at traffic lights.                         |

**Statistics**

|                                |        |         |     |     |     |     |
|--------------------------------|--------|---------|-----|-----|-----|-----|
| Average                        | 29,155 | 49,390  | 3%  | 28  | 38  | 4   |
| Coefficient of Variation (COV) | 85%    | 80%     | 12% | 38% | 56% | 47% |
| Range: Minimum                 | 6,600  | 11,200  | 2%  | 16  | 13  | 2   |
| Range: Maximum                 | 64,750 | 112,300 | 4%  | 46  | 75  | 8   |

Note: Complete data can be found in the Texas PP database.

## APPENDIX B: EXAMPLE OF MATERIAL PROPERTIES FOR SH 114

**Table B-1. Permanent Deformation Parameters from Repeated Load Testing.**

| Layer Material  | Binder            | $\alpha$      |        | $\mu$ |        |       |
|---|-------------------|---------------|--------|-------|--------|-------|
|   |                   | 77 °F         | 104 °F | 77 °F | 104 °F |       |
| <b>SH 114: Superpave Section</b>  |                   |               |        |       |        |       |
| Layer 1   | ½" HDSMA          | 6.8% PG 70-28 | 0.809  | 0.611 | 0.210  | 0.219 |
| Layer 2   | ¾" SFHMA          | 4.2% PG 76-22 | 0.765  | 0.594 | 0.221  | 0.232 |
| Layer 3   | 1" SFHMA          | 4.0% PG 70-22 | 0.887  | 0.678 | 0.182  | 0.192 |
| Layer 4   | ¾" SFHMA<br>(RBL) | 4.2% PG 64-22 | 0.721  | 0.565 | 0.250  | 0.281 |
| <b>SH 114: Conventional Section</b>                                     |                   |               |        |       |        |       |
| Layer 1   | ½" HDSMA          | 6.8% PG 70-28 | 0.809  | 0.611 | 0.210  | 0.219 |
| Layer 2   | Type C            | 4.4% PG 70-22 | 0.747  | 0.586 | 0.242  | 0.251 |
| Layer 3   | Type B            | 4.5% PG 64-22 | 0.819  | 0.659 | 0.203  | 0.228 |
| Layer 4   | Type C (RBL)      | 5.3% PG 64-22 | 0.693  | 0.544 | 0.261  | 0.283 |
| Except for Layer 1 (igneous/granite), all aggregate type was limestone. |                   |               |        |       |        |       |

Note: Complete data for all the Texas PP sections can be found in the Texas PP database.





## APPENDIX C: FIELD PERFORMANCE TESTING OF SELECTED PP SECTIONS



**Figure C-1. Example Pictorial View of Some Texas PP Sections.**

Note: Complete data for all the Texas PP sections can be found in the Texas PP database.

**APPENDIX C: FIELD PERFORMANCE TESTING OF SELECTED PP SECTIONS (CONTINUED)**

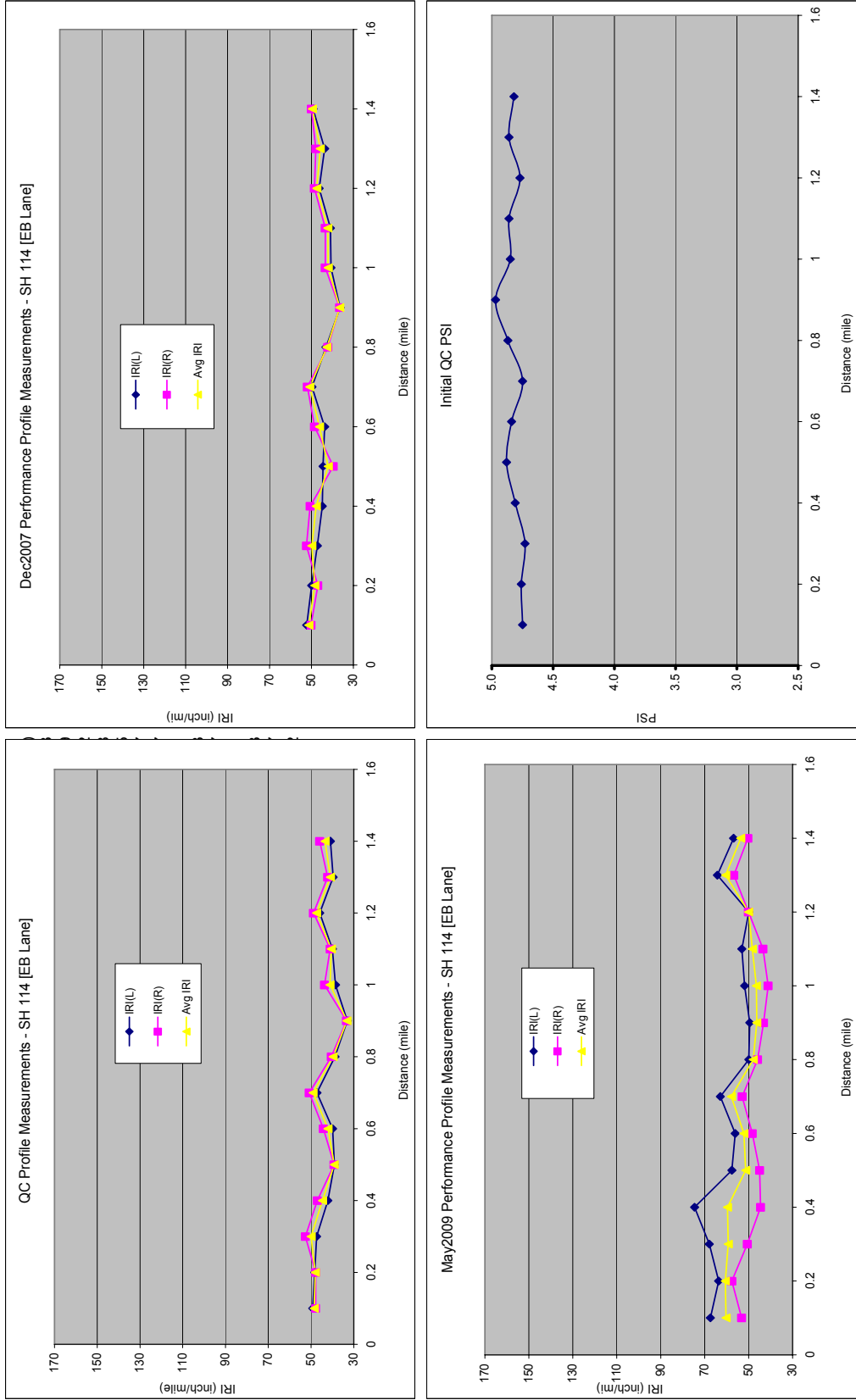


**Figure C-2. Example IRI and PSI Plots for SH 114 – Superpave (Fort Worth).**

Note: Complete data for all the Texas PP sections can be found in the Texas PP database.

**APPENDIX C: FIELD PERFORMANCE TESTING OF SELECTED PP SECTIONS (CONTINUED)**

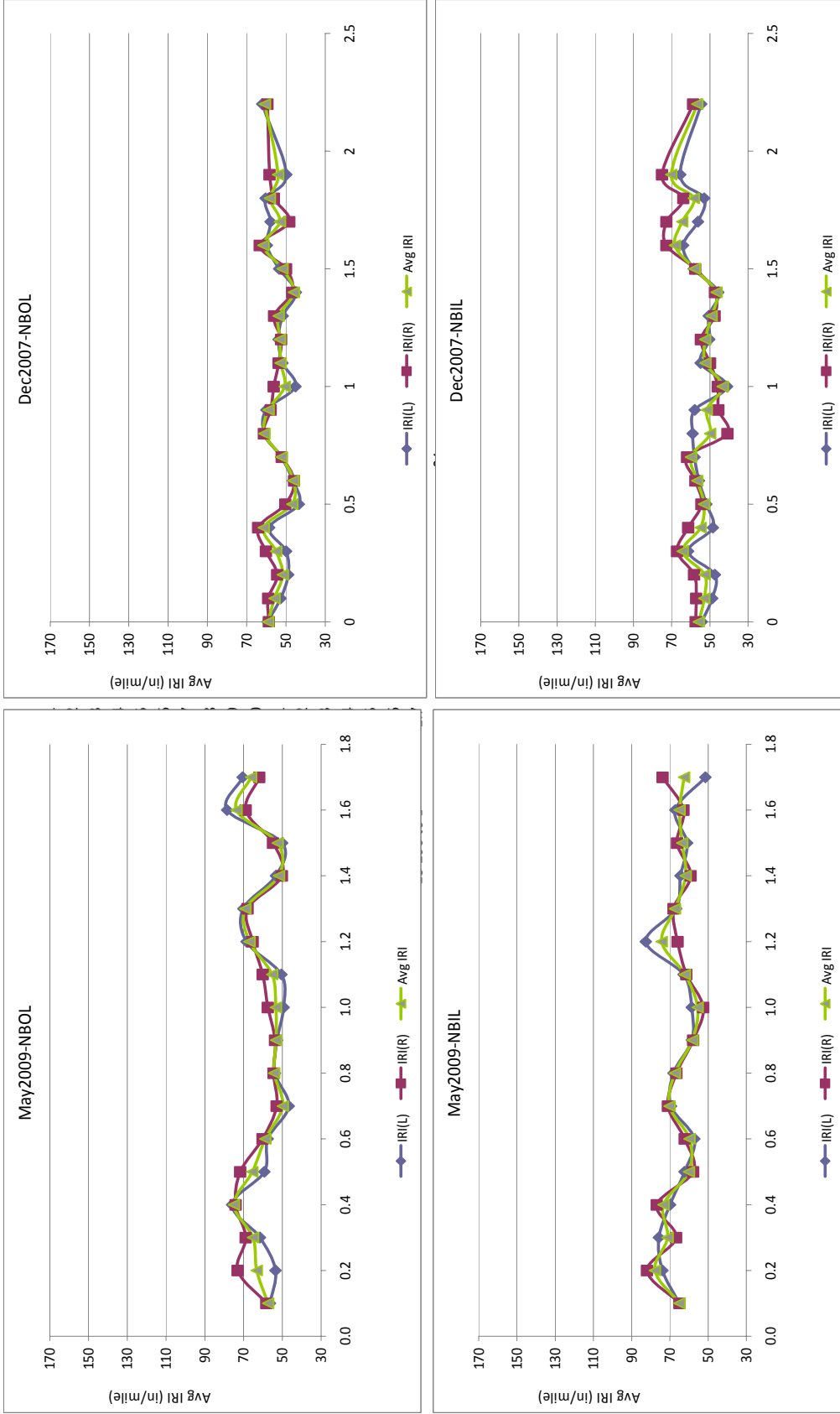


**Figure C-3. Example IRI Plots for IH 35 - Superpave (Hillsboro).**

Note: Complete data for all the Texas PP sections can be found in the Texas PP database.

## APPENDIX C: FIELD PERFORMANCE TESTING OF SELECTED PP SECTIONS (CONTINUED)

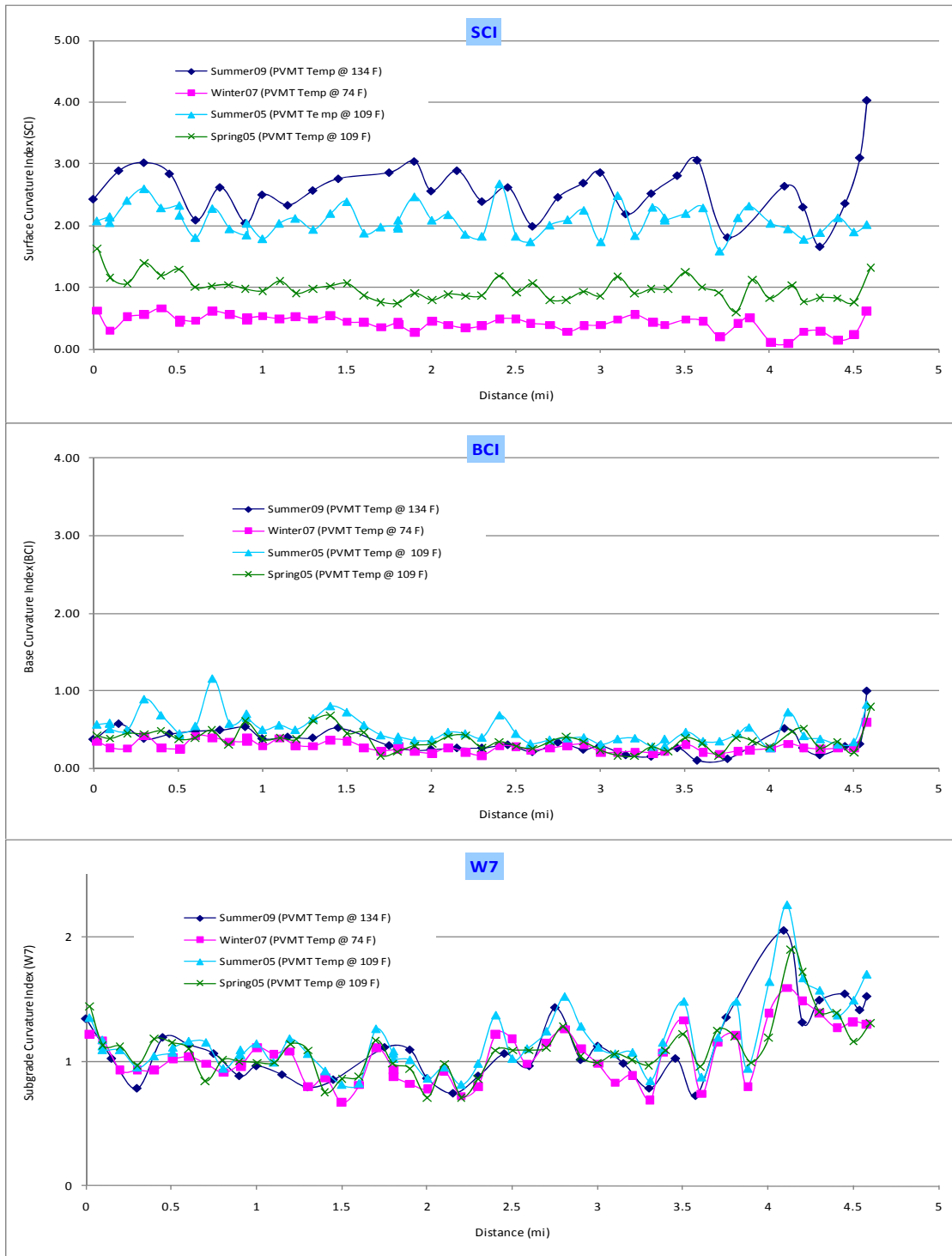


**Figure C-4. Example Curvature Index Plots for IH 35 Laredo – ZMW01.**

Note: Complete data for all the Texas PP sections can be found in the Texas PP database.

## APPENDIX C: FIELD PERFORMANCE TESTING OF SELECTED PP SECTIONS (CONTINUED)

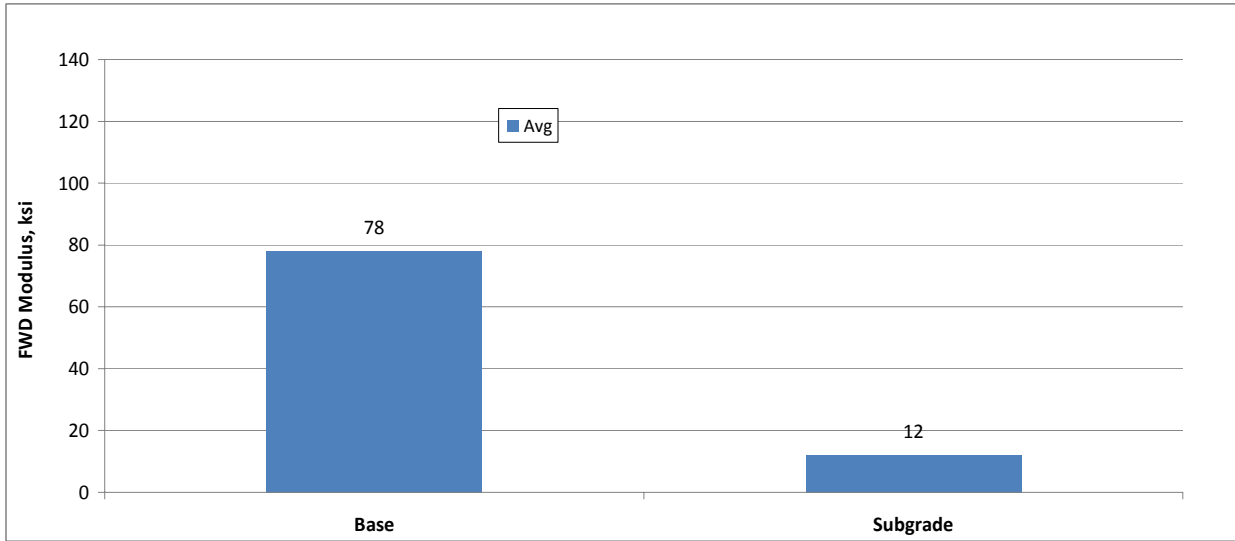
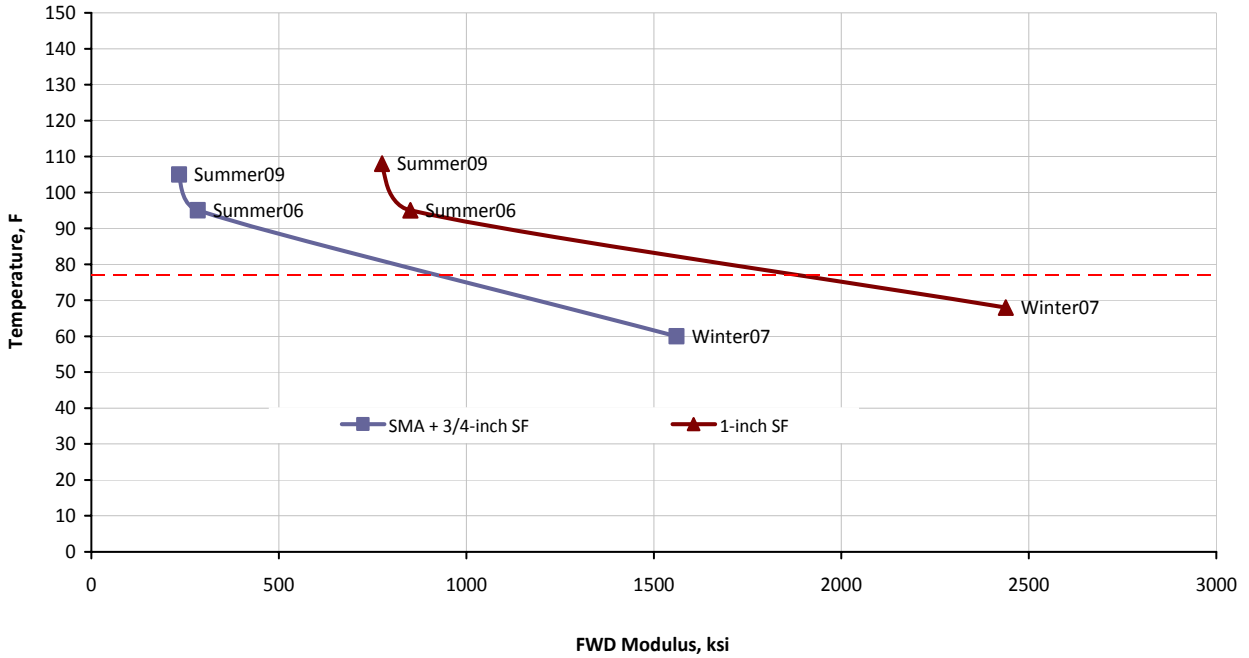


**Figure C-5. Example Moduli Plots for SH 114 – Superpave.**

Note: Complete data for all the Texas PP sections can be found in the Texas PP database.

## APPENDIX C: FIELD PERFORMANCE TESTING OF SELECTED PP SECTIONS (CONTINUED)

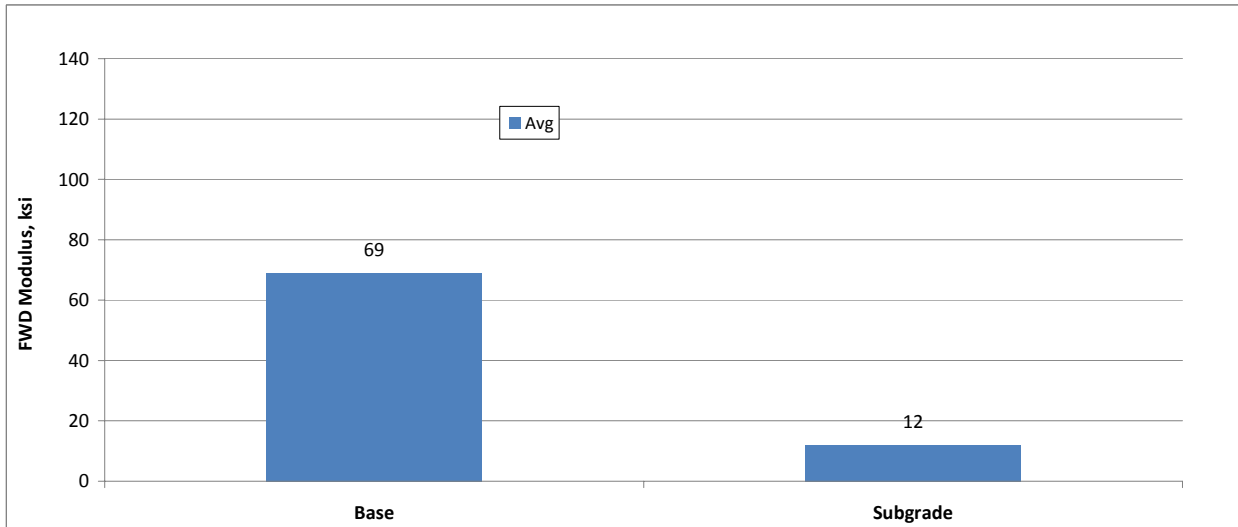
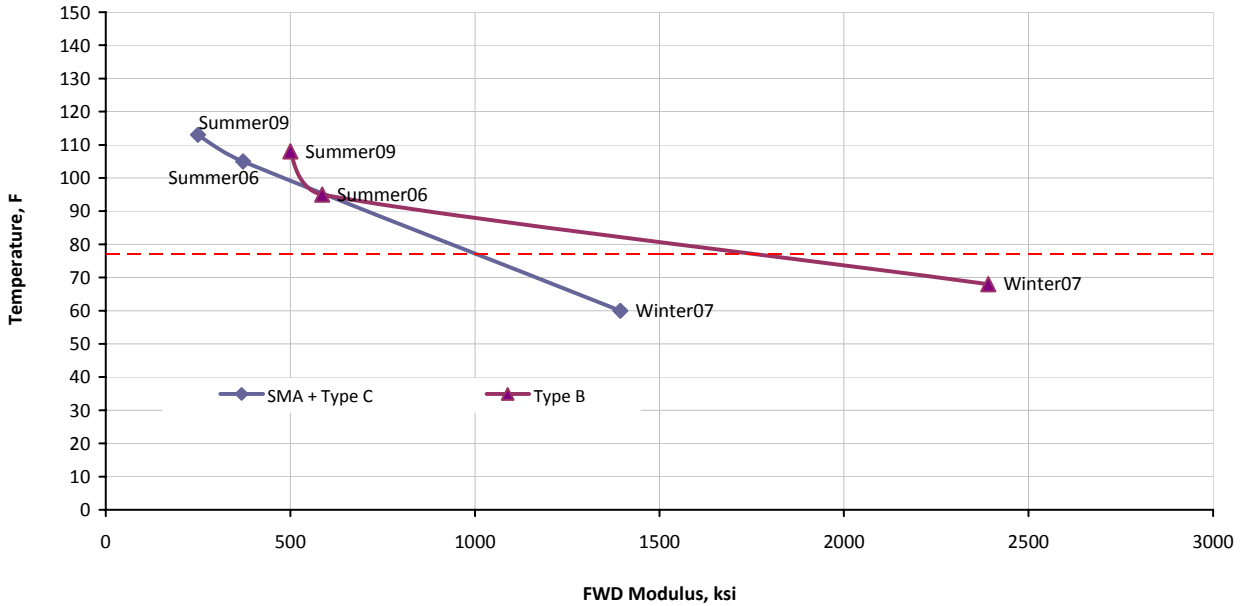


**Figure C-6. Example Moduli Plots for SH 114 – Conventional.**

Note: Complete data for all the Texas PP sections can be found in the Texas PP database.

## APPENDIX C: FIELD PERFORMANCE TESTING OF SELECTED PP SECTIONS (CONTINUED)

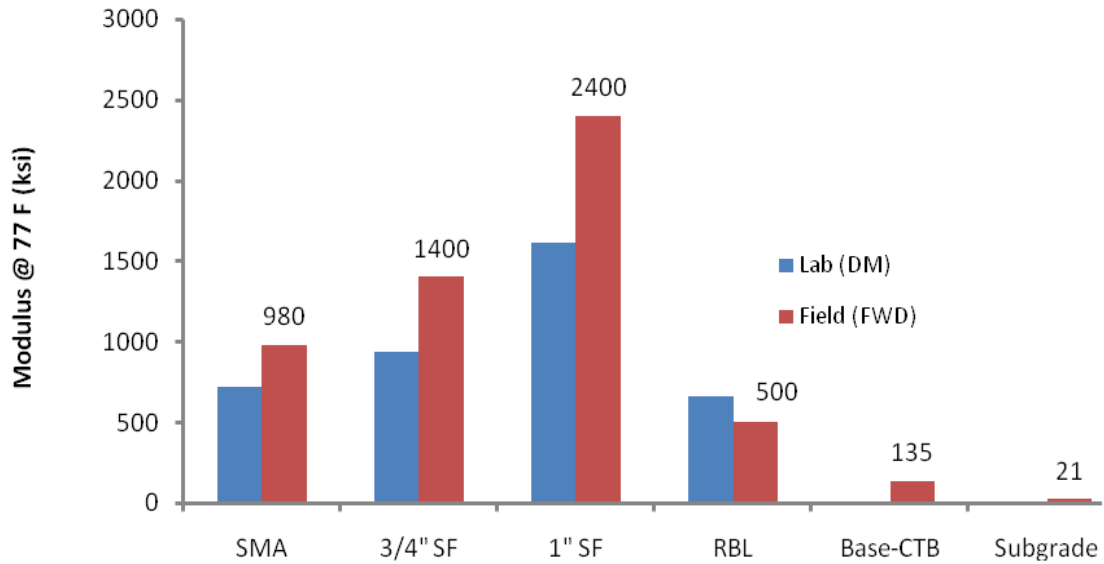


**Figure C-7. Example FWD Layer Moduli Values for IH 35 – ZUMW02.**

Note: Complete data for all the Texas PP sections can be found in the Texas PP database.





## APPENDIX D: MDD DEFLECTIONS AND STRAIN ANALYSES FOR IH 35 (LAREDO)

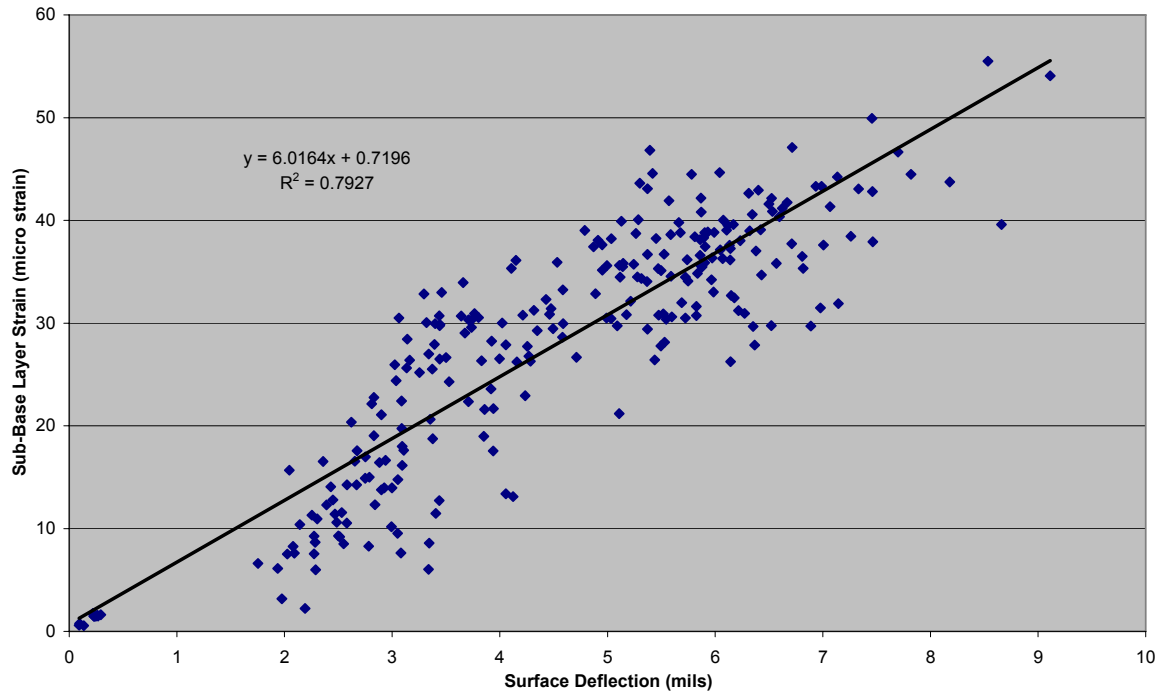


**Figure D-1. Surface Deflection vs. Subbase Vertical Strain – IH 35 ZMW02.**

Note: Complete data for all the Texas PP sections can be found in the Texas PP database.

**APPENDIX D: MDD DEFLECTIONS AND STRAIN ANALYSES  
FOR IH 35 (LAREDO) (CONTINUED)**

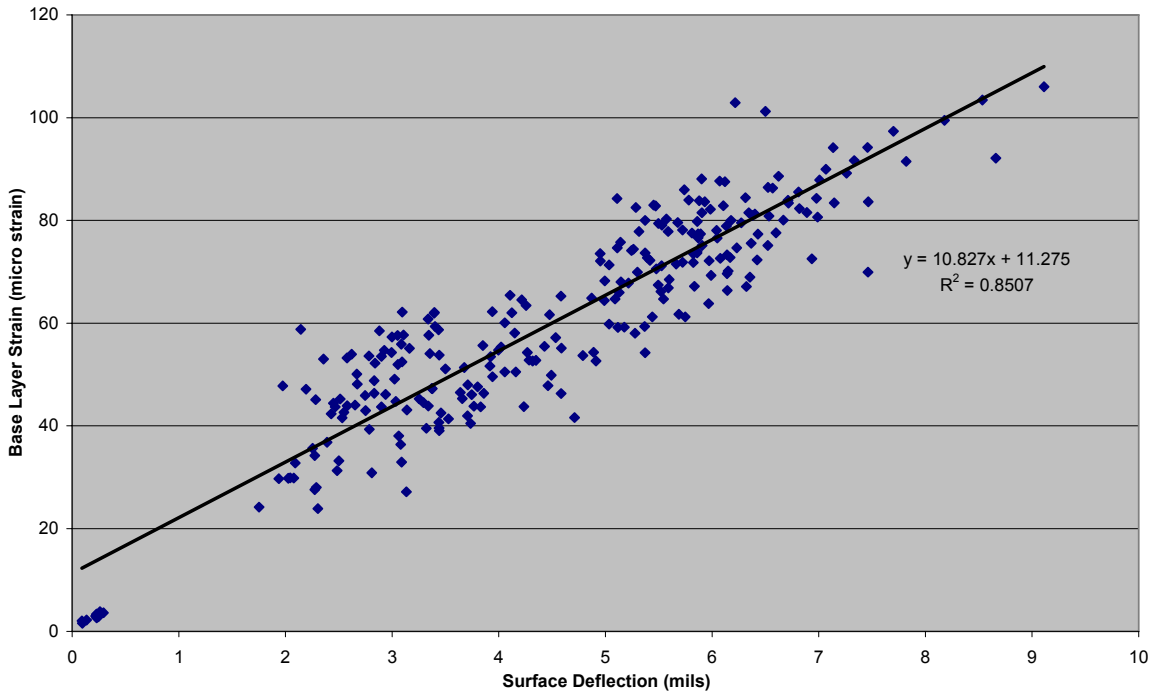


**Figure D-2. Surface Deflection vs. Base Layer Vertical Strain – IH 35 ZMW02.**

Note: Complete data for all the Texas PP sections can be found in the Texas PP database.

**APPENDIX D: MDD DEFLECTIONS AND STRAIN ANALYSES  
FOR IH 35 (LAREDO) (CONTINUED)**

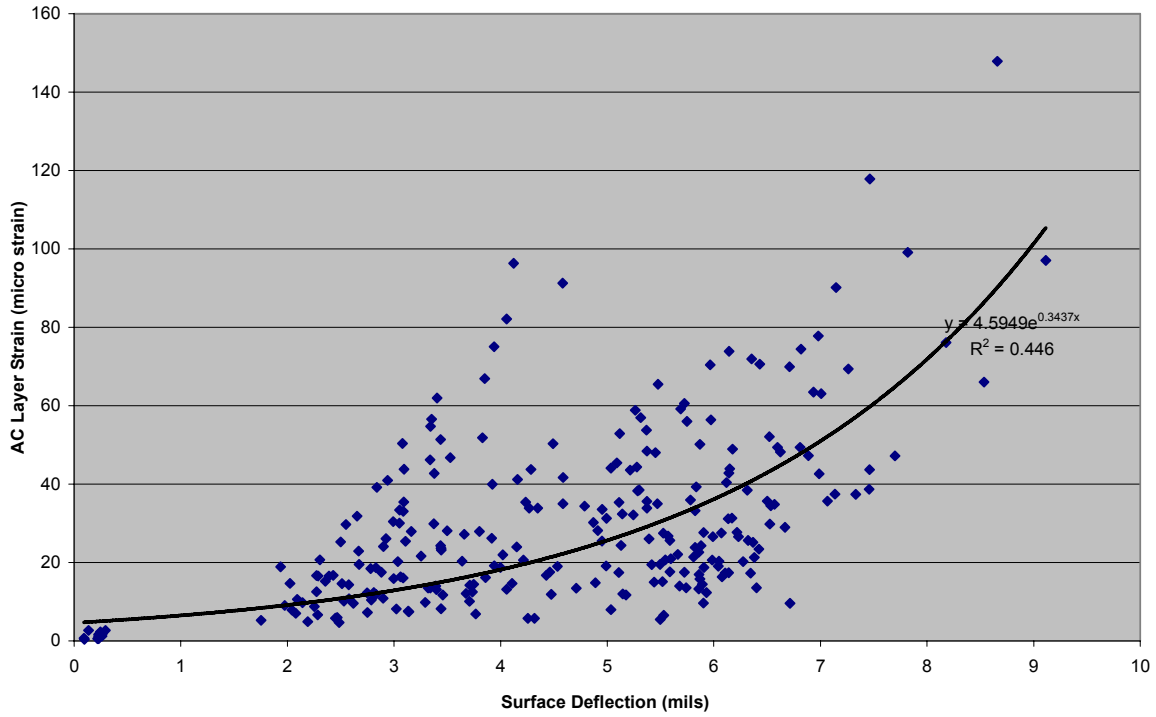


**Figure D-3. Surface Deflection vs. Surface Layer Vertical Strain – IH 35 ZMW02.**

Note: Complete data for all the Texas PP sections can be found in the Texas PP database.

